UNIVERSITÀ
POLITECNICA
DELLE MARCHE

Marco Palma

The application of Structure from Motion photogrammetry as innovative method to assess marine benthic habitats and support their management

Scienze della Vita e dell' Ambiente

PhD
Academic Year: 2015–2018

Supervisor: Prof. Carlo Cerrano
October 2018

UNIVERSITÀ
POLITECNICA
DELLE MARCHE

Scienze della Vita e dell' Ambiente

PhD

Academic Year: 2015–2018

Marco Palma

The application of Structure from Motion photogrammetry as innovative method to assess marine benthic habitats and support their management

Supervisor: Prof. Carlo Cerrano
October 2018

Submitted in partial fulfilment of the requirements of the degree of Doctor of Philosophy

Abstract

Global environmental changes and human activities are having significant effects on the composition of marine benthic habitats, disturbing the ecological functioning of many ecosystems. Yet, quantifying ecological responses to habitat changes is challenging because of limitation of current field methods and technology. The aim of this research is to improve the characterization of benthic marine communities by using Structure for Motion (SfM)-based methods. The objectives are (i) to provide a SfM-framework to assess the spatial composition of benthic communities and uncover the scale-specific effects that determine sample representativeness; (ii) to apply and test the framework to study the effects of human and environmental pressures on coral reefs; and (iii) to propose a new method for investigating the population structure and biomass of benthic tree-shaped species. The research was carried out at the Partial Marine Reserve of Ponta do Ouro (PPMR, Mozambique) and at the Marine Protected Area of Portofino (Italy).

At PPMR, the findings show that the best sampling size is 25 m^2. This size allowed capturing the diversity, abundance, structural complexity and morphological functions of reefs' organisms, and investigating changes driven by anthropic activities (i.e. scuba diving). Highly dove sites had low taxa diversity and density, and were characterized by mainly resistant-to-physical-impact organisms (i.e. sponges and algae) of big sizes and with complex shapes. On the contrary, low or moderately dove sites presented fragile-to-physical-impact organisms (i.e. *Acropora* spp.). This research also demonstrated that in addition to abundance and morphological information, the use of SfM point clouds over tree-shaped organisms allows to have accurate prediction of biomass, avoiding to conduct destructive sampling and supporting calculation of secondary production.

To support marine management using SfM to investigate benthic communities, this research emphasizes the need to (i) recognise the need of standardised approaches of SfM method to identify relevant scales for conservation; (ii) develop better approaches to derive quantitative information on marine organisms biodiversity, biomass and on their structural habitat, and (iii) establish further knowledge on the spatial variation of benthic communities as a result of human pressure.

Keywords: SfM, gorgonian, coral reefs, scuba divers, ortho-mosaics, point clouds, conservation, management

This research project was funded by "EUREKA", European Social Funds (FSE), Programma Operativo Regionale (POR) 2014/2020 Regione Marche (Italy).

Acknowledgements

Questa tesi é a conclusione di un lungo percorso di crescita professionale e di ricerca scientifica che mi ha dato la possibilita di congiungere la passione per la conservazione con l'interesse per l'innovazione e le nove tecnologie. Produrre nuove applicazioni pratiche per migliorare esistenti sistemi é stato obiettivo ultimo di questo lavoro di ricerca sempre supportato dalla fiducia e dalle infallibili intuizioni del mio supervisore Prof. Carlo Cerrano.

Questa ricerca é stata occasione irripetibile di approfondimento e sperimentazione, di conoscenza e multidisciplinaritá. Devo ringraziare per questo la ditta UBICA srl, l'Ateneo dell'Universitá Politecnica delle Marche e la Regione Marche che tramite il progetto EUREKA (Fondi Sociali Europei, Programma Operativo Regionale (POR) 2014/2020) hanno supportato finanziariamente la ricerca. Un ringraziamento particolare ai membri della UBICA srl che mi hanno sempre supportato nelle attivitá di ricerca e con i quali ho condiviso ogni fase del lavoro realizzato.

Un ringraziamento a Dr. Monica Rivas Casado della Cranfield University per la sua energia, positivitá, supporto e curiositá scientifica che mi hanno permesso di superare i grandi ostacoli del publicare su riviste scientifiche. Grazie al gruppo di ricercatori, dottoranti e studenti del laboratorio di zoologia con i quali ho avuto occasione di consolidare forti amicizie.

Infine un grazie a mia moglie Chiara, con la quale ho condiviso le frustrazioni e le gioie quotidiane di questi tre anni, e che, piú di chiunque, mi ha in ogni modo ed istante supportato.

Al prossimo Nebbiolo

Contents

List of Figures

List of Tables

Chapter 1

Introduction

Marine habitats are essential element of Earth's ecosystem and provide a wide range of services for human life. They are also intensively impacted by human activities: urbanization, coastal runoff, excess of nutrient and chemicals, have impaired natural biological regimes and caused a widespread decline of marine species and habitats worldwide (Thakur et al., 2018; Doney, 2010). Coral reefs and coralligenous habitats are for example two of the most vulnerable systems on earth, undergoing major decline due to short term human and natural threats (Hughes et al., 2017; Cerrano et al., 2010). The impact of all these changes suggests the need to investigate marine habitats in their geographical extent, ecological functions and conservation status (Lecours et al., 2015). This is the ambition of many governmental agendas that promote topographic investigations, habitat, and biotope marine mapping to protect marine biodiversity and services (Hong Kong Special Administrative Region, 2016; Buhl-Mortensen et al., 2015; Commission, 2011).

Research studies have demonstrated that mapping marine habitats supports effective management of marine environment (i.e. monitoring) (Van Dover et al., 2017; Lecours et al., 2015; Brown et al., 2011). However, mapping marine habitats and species at high resolution and large spatial scales is impaired by current investment changes and technological approaches (Lecours et al., 2015). Conventional seabed survey methods are limited or inadequate for extended and high-resolution mapping (Brown et al., 2011). To this end, only the 5-10% seabed ecosystems has been surveyed at similar fine resolution of terrestrial system (Wright and Heyman, 2008). The lack of high resolution information over large spatial scales, has limited our understanding on species distribution pattern, ecological dynamics, and the design of conservation strategies (González-Rivero et al., 2014; Mengerink et al., 2014; Brown et al., 2011).

Hence, the application of validated technologies in terrestrial environment have been suggested in the marine field for collecting quantitative information on the impacts of anthropogenic and natural factors on benthic species and habitats (Harris and Baker, 2012; Harris, 2012). In this direction, marine research has started to adopt more interdisciplinary approaches by using for example using the Structure for Motion (SfM) Photogrammetry (Westoby et al., 2012).

1.1 What is Structure from Motion photogrammetry?

The Structure from Motion is an optical based technology for estimating the 3D structure of a scene from 2D overlapping images, acquired by a moving sensor (Westoby et al., 2012). In SfM photogrammetry the internal camera geometry, the camera position and the camera orientation are automatically calculated by the algorithms processing the images (Westoby et al., 2012). An algorithm, scale invariant feature transform (SIFT), processes the image dataset by identifying common feature points within the collected images, and establishes 3D spatial relationships in an arbitrary coordinate system (Micheletti et al., 2015b). A second algorithm, sparse bundle adjustment, transforms the measured image coordinates into coloured 3D points creating a sparse point cloud (e.g. Snavely et al. (2008)). The bundle adjustment implements the collinearity condition between common points between images to establish a mathematically rigorous relationship with the 3D points (Snavely et al., 2008). The "self-calibration" of the bundle adjustment algorithm, models and estimates additional parameters of distortions associated with the consumer cameras, and supports the processing of images coming from different sensors qualities (Kenefick et al., 1972; Faig and Moniwa, 1973). Multi View Stereo (MVS) techniques intensify the sparse point cloud, generate very high-resolution datasets by removing gross errors, and provide dense point clouds (e.g. Furukawa and Ponce (2010); Rothermel et al. (2012). 3D models, ortho rectified mosaics, Digital Terrain Models (DTM) are generated by interpolating 3D point cloud (Westoby et al., 2012).

The SfM has become a competitive technologies in close range remote sensing because low-cost and time-efficient. In fact, a wide range of camera sensors ranging from smartphones cameras (Micheletti et al., 2015a) to action cameras and DLCS cameras (Ingwer et al., 2015), can be used for SfM surveys providing highly accurate 3D point clouds. In contrast, laser scanning systems, which measure the time of an emitted laser pulse to be reflected off and return to the sensor, provides the highest quality 3D point clouds but at lower densities than SfM and more expensive equipment and specific knowledge is required (Wallace et al., 2016) . Therefore SfM is revolutionizing traditional methods for data collection and data processing in ecology.

In terrestrial research, the use of SfM encouraged the growth of "personal remote sensing" of landscapes at high spatial and temporal resolution (Dandois et al., 2015). It has been applied for a wide range of purposes and replaced in most cases the use of aerial or terrestrial laser scanning surveys; from mapping canopy height and estimating their density, to investigating the extent and coverage of lichen and moss on bare soils (Dandois et al., 2015; Liang et al., 2015). In marine field, SfM has been successfully applied in aerial and underwater application. Aerial studies demonstrated the effectiveness of SfM in mapping coastal and shallow areas at high resolution by using drones and kites (Levy et al., 2018; Chirayath and Earle, 2016; Currier, 2015). Underwater studies tested SfM technology by using "out of the shelf cameras" handled by scuba diver (Storlazzi et al., 2016), cameras equipped on semiautonomous underwater vehicles (Bryson et al., 2017; González-Rivero et al., 2014) or cameras coupled with autonomously navigated vehicles (Williams et al., 2012). Researchers have started defining new frameworks to integrated remote sensing methods to underwater habitat monitoring for improving the understanding of key aspects of habitat dynamics, provision and productivity, and estimating their structural complexity at multiple scale (Storlazzi et al., 2016; Ferrari et al., 2016; Figueira et al., 2015; Leon et al., 2015). For example, measuring habitat structural complexity of coral reefs by using linear rugosity calculations has greatly contributed to our understanding of the reef functioning (Graham and Nash, 2013). Traditional methods as chain transect have been replaced by using linear or surface rugosity calculation on 3D model generated by SfM (Storlazzi et al., 2016) and the SfM accuracy in calculating the habitat complexity has been estimated in different environmental conditions and on target taxonomical groups (Bryson et al., 2017). These types of approaches allows avoiding contact with the substrate, to perform rapid underwater surveys and to replicate multiple measurements at known spatial resolutions (Leon et al., 2015).

Recent applications also include investigations on the morphological complexity of reefs from single organisms to reef-scape scales (10 km^2) (Ferrari et al., 2016). However, few SfM based studies investigated the correlation between coral reef morphological complexity and species composition (Bryson et al., 2017). None of these studies investigated the composition of benthic communities at high resolution and across wide areas of orthorectfied mosaics or point cloud datasets. Ortho- mosaics generated from SfM data processing are new informative layers to support detailed ecological studies and habitat mapping. For example, they can inform about organisms varying in dimension, shape, species and abundance interact at seascape level, and how environmental and human pressures act over time in selecting and designing benthic communities. Also, SfM point clouds are commonly used for estimating relevant metrics in terrestrial forestry (i.e. canopy coverture, trees, steam diameters) (Liang et al., 2015), but no studies have processed SfM point clouds in the underwater field to estimate population structure and morphometrics, for example of tree shaped marine benthic species (i.e. gorgonians).

To date, the lack of a framework that standardize SfM sampling protocols and data processing for habitat characterization, limits the use of SfM technologies in experimental studies and monitoring programs. Therefore, it is important to investigate potential benefits of SfM applications to study marine benthic communities and to respond to national and international policies.

1.2 Knowledge gap and research needs

Studying benthic communities is the first step to assess the potential impact of human and environmental pressures in marine environment and for the development of appropriate management strategies. Thus, to quantify ecological responses to habitat changes, there is the need of tools supporting a comprehensive knowledge of habitats and organisms and their interactions. Therefore, this research investigates the use of

SfM in marine research and identified two key research needs about its applications to support marine management.

First, there is a need for studies that standardize and synthesize SfM approaches to study marine communities at seascape scale (González-Rivero et al., 2014). To date, SfM approaches have been applied at organisms-scale and used the 3D structure of the seascape as proxy of organisms growth, habitat complexity and biodiversity conditions (Ferrari et al., 2017; Bryson et al., 2017). However, this research is limited by the type of organism (i.e. stout branched coral) and the use of 3D models within which habitat complexity has been quantified, making investigations difficult about the spatial composition of organisms.

Second, there is the need for studies that uses SfM approaches to derive quantitative information on marine organisms biodiversity, biomass and on their structural habitat. To date, sampling methodologies used to characterize benthic communities are time-consuming, limited by small sampling surfaces defined *a-priori* (i.e. quadrat samples size), and often require destructive sampling (Mistri and Ceccherelli, 1994). These approaches limit our ability to understand the spatial distribution of species and habitats, and consequently their conservation status.

1.3 Aim and objectives

The aim of this study is to improve the characterization of benthic marine communities by using SfM, and to support the development of targeted marine management strategies by providing standardised methods for assessing benthic composition and organisms' morphometrics at seascape scale. This aim will be met through the following objectives:

Objective 1: to provide a framework to assess the spatial composition of benthic communities using SfM ortho-mosaics and uncover the scale-specific effects that determine sample representativeness (Chapter 2).

Objective 2: to apply and test the framework to study the effects of human and environmental pressures on coral reefs (Chapter 3).

Objective 3: to propose a new method for investigating the population structure (e.g. maximal height, abundance) and biomass of benthic tree-shaped species (i.e. gorgonians) by using scaled point cloud from SfM (Chapter 4).

Case study: The study is applied to the Ponta do Ouro Partial Marine Reserve (PPMR) (Mozambique) and to the Portofino Marine Protected Area (Italy).

1.3.1 Thesis outline

The thesis has been written in a paper format, and thus the novel contributions to science are written as individual academic journal articles (Chapter 2 to 4). Chapter 2 has been published in Remote Sensing (Palma et al., 2017) and Chapter 4 has been published in at Remote Sensing (Palma et al., 2018), Chapter 3 will be submitted to People and Nature for review, after completion of this thesis. All original work was carried out by the author of this thesis, and the contributions of the co-authors were what would normally be expected from supervisors and advisors (Table 1.1). Please note that due to the format of the thesis, repetition in data description and methodology occur (especially in Chapter 2 and 3).

Chapter 2 presents a multiple scale framework to standardize SfM data collection method, data processing and ortho-mosaic analysis. It provides a methodology to assesses the minimal sample size (i.e. extension and number of replies) to be used to monitor coral reef community at PPMR, and to calculate quantitative metrics (i.e. shape, biodiversity and fractality of coral communities) for investigating the spatial composition of benthic communities at seascape scale (Objective 1).

Chapter 3 presents a field study investigating the structural composition of benthic communities in coral reefs and their responses to scuba diving and environmental conditions by applying the SfM framework (Chapter 2). This chapter outlines the effect of scuba diving and environmental pressures to shape the structural composition of coral reefs and highlights the potential of using the SfM framework for spatial and temporal-based monitoring of coral reefs (Objective 2).

Chapter 4 presents a novel and transferable method to calculate gorgonians' metrics (i.e. max high, max width, fan surface, abundance and biomass) by processing point cloud generated through SfM. The methods bases on interpolation of organisms point cloud generated by SfM and avoids the reliance on *in-situ* collection of gorgonian organism. The chapter provides guidance and is a base for effective approaches to marine monitoring (Objective 3).

Chapter 5 discusses how the results presented in the previous chapters contributes to identifying the best approaches to use SfM and supporting the development of SfM-targeted marine monitoring strategies.

Additionally, **Appendices** are included at the end of the document, which provide more detail on the cases of study, statistical analysis, and methodologies.

Table 1.1: Authors' contributions to Chapters, including those already submitted for publication in peer-reviewed academic journals.

Authors	Chapter 2	Chapter 3	Chapter 4
M. Palma	Data collection, analysis, methodology development, discussion, layout and writing	Data collection, analysis, methodology development, discussion, layout and writing	Data collection, analysis, methodology development, discussion, layout and writing
C. Cerrano (supervisor)	Guidance on structure, advice, editing	Guidance on structure, editing	Guidance on structure, advice, editing
M. Rivas Casado (external collaborator)	Guidance on structure, advice, editing	Conceptual advice	Guidance on structure, advice, editing
U. Pantaleo (external collaborator)	Conceptual advice	-	Conceptual advice
D. Pica (external collaborator)	-	-	Conceptual advice
G. Pavoni (external collaborator)	-	-	Conceptual advice
C. Magliozzi (external collaborator)	-	Guidance on structure, advice, editing	-
G. Coro (external collaborator)	-	Conceptual advice	-

Chapter 2

High Resolution Orthomosaics of African Coral Reefs: A Tool for Wide-Scale Benthic Monitoring

[1]

Abstract

Coral reefs play a key role in coastal protection and habitat provision. They are also well known for their recreational value. Attempts to protect these ecosystems have not successfully stopped large-scale degradation. Significant efforts have been made by government and research organizations to ensure that coral reefs are monitored systematically to gain a deeper understanding of the causes, the effects and the extent of threats affecting coral reefs. However, further research is needed to fully understand the importance that sampling design has on coral reef characterization and assessment. This study examines the effect that sampling design has on the estimation of seascape metrics when coupling semi-autonomous underwater vehicles, structure-from-motion photogrammetry techniques and high resolution (0.4 cm) underwater imagery. For this purpose, we use FRAGSTATS v4 to estimate key seascape metrics that enable quantification of the area, density, edge, shape, contagion, interspersion and diversity of sessile organisms for a range of sampling scales (0.5 m × 0.5 m, 2 m × 2 m, 5 m × 5 m, 7 m × 7 m), quadrat densities (from 1–100 quadrats) and sampling strategies (nested vs. random) within a 1655 m^2 case study area in Ponta do Ouro Partial Marine Reserve (Mozambique). Results show that the benthic community is rather disaggregated

[1]Palma, M., Rivas Casado, M., Pantaleo, U. and Cerrano, C., 2017. High Resolution Orthomosaics of African Coral Reefs: A Tool for Wide-Scale Benthic Monitoring. Remote Sensing, 9(7), p.705.
Open Access
The spelling of the original published manuscript has been adjusted to fit the format of this thesis.

within a rocky matrix; the embedded patches frequently have a small size and a regular shape; and the population is highly represented by soft corals. The genus *Acropora* is the more frequent and shows bigger colonies in the group of hard corals. Each of the seascape metrics has specific requirements of the sampling scale and quadrat density for robust estimation. Overall, the majority of the metrics were accurately identified by sampling scales equal to or coarser than 5 m × 5 m and quadrat densities equal to or larger than 30. The study indicates that special attention needs to be dedicated to the design of coral reef monitoring programmes, with decisions being based on the seascape metrics and statistics being determined. The results presented here are representative of the eastern South Africa coral reefs and are expected to be transferable to coral reefs with similar characteristics. The work presented here is limited to one study site and further research is required to confirm the findings.

Keywords:seascape metrics; structure-from-motion;FRAGSTATS; photogrammetry; sampling scale; quadrat density; sampling strategy; sampling framework

2.1 Introduction

Coral reefs provide key provisioning, cultural and regulating ecosystem services (Hilmi et al., 2014; Laurans et al., 2013). Their economic value has been estimated in recent studies through the ecosystem services theory developed by Samonte et al. (2016); Seenprachawong (2016) and the Millennium Ecosystem Assessment's classification (Assessment, 2003). Within the context of provisioning and cultural services, coral reefs provide an important protein source and a basin for livelihoods for fisheries in addition to scenic beauty for recreational tourism (Pascal et al., 2016). Regarding regulating services, coral reefs provide coastal protection by dissipating the waves energy (Barbier et al., 2011) and contribute to the regulation of the coastal line erosion and sedimentation (Pascal et al., 2016). The benefits of coral reefs are therefore vast and varied. However, anthropogenic threats at the regional and global scale have considerably impacted coral reefs, with 19% of reefs considered completely lost and 60–75% of reefs threatened by 2011 (Wilkinson and Souter, 2008; Burke et al., 2012; Mora, 2015).

The increase of extreme weather events impacting the coast (Cheal et al., 2017) has also played a significant role in large-scale degradation. As a result, coral reef protection has become a priority in many governmental agendas (e.g., Hong Kong Special Administrative Region (2016)). This has resulted in the development and implementation of scientific surveys and monitoring programs aimed at evaluating the causes, effects and extent of coral threats (e.g., sedimentation, bleaching and climate change) (González-Rivero et al., 2016; Hattori and Shibuno, 2015; Hedley et al., 2016).

In general, wide-area (>1500 m^2) coral reef monitoring methods are based on remote sensing approaches that range from autonomous or semi-autonomous underwater vehicles (Beijbom et al., 2012; Friedman et al., 2012; Williams et al., 2012; Ferrari et al., 2016; González-Rivero et al., 2016) to satellite and airborne imagery (Costa et al., 2009; De'ath et al., 2012; Zhang et al., 2013; Barnes et al., 2015). For the particular case of wide-area (>1500 m^2) in situ monitoring, the key limitations are cost, access to the site and the spatio-temporal extent to be covered (Hedley et al., 2016). In situ refers hereinafter to all techniques that require human presence at the site to obtain relevant samples (e.g., photographs or biological samples), and its meaning is specific to this manuscript. In situ methodologies provide higher spatial resolution than wide-area (>1500 m^2) remote sensing methods (e.g., satellites) and are essential for the understanding of very fine ecological processes (Lecours et al., 2015; Hedley et al., 2016). New technologies and analytical solutions (e.g., autonomous and semi-autonomous underwater vehicles, boat-based systems and close range Structure-from-Motion (SfM)) have been developed and can help fulfil the need for wide-area (>1500 m^2) high resolution data provision (Williams et al., 2012; Leon et al., 2015; Ferrari et al., 2016; González-Rivero et al., 2016; Storlazzi et al., 2016). This scientific advance in coral reef monitoring relies on the integration of low cost off-the-shelf cameras and state of the art photogrammetric techniques (i.e., SfM) (Figueira et al., 2015; Carrivick et al., 2016). The resulting data products include high resolution (finer than 5 cm) Digital Elevation Models (DEMs), point clouds and two-dimensional mosaics (Westoby et al., 2012; McCarthy and Benjamin, 2014; Ferrari et al., 2016), which enable the 2D and 3D analysis of coral reef ecological processes at different scales through the use of key metrics (Casella et al., 2016; Storlazzi et al., 2016; Figueira et al., 2015; González-Rivero et al., 2014; Ferrari et al., 2016; Leon et al., 2015). Examples of the use of these techniques include Burn (Burns et al., 2016), Chirayath (Chirayath and Earle, 2016), Gutierrez (Gutiérrez-Heredia et al., 2015) and Lavy (Lavy et al., 2015). Burns (Burns et al., 2016) used 3D SfM-derived models to estimate key metrics that informed on changes to the benthic habitat along 25 m long transects and covering around 250 m^2. Chirayath (Chirayath and Earle, 2016) applied SfM techniques to map a 15 km^2 coral reef area in the Shark Bay (Australia) and to generate an accurate bathymetric map from an unmanned aerial vehicle. Gutierrez (Gutiérrez-Heredia et al., 2015) applied SfM to generate 3D models of the benthic organisms for taxonomic identification purposes, whereas Lavy (Lavy et al., 2015) applied SfM techniques to derive morphological measurement of corals.

Several authors have looked at the application of seascape ecology metrics to characterize the ecological processes of coral reefs Boström et al. (2011); Wedding et al. (2011a). However, little effort has yet been made to define the appropriate sampling strategy to accurately determine each of the metrics; the ecological rational for scale selection is usually unsupported Boström et al. (2011). Generally, scale selection is based on arbitrary choices or convention, albeit scale having an impact on seascape metric estimation (Kendall and Miller, 2008). The importance of standardized sampling protocols has already been recognized by several authors (Boström et al., 2011). For example, Lecours et al. (2015) recognizes the need for multiple scale approaches in benthic habitat mapping and states that sampling should be planned in order to describe those variables relevant for the study. Boström et al. (2011) recognizes the design of a survey as a key future research priority for seascape ecology; the wide range of spatio-temporal scales used in seascape studies inhibits the ability to directly compare studies' outcomes, identify general patterns, predict consequences across systems and design coastal reserves based on relevant information. Kendall and Miller (2008) underline the negative effects of changes in map resolution when representing ecological landscape indexes. Garrabou et al. (1998, 2002) proposed the calculation of landscape metrics at centimeter resolution in accord with the principles of landscape ecology Turner (1989).

There are multiple studies that (Costa et al., 2009; Pittman et al., 2009; Wedding et al., 2008; Purkis et al., 2008) investigate the effect that the sampling design (i.e., the combined effect of scale, quadrat density and sampling strategy) has on metric estimation. For example, Costa et al. (2009) carried out a comparative assessment for bathymetry and intensity characterization at two different spatial scales (4 m × 5000 m and 4 m × 500 m), whereas Pittman et al. (2009) quantified seven different morphometrics at multiple scales (i.e., 15 m, 25 m, 50 m, 100 m, 200 m, 300 m radius) from a 4 m bathymetry grid. Both studies showed that the spatial scale had an influence on the derived metrics. Wedding et al. (2008) used a stratified sampling strategy to estimate rugosity and compare it to rugosity estimates obtained from a DEM at four grid sizes (i.e., 4 cm, 10 cm, 15 cm and 25 cm). Results showed that the 4 m grid was the only grid size showing a significant positive association with the in situ rugosity. The author proposed the method as non-substitutive of the finer scale rugosity methods for characterizing coral reef communities, but as an effective alternative for broad scale assessments. Purkis et al. (2008) used a kernel radius of 4 m, 8 m, 20 m and 40 m with an increment of 20 m–400 m to estimate rugosity and habitat. In their study, results indicated that the habitat of up to (but likely not exceeding) 40 m away, most strongly influenced the diversity and particularly the abundance of certain fish guilds.

Here, multiple sample scales and quadrat densities applied on a high resolution (1.8 cm) wide area (>1500 m^2) dataset, where sample scale indicates the sampling quadrat size and quadrat density refers to the number of quadrats taken within a target area, will be compared. The aim of the study is to develop an SfM-based monitoring framework for the estimation of seascape metrics using semi-autonomous vehicles with embedded cameras for imagery collection for the case of the study area of Ponta do Ouro, Mozambique. This will be achieved through the following overarching objectives:

(1) to quantify the trade-offs between sample scale and robustness in seascape metric estimation;

(2) to quantify the trade-offs between sample quadrat density and robustness in seascape metrics estimation;

(3) to define a set of guidelines for seascape metric estimation based on findings from (1) and (2).

2.2 Material and Methods

2.2.1 Study Site

The study area is located in the Partial Marine Reserve of Ponta do Ouro, Mozambique (Figure 2.1a) and is part of the Isimangaliso Wetland Park, which protects the southernmost tropical coral reefs of the African continent (Schleyer, 2000). The coral reef system is dominated by non-accretive corals running parallel to the coastline at 1–2 km from the shore (Ramsay, 1994, 1996). Outcrops are present (Figure 2.1b,c) and originate from fossilization of Late Pleistocene beaches and dunes (Schleyer and Celliers, 2004) that form very flat structures (Riegl, 1993). The area is characterized by high levels of endemic species (Jordan and Samways, 2001; Celliers and Schleyer, 2008; Robertson et al., 1996) with the coral cover being dominated by soft corals that are tolerant to strong wave energy and sediment resuspension (Dai, 1990; Riegl, 1995; Schumann and Orren, 1980; Schleyer et al., 2008).

Figure 2.1: (**a**) Location of the study site in the Partial Marine Protected Area of Ponta do Ouro (Mozambique); (**b**) detailed image showing the fossils dune outcrops along the sandy littoral; (**c**) detailed image showing the submerged outcrops at the dive site.

2.2.2 Data Acquisition

Data collection was carried out by two SCUBA divers using a Sierra Dive Xtras (Xtras, Ltd., Mukilteo, WA, USA) Diver Propulsion Vehicle (DPV) equipped with a

GoPro Hero3 Silver (Woodman Labs, Inc., San Mateo, CA, USA) and an Asus Google Nexus 7 tablet (Google Inc., Mountain View, CA, USA) embedded within an Alltab dry case system (Alleco Ltd., Helsinki, Finland) (Figure 2.2). The camera was set to time-lapse mode, recording nadir images at 1 Hz frequency with a focal length equivalent to 21 mm. Inertial navigation data obtained from the gyroscope and the accelerometer were logged via an Ubica Underwater Position System (UUPS) (Ferraris et al., 2017) be-spoke application. The logged data were then used to derived camera pitch, yaw and roll.

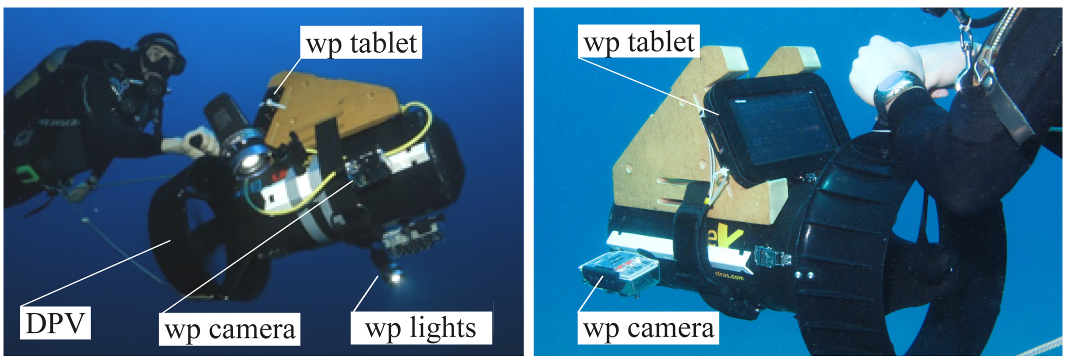

Figure 2.2: (**a**) A general photograph of the Diver Propulsion Vehicle (DPV) equipped with the Hero3 Silver camera, the waterproof tablet and the lights; (**b**) detailed image of the waterproof camera and tablet. "wp" stands for waterproof.

The sampling path was defined by two 50 m ancillary tapes distributed following homogeneous seascape characteristics identified in a pre-deployment survey (Figure 2.1c). The exact path followed by the diver was recorded via a towed buoy with an integrated Etrex10 GPS (Garmin Ltd., Lenexa, KS, USA). The GPS coordinates were recorded in Wide Area Augmentation System (WAAS) mode at 1 Hz frequency and projected into the Universal Transverse Mercator (UTM) fuse 36 Southern Hemisphere coordinate system, defined by the World Geodetic System (WGS84), within a Geographical Information System (GIS) environment (ArcGIS 10.1, Redlands, CA, USA). The diver maintained an average swimming speed of 0.75 m s^{-1} and an average distance to the sea bottom of 2.7 m, with the range being between 1.5 m and 3 m and with each frame covering 3 m^2 (Figure 2.3a).

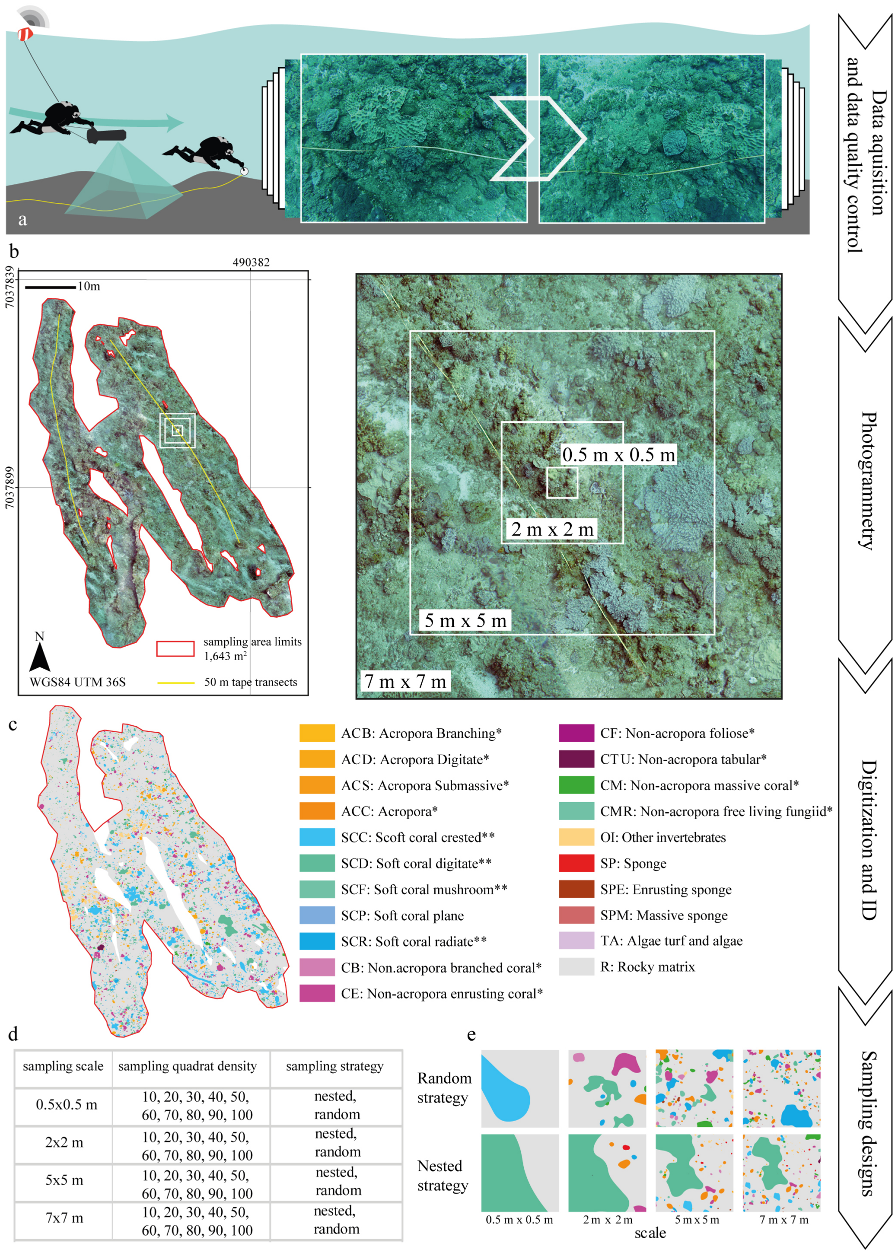

sampling scale	sampling quadrat density	sampling strategy
0.5x0.5 m	10, 20, 30, 40, 50, 60, 70, 80, 90, 100	nested, random
2x2 m	10, 20, 30, 40, 50, 60, 70, 80, 90, 100	nested, random
5x5 m	10, 20, 30, 40, 50, 60, 70, 80, 90, 100	nested, random
7x7 m	10, 20, 30, 40, 50, 60, 70, 80, 90, 100	nested, random

Figure 2.3: Schematic workflow overview for the field data collection and data analysis implemented: (**a**) transect deployment and image collection (left) and detailed example of the collected imagery (right); (**b**) processed orthoimage of the transects with the example of nested quadrats (left) and the detail of the nested sampling scales applied (right); (**c**) digitized output showing the abundance of different classes of benthic organisms; (**d**) summary of sampling scale, quadrat density and strategy applied; (**e**) graphical example of the digitized sessile organisms within different sampling scales. * and ** refer to the classification proposed byEdinger and Risk (2000) and the classes used by Schleyer and Celliers (2004), respectively. ID stands for Identification Code.

Consecutive frames were taken with an approximate overlap of 70% along and 45% across the path. The sampling was performed in the central area of the reef covering a total of 1655 m^2 at an average depth of −22 m AMSL. All datasets were acquired on the 8 May 2015 during one single dive with a SCUBA dive. Data were collected during steady and calm sea-weather condition with good visibility (estimated 20 m) and avoiding the lowest and the highest tides. All the underwater imagery was collected within 15 min. A total of four hours was required to set up the equipment on site (e.g., mount the camera, deploy the tape underwater, set up the parameters, implement the field briefing). An additional hour was required after the dive to check that all the imagery had been captured correctly and the UUPS had logged all of the required information. An extra 20 min were required to pack the equipment.

2.2.3 Photogrammetric Process and Digitization

A total of 1192 images collected were visually inspected, and only those with the right characteristics (i.e., 3200 × 2400 pixel high image quality and consecutive spatial coverage) were considered for further analysis (Figure 2.3a). A total of 8 h were required to visually inspect all the frames acquired. From the initial set of images, 1182 were included in the photogrammetry process. All the frames were captured at 1 cm resolution with a final orthoimage resolution of 1.8 cm. The metadata of each JPEG were stored in Exchangeable Image File format (EXIF) along with other camera parameters (e.g., camera model and optical lens characteristics) and directly loaded into Photoscan (Agisoft LLC., St. Petersburg, Russia). The exact position of each frame centroid was estimated by coupling the camera recording time with the GPS watch based on Roelfsema et al. Roelfsema et al. (2013). pixGPS (BR Software, Asker, Norway) was used for that purpose. The coordinates for each of the frames were used to georeference (scale, translate and rotate) the imagery into the coordinate system defined by the World Geodetic System (WGS84) and to minimize geometric distortions. Image coregistration errors were automatically estimated by Photoscan as the difference between the positions measured through GPS and the coordinates derived from the imagery. The overall process to obtain the orthoimage took 12 h of processing time based on the performance of an Asus laptop (Beitou District, Taipei, Taiwan) with an Intel Core i7-3630QM 2.40-GHz processor (Intel Corporation, Santa Clara, CA, USA), 16 Gb RAM and graphic card NVIDIA Geoforce GTX 670M (NVIDIA Corporation, Santa Clara, CA, USA).

Mega-epibenthic sessile organisms (i.e., seabed living organisms with a body diameter of 5 cm approximately) were manually identified and digitized to the finest possible taxonomic level and then clustered according with common morphological characteristics following the approach by Edinger and Risk (2000) and the descriptions published by Schleyer and Celliers (2004). The morphological classification also accounted for non-coral organisms, such as sponges and other sessile invertebrates (i.e., tunicates and ascidians). The orthoimage was digitized manually and classified within ArcGIS (Figures 2.3b,c and 2.4a,b). The background rocky substrate, within which patches were embedded as "islands", was considered as the seascape matrix (i.e., rocky matrix) following the island biogeography theory proposed by MacArthur and Wilson (2015). The digitization process required 21 days (i.e., 147 h at 7 h per day). A total of 7547 individual organisms were digitized from the orthoimage.

2.2.4 Seascape Metric Estimation

Seascape metrics were estimated from the orthoimage for a set of different sampling designs described by all the possible combinations of a range of sampling scales, quadrat densities and sampling strategies. Within the scope of this study, the sampling scale refers to the size of the sampling quadrats and ranged from 0.5 m × 0.5 m–7 m × 7 m (Figure 2.3d); the quadrat density is the number of quadrats taken within the target area and ranged from 10–100 in consecutive increments of 10 quadrats; and the sampling strategy refers to the spatial distribution of the samples (i.e., nested or random) (Figure 2.3e). The sampling designs were overlaid onto the orthoimage within ArcGIS.

Nested sampling approaches require the overlap of quadrat centroids of consecutively increasing scales. Each scale appears only once in each set of overlapped centroids, with each set being randomly distributed across the reef. The range of values considered for the sampling scale, quadrat density and sampling strategy was selected based on the size of the sessile organisms, their spatial distribution, the magnitude of the effects to be measured and standard sampling protocols for coral reefs (Weinberg, 1981; Bianchi et al., 2004; Guinda et al., 2014; Ferrari et al., 2016). A total of three replications were obtained for each combination of sample scale, quadrat density and sampling strategy to account for spatial variability. All quadrats were inspected to ensure that at least 60% of their surface fell within the extent of the coral reef area. Although the centroid of the quadrat was always forced to be within the surveyed area, this did not guarantee that all the quadrat fell within the boundary. Those quadrats with more than 40% of their surface falling outside the coral reef boundaries were excluded from the analysis. The spatial distribution of sampling quadrats was automated in ArcGIS using a range of tools (i.e., create random points, buffer, envelope feature to polygon, iterate feature classes, clip, invert, merge and polygon to raster) within the ArcMAP model builder.

Seascape metrics were derived using FRAGSTATS v4 (Amherst, MA, USA) (Mcgarigal et al., 2002), a software developed to compute a wide variety of landscape metrics for categorical map patterns that has successfully been applied for seascape ecology (Garrabou et al., 1998; Teixido et al., 2002; Kendall and Miller, 2008; Wedding et al., 2011a). Only metrics that could be automatically derived from FRAGSTATS were considered within this study because of their potential to enhance the autonomy of the framework. From the more traditional metrics used for coral reef characterization, only cover was calculated, as it is a key metric used to assess the benthic community composition.

FRAGSTATS estimates key landscape metrics, hereinafter referred to as seascape metrics, based on the disposition of the patches within the landscape (i.e., seascape). Here, a patch is each of the digitized individual polygons (Figure 2.4). A set of metrics defining area-density-edge, shape, contagion and interspersion, as well as diversity was selected based on their relevance to seascape ecology composition (Table 2.1).

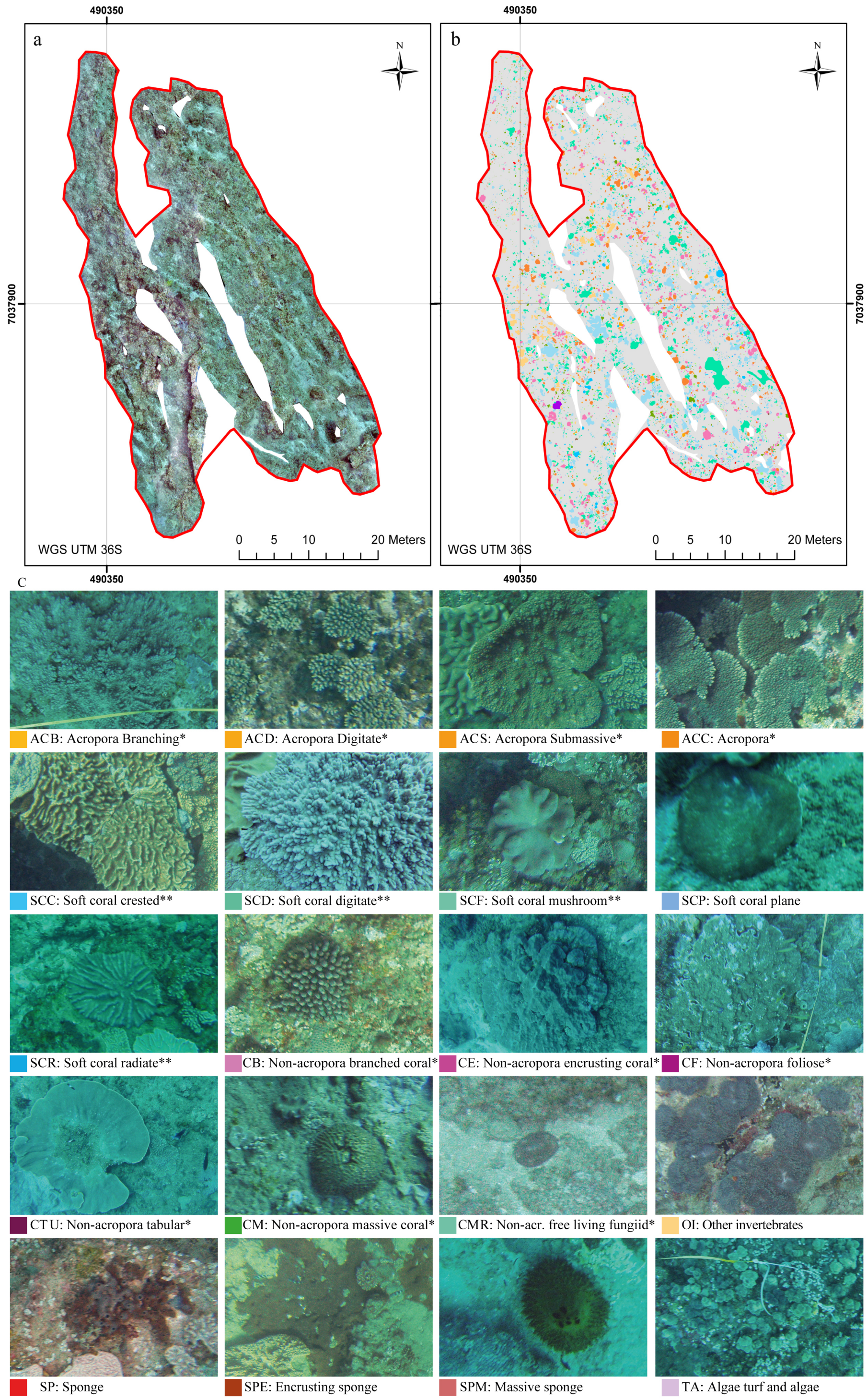

Figure 2.4: (**a**) The processed orthoimage; (**b**) the map of the digitized benthic organisms; (**c**) the configuration of the digitized sessile organism within the case study area of Ponta do Ouro Partial Marine Reserve (Mozambique). * and ** refer to the classification proposed by Edinger and Risk (2000) and the classes used by Schleyer and Celliers (2004), respectively.

Area-density-edge metrics relate to the number and size of sessile organisms and the amount of edges created by them. Here, the edge is the border between adjacent patches. This group of metrics includes the Landscape Shape Index (LSI) and the Largest Patch Index (LPI) (Mcgarigal et al., 2002). LSI informs about the morphological aggregation of the patches within a standardized seascape square. The value of LSI increases without limit from 1 upwards as the seascape becomes disaggregated, where 1 represents minimum disaggregation. LPI informs about the clumpiness of the seascape as the percentage value within a standardized seascape square. It is a measure of patch dominance; LPI values of 100% indicate that the seascape unit is dominated by a single patch. Both LSI and LPI provide information on the composition of the sessile organism communities in size per class and on the structure of the reef; seascapes that are highly subdivided into small patches are characteristics of low colonized substrates where colonies have difficulties settling and cannot reach typical dimensions. This can be caused by multiple factors, such as sediment resuspension and deposition or high wave energy (Schleyer et al., 2008).

Shape metrics (i.e., Perimeter Area Ratio (PARA)(Mcgarigal et al., 2002; McGarigal and Marks, 1995)) are directly estimated from the shape of the organisms. In particular, PARA estimates the ratio between the perimeter and the area of all the patches within the seascape unit and provides information on the shape complexity of the patches in the seascape; an increase in the size of the patch results in a decrease in the value of PARA. PARA is always larger than 0 and does not have an upper limit. The PARA value could be interpreted as a good indicator of the growth conditions of corals; corals show constant radial allometric growth (Dornelas et al., 2017), but this can be affected by external factors, such as intra-specific and inter-specific competition and hydrodynamic conditions. Under affected allometric growth conditions, larger PARA values are to be expected.

Contagion and dispersion metrics (i.e., Aggregation Index (AI) and Division index (DIVISION)) (Mcgarigal et al., 2002) look at the seascape texture by examining the aggregation and intermix of the class of organisms. AI (He et al., 2000; Mcgarigal et al., 2002) quantifies the adjacencies per patch type within the seascape and informs on the homogeneity of the composition of the benthic communities. It ranges from 0%

(maximum patch disaggregation) to 100% (maximum patch aggregation). High values of AI indicate that the classes of patches are more clustered within the landscape. This could inform about the reproductive biology of the species considered and the population dynamics; species with short larval dispersion tend to create clusters of individuals near the organism. These species are more sensitive to local extinctions (Cowen and Sponaugle, 2009). Instead, DIVISION measures the heterogeneity of the seascape and estimates the variability in patch types within the seascape. DIVISION ranges from 0–1, where a 0 value indicates maximum aggregation, and values close to 1 indicate maximum disaggregation. These indexes provide information on the composition of the coral and the planar morphology of the colonies within the seascape; heterogeneous seascapes are composed by a varied benthic community or placed at the edge of the reef, where just a few individuals per specie are settled.

Diversity metrics focus on the number of organisms and their distribution within the seascape. They are an indication of the resilience of the coral reef and its ability to withstand significant disturbances (Nyström, 2006). Within this group, five key metrics have been estimated: Patch Richness (PR), Shannon's Diversity Index (SHDI), Simpson's Diversity Index (SIDI), Shannon's Evenness Index (SHEI) and Simpson's Evenness Index (SIEI) (Mcgarigal et al., 2002). PR informs about the number of patches present within the seascape. SHDI (Spellerberg and Fedor, 2003) informs about the number of different patch types within the seascape and how evenly these types are distributed. SHDI can present any positive value from 0 upwards. Larger SHDI values represent greater evenness amongst patch types within the seascape. SIDI (Somerfield et al., 2008) informs about the probability that two entities (i.e., pixels) taken at random from the same seascape belong to different patch types and ranges between 0 and 1. Larger SIDI values indicate a greater probability that two pixels are from different patch types. Both SHEI and SIEI estimate the proportion of the maximum Shannon's or Simpson's diversity index, respectively. SHEI and SIEI range from 0–1, where 1 indicates that the area is distributed evenly among patch types.

Table 2.1: Seascape metrics estimated for the case study area of Ponta do Ouro Marine Reserve (Mozambique). The seascape metric descriptions are based on those for landscape analysis obtained from FRAGSTATS v4 (Mcgarigal et al., 2002). All metrics are dimensionless except for the Largest Patch Index (LPI) (%), AI (%) and DIVISION (ratio). Here, patch refers to each of the digitized individual polygons falling within a given morphological class.

Metrics	Index	Description
Area Density Edge	Landscape Shape Index (LSI)	Normalized ratio of edge (i.e., patch perimeters) to area (i.e., seascape defined by the sampling scale) in which the total length of edge is compared to a seascape with a standard shape (square) of the same size and without any internal edge. LSI = 1 when the seascape consists of a single square patch; LSI increases without limit as the morphology becomes more disaggregated. LSI provides a simple measure of morphological aggregation or clumpiness.
	Largest Patch Index (LPI)	Percentage of the seascape comprised of the single largest patch. LPI approaches 0 when the largest patch is increasingly small. LPI = 100 when the entire seascape consists of a single patch; that is, when the largest patch comprises 100% of the seascape.
Shape	Perimeter Area Ratio (PARA)	Simple ratio of patch perimeter to area in which patch shape is confounded with patch size. The ratio is not standardized to a simple Euclidean shape (e.g., square); an increase in patch size will cause a decrease in the perimeter-area ratio.
Contagion Interspersion	Aggregation Index (AI)	The ratio of the observed number of like adjacencies to the maximum possible number of like adjacencies given the proportion of the seascape comprised of each patch type (%). The maximum number of like adjacencies is achieved when the morphological class is clumped into a single compact patch, which does not have to be a square.
	Division Index (DIVISION)	The probability that two randomly chosen pixels in the seascape are not situated in the same patch.Maximum values are achieved when the seascape is maximally subdivided; that is, when every pixel is a separate patch.
Diversity	Patch Richness (PR)	Number of patch types present in the seascape.
	Shannon's Diversity Index (SHDI)	Represent the amount of "information" per morphological class; larger values indicate a greater number of patch types and /or greater evenness among types.
	Simpson's Diversity Index (SIDI)	The probability that any two pixels selected at random would correspond to different patch types; the larger the values the greater the likelihood than any two randomly drawn pixels would be different patch types.
	Shannon's Evenness Index (SHEI)	Proportion of maximum Shannon's Diversity Index based on the distribution of area among patch types and typically given as the observed level diversity divided by the maximum possible diversity given the patch richness. SHEI = 1 when the area is distributed evenly among patch types.
	Simpson's Evenness Index (SIEI)	Proportion of maximum Simpson's Diversity Index based on the distribution of area among patch types and typically given as the observed level diversity divided by the maximum possible diversity given the patch richness. SIEI = 1 when the area is distributed evenly among patch types.

2.2.5 Data Analysis

Composition and abundance for the full extent of the mapped coral reef area were estimated based on the digitized sessile organism classes (Figures 2.3c and 2.4). The minimum and maximum cover of individual sessile organisms (total surface in m^2) identified within each quadrat for each morphological class (Schleyer and Celliers, 2004; Edinger and Risk, 2000) were estimated. The average dimension, as well as the total count of individuals within each morphological class were also reported. Robustness in metric estimation was assessed for each sampling design based on the difference between the metric value estimated for a specific sampling design and (i) that obtained for the whole surveyed area or (ii) that obtained for the most comprehensive sampling design considered (i.e., 7 m × 7 m and 100 quadrats). The effect on both measures of central tendency (e.g., mean, median) and dispersion (e.g., range, standard deviation) was assessed. Descriptive statistics and box-plots were used for that purpose. General trend patterns were derived from these observations and used to compile a set of general guidelines for coral reef sampling.

2.3 Results

The line transect defined by the metric tape accounted for 650 m. The coregistration error of the generated orthoimage was 4.08 m and 6.8 m for the x and y axis, respectively. Within the whole mapped area (1655 m^2), the benthic organisms covered 335.54 m^2, which equates to a total cover of 20.27%. The coral reef was dominated by soft (Alcyonacea, 62.1% of the total cover) and hard corals (Scleractinia, 31.00% of the total cover) (Figure 2.5). Within the soft corals, the dominant morphological classes were (i) Soft Crested Coral (SCC) (soft corals that are rigid with mounted parallel lobes and low in profile) and (ii) Soft Corals with Digitate lobules (SCD). These groups presented the largest individual organism cover values (7 m^2) and were represented by the genera *Lobophytum*, *Sinularia* and *Sarcophyton* (Table 2.2). Hard corals were mainly represented by the genus *Acropora* (44.32% of the total hard colony community). The more frequent class in the group was *Acropora* with digitated and stubby branches

(ACD), presenting also the largest surface dimensions (Table 2.2).

Non-*Acropora* Massive or Multilobate Corals (CM) include *Platygyra* spp., *Montastrea* spp., *Galaxea* spp., *Favites* spp., *Favia* spp. and *Turbinaria* sp.. The average size for this morphological class was 0.019 m^2. In addition to the above groups, 141 colonies of free-living fungiid corals were identified. These showed an average dimension of 0.006129 m^2 (Table 2.2) and also included 11 encrusting and dome-shaped sponges. The Other Invertebrates (OI) presented the largest variance in surface dimension with the tunicate *Atriolum robustum*, accounting for 0.0008 m^2, and the actinias *Stichodactyla* spp., accounting for 1.04 m^2. The background rocky substrate accounted for 1150.55 m^2 of the total area (69.52%). The 10.27% (168.84 m^2) of the overall coral reef area sampled, where individual organisms could not be identified, was not digitized.

The exclusion of quadrats with more than 40% of the area falling outside the coral reef boundary or presenting non-textured classes did not influence the overall analysis; the number of samples available was large enough for the robust estimation of the descriptive statistics, boxplots and associated metrics of species abundance and composition (Table 2.3).

The effect of scale, quadrant density and sampling strategy on cover estimation is summarized in Figure 2.5. Sampling scales coarser than 5 m × 5 m provide similar cover estimates to those obtained for the overall surveyed area, with the finest scale (0.5 m × 0.5 m) failing to accurately represent cover estimates. This pattern is more noticeable for random sampling strategies than for nested strategies. Regarding the quadrat density applied, no particular patterns can be observed as the number of quadrats used in the survey is increased. However, sampling designs where the combined area surveyed by the quadrats contains in excess of 100 m^2 of benthic organisms closely resembles the cover distributions observed within the whole surveyed area.

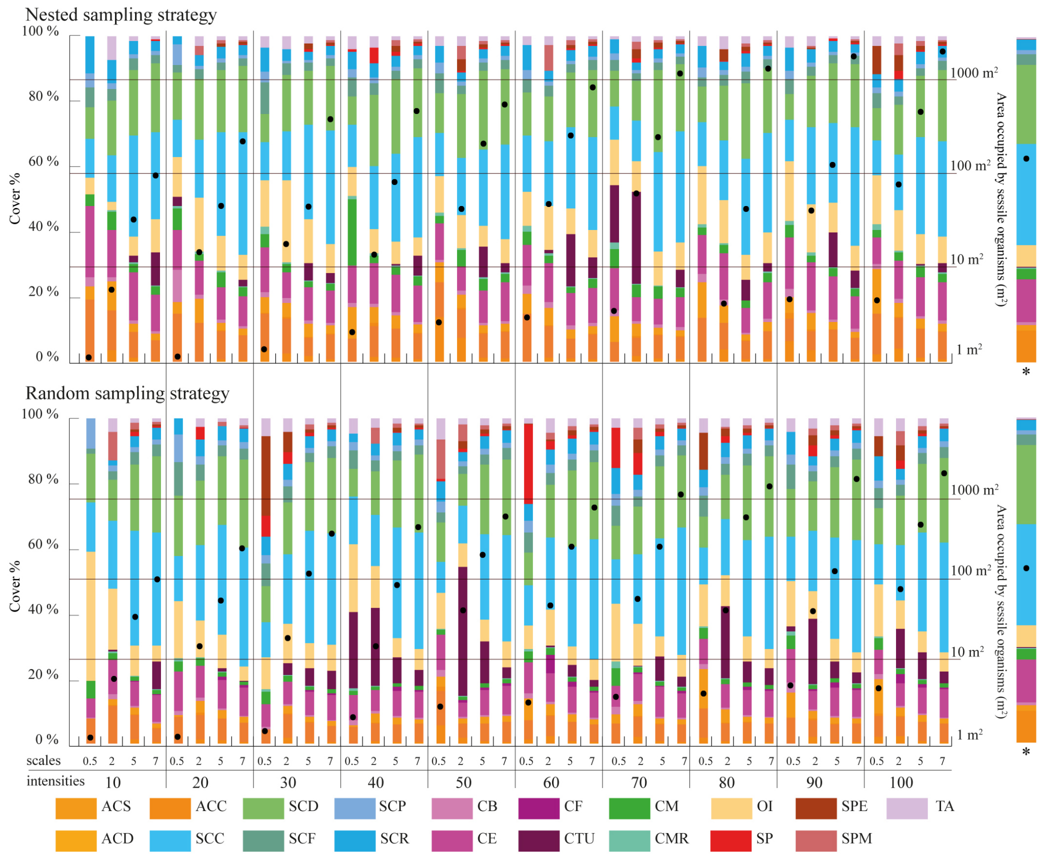

Figure 2.5: Percentage of cover per morphological class for each sampling design considered in the study. The proportion is estimated as the ratio between the area occupied by each morphological class over the total area covered by the sessile organisms within each sampling design. The values presented refer to the average cover of the three replicates taken within each sampling design. The "*" indicates the total area covered by the sessile organisms in each sampling design estimated as the average of the three replicates taken. The last column shows the cover per morphological class for the totality of the coral reef surveyed.

For area-density-edge metrics, the overall area surveyed scores an LSI value of 2.91 (Table 2.4). The LPI value for the sampled coral reef is 0.47% (Table 2.4). The LSI values for independent quadrats range between one and eight, showing that there is spatial heterogeneity in aggregation across the coral reef. The dispersion of LPI values obtained within some of the sampling design tested is large, with LPI values ranging from 0%–100% in some cases. For both LSI and LPI, the sampling quadrat density has a larger impact on the estimation of the measures of dispersion (e.g., range, standard deviation) than on the estimation of measures of central tendency (e.g., mean, median). For LSI, quadrat densities above 70 are required to characterize the measures of dispersion for nested strategies to the same level as the most comprehensive quadrat density applied (i.e., 100), whereas quadrat densities above 40 are required for random strategies. For LPI, quadrat densities above 40 and 30 are required to characterize the measures of dispersion for nested and random strategies, respectively. In contrast, the sampling scale has a larger impact on the measures of central tendency than on the measures of dispersion. The finest scale (0.5 m × 0.5 m) presents the largest deviations from the seascape metrics obtained for the overall coral reef area. For LPI, sampling scales of 5 m × 5 m and 7 m × 7 m provided good approximations to the metrics obtained for the totality of the coral reef area for both nested and random strategies (Figures 2.6 and 2.7). However, for LSI, coarse scales (7 m × 7 m) were required for both nested and random strategies.

Table 2.2: Description of the key morphological classes of benthic organisms and their count, maximum (max), minimum (min) and average dimensions (m^2), identified within the coral reef studied in the Partial Marine Reserve of Ponta do Ouro (Mozambique).

Acronym	Description	Count	Average Dimension	Max Dimension	Min Dimension
ACB	*Acropora*, branching (e.g., *A. austera*)	15	0.384 ± 0.016	0.716	0.225
ACD	*Acropora*, digitate, stubby (e.g., *A. humilis*)	465	0.069 ± 0.010	0.821	0.044
ACS	*Acropora*, columns and blades, very stout (e.g., *A. palifera* and *A. cuneata*)	109	0.054 ± 0.068	0.467	0.001
ACC	*Acropora*, stout branches, low bushy shape	20	0.045 ± 0.041	0.148	0.005
CM	Non-*Acropora* massive or multilobate corals (e.g., *Platygyra* spp. and *Galaxea* spp.)	559	0.019 ± 0.038	0.544	0.0005
CE	Low relief, often small colonies (e.g. *Porites* spp.)	533	0.083 ± 0.112	1.281	0.002
CTU	Tabular coral (e.g., *Turbinaria* sp.)	4	0.300 ± 0.573	1.160	0.009
CMR	Free-living fungiid corals	141	0.006 ± 0.004	0.034	0.015
CB	Branching non-*Acropora* corals (e.g., *Pocillopora* spp.)	275	0.011 ± 0.012	0.089	0.065
CF	Foliose, either horizontal or vertical, non-*Acropora*, (e.g., *Montipora* spp., *Echinopora* spp.)	2	0.065 ± 0.069	0.1138	0.0164
OI	Other invertebrates inclusive of gasterops, tunicates, echinoderms and other hexacorals	339	0.067 ± 0.134	1.044	0.00008
SCF	Erect in profile, but soft and pliable with an expanded disk and stalk (e.g., *Sarcophyton* spp.)	461	0.023 ± 0.021	0.137	0.046
SCD	Soft and pliable colonies (e.g., *Sinularia* spp.)	1916	0.042 ± 0.205	7.6134	0.045
SCC	Low in profile and rigid with mounded radial (e.g., *L. latilobatum*)	1721	0.061 ± 0.197	4.376	0.645
SCR	Low in profile and rigid with erect radial or parallel lobes (e.g., *L. crassum*).	342	0.032 ± 0.068	0.974	0.002
SCP	Low in profile and plane on the surface (e.g., *L. depressum*)	466	0.009 ± 0.007	0.0562	0.0007
SP	General sponges	6	0.041 ± 0.031	0.092	0.001
SPM	Massive or dome-like sponges	3	0.075 ± 0.038	0.119	0.046
SPE	Encrusting sponges	2	0.070 ± 0.022	0.086	0.055
TA	Algae and algal turf	168	0.010 ± 0.018	0.144	0.0004

The PARA shape metric (Figures 2.6 and 2.7) reaches values of 4.5×10^5 (Table 2.4) for the whole area surveyed. The multiple sampling scales considered report different results in terms of measures of dispersion. Scales finer than 2 m × 2 m report dispersion values considerably larger than coarser scales and are characterized by PARA metric overestimation. The pattern is more prominent for nested strategies, where PARA values of individual quadrats reach magnitudes of 3×10^6, whereas for random strategies, the maximum values do not exceed magnitudes of 1.6×10^6. The quadrat density also influences the estimation of the measures of dispersion, with the range of PARA decreasing as the number of quadrats increases for both nested and random sampling strategies. Quadrat densities of 40 and 30 provide similar results to those obtained for the maximum quadrat densities applied (i.e., 100) for nested and random strategies, respectively.

Table 2.3: Sample size per combination of sampling scale, quadrat density and strategy considered, after exclusion of non-valid samples (i.e., quadrats with more than 40% of the area falling outside the coral reef boundary or presenting non-textured morphological class).

Scale	**0.5 m × 0.5 m**		**2 m × 2 m**		**5 m × 5 m**		**7 m × 7 m**		**Expected**
Density	**Random**	**Nested**	**Random**	**Nested**	**Random**	**Nested**	**Random**	**Nested**	
10	24	25	29	28	28	28	27	27	30
20	50	49	54	56	53	53	44	44	60
30	73	70	78	83	80	80	73	73	90
40	91	98	113	116	108	108	109	109	120
50	127	117	142	142	136	136	130	130	150
60	145	146	178	176	167	167	161	162	180
70	164	161	201	204	202	202	190	190	210
80	191	187	237	234	225	225	223	223	240
90	213	216	260	265	244	245	250	250	270
100	240	239	287	290	291	290	270	282	300

Table 2.4: Seascape metric values obtained for the total coral reef area surveyed. The metrics reported include: Landscape Shape Index (LSI), Large Patch Index (LPI), Perimeter Area Ratio (PARA), Aggregation Index (AI), Division Index (DIVISION), Patch Richness (PR), Shannon's Diversity Index (SHDI), Simpson's Diversity Index (SIDI), Shannon's Evenness Index (SHEI) and Simpson's Evenness Index (SIEI).

Acronym	**Value**	**Acronym**	**Value**
LSI	2.91	LPI	0.47%
PARA	4.52 e^5	AI	95.61%
DIVISION	0.99%	PR	23
SHDI	1.94	SIDI	0.78
SHEI	0.62	SIEI	0.83

The contagion and dispersion metric AI scores 95.6% (Table 2.4) for the case study area. The value of AI for independent quadrats oscillates between 70% and 100% approximately. For nested strategies, scales equal to or coarser than 5 m × 5 m underestimate the value of AI, whereas scales equal to or finer than 2 m × 2 m overestimate the value of the index. A similar pattern is observed for random strategies where scales equal to or coarser than 2 m × 2 m underestimate the metric value, and scales of 0.5 m × 0.5 m overestimate it. For both nested and random strategies, the finest scale considered (0.5 m × 0.5 m) results in large dispersion measurements, whereas coarser scales (i.e., coarser than 2 m × 2 m and 5 m × 5 m for nested and random, respectively) present similar dispersion estimates amongst each other. Quadrat density also influences the estimation of the measures of dispersion, with quadrat densities above 20 and 30 providing similar dispersion estimates to more dense designs for nested and random strategies, respectively.

In the particular case of DIVISION, the value for the overall area is 0.99% (Table 2.4). The DIVISION values of independent quadrats range from its plausible minimum to its maximum, this indicating that the index is highly dependent on the spatial heterogeneity of the site. The effect of sampling design for both nested and random strategies follows a similar pattern; measures of central tendency become more accurate as the quadrat scale increases, with scales finer than 2 m × 2 m reporting slight departures from the metric value obtained for the overall coral reef area. Sampling quadrat densities equal to or larger than 40 provide estimations of the dispersion measures close to those obtained for the most comprehensive density considered (i.e., 100).

The diversity metrics PR (23), SHDI (1.94), SIDI (0.78), SHEI (0.62) and SIEI (0.83) obtained for the overall area are also affected by changes in sampling design (Table 2.4, Figures 2.8 and 2.9). For PR, none of the sampling designs considered in this study capture the total number of different patch types present within the seascape for both nested and random sampling strategies. The mean PR obtained for independent sampling designs does not exceed a value of 14 in any instance, with PR values obtained for individual quadrats ranging from 0–18. Sampling scale has an important effect on the estimation of measures of central tendency and dispersion for PR; the larger the scale, the larger the number of different patch types identified. The fine scales tested (equal or finer than 2 m × 2 m) do not provide representative values of PR. The effect of quadrat density is not so apparent, with quadrat densities of 10 providing similar results in terms of measures of dispersion and central tendency to those obtained with 100 quadrats.

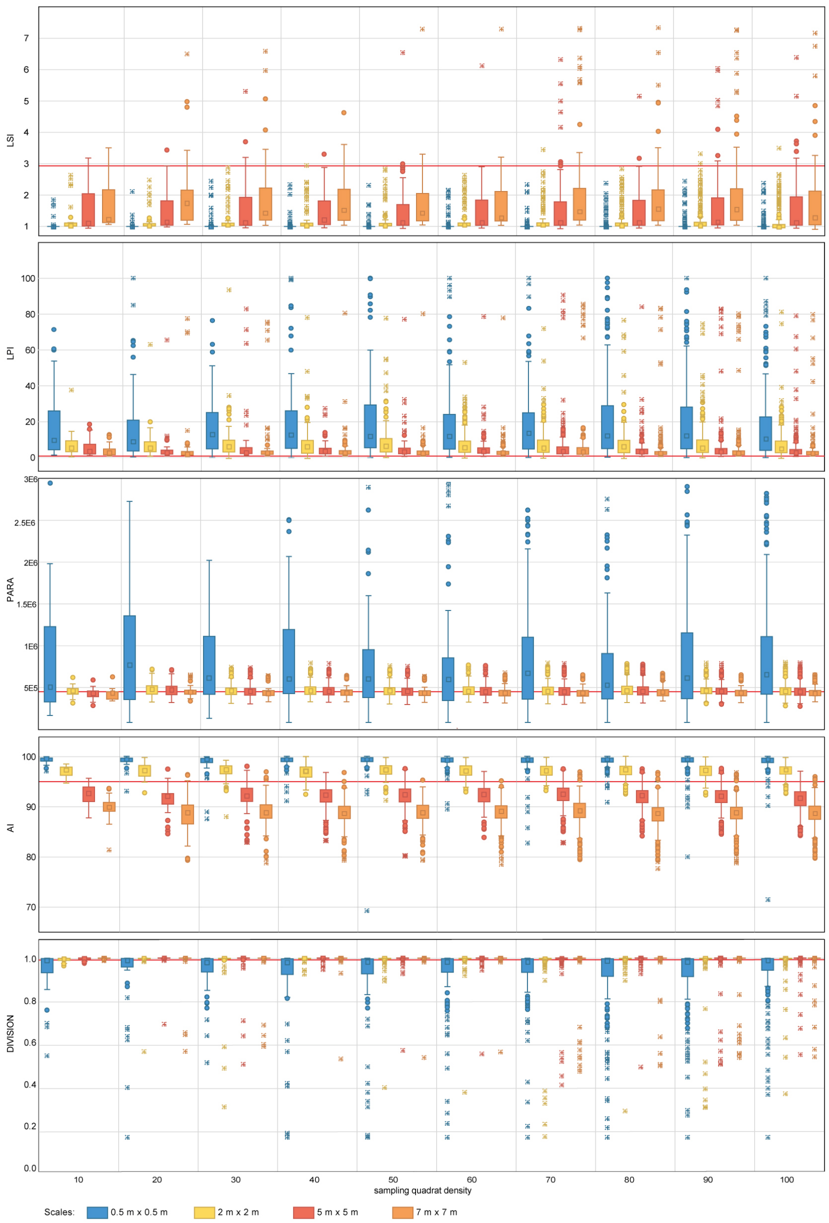

Figure 2.6: Area-density-edge, shape, contagion and interspersion metric values obtained for the nested sampling strategy for the range of scales and quadrat densities considered. The red horizontal line indicates the metric value obtained on the total area mapped. LSI, LPI, PARA, AI and DIVISION stand for Landscape Shape Index, Largest Patch Index, Perimeter Area Ration Mean, Aggregation Index and Division Index, respectively. The boxplots show the first, second (median), third and fourth quartiles. Circles and crosses indicate outliers and extreme values, respectively.

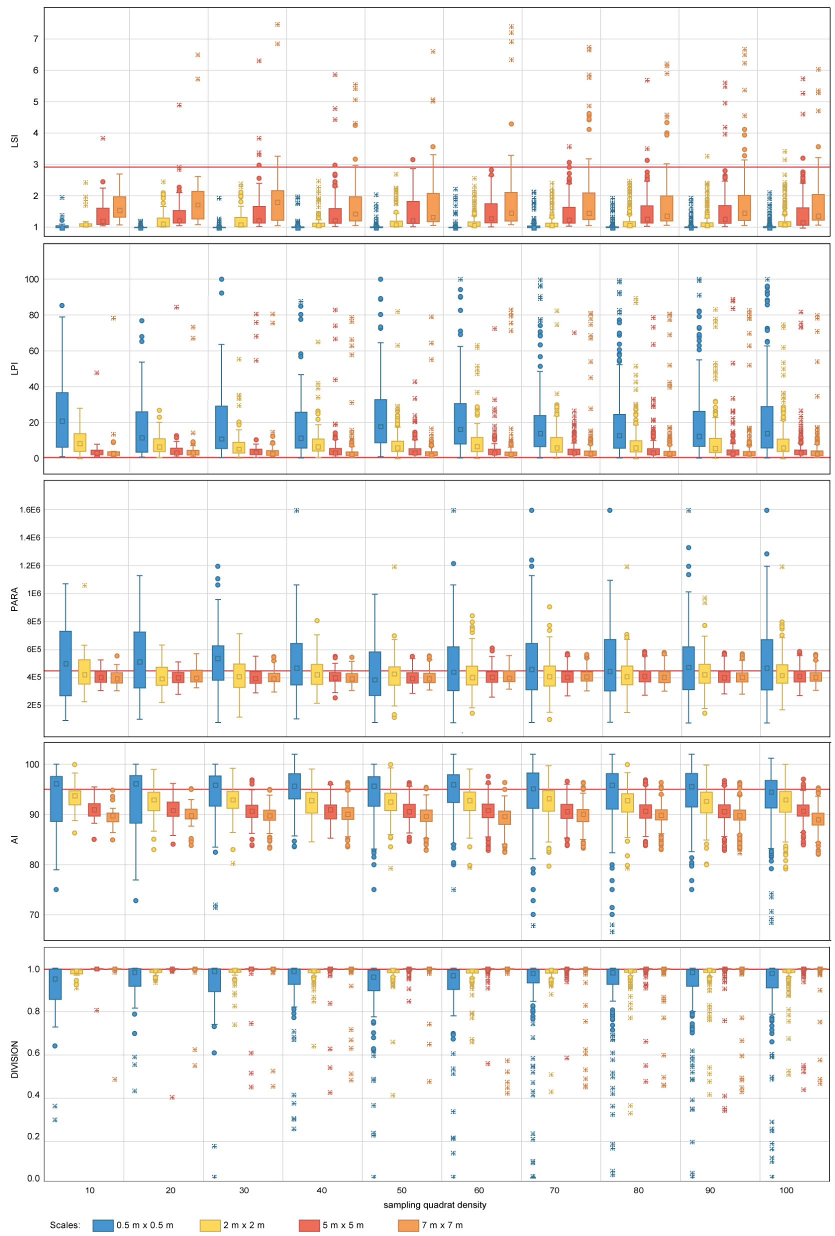

Figure 2.7: Area-density-edge, shape, contagion and interspersion metric values obtained for the random sampling strategy for the range of scales and quadrat densities considered. The red horizontal line indicates the metric value obtained on the total area mapped. LSI, LPI, PARA, AI and DIVISION stand for Landscape Shape Index, Largest Patch Index, Perimeter Area Ration Mean, Aggregation Index and Division Index, respectively. The boxplots show the first, second (median), third and fourth quartiles. Circles and crosses indicate outliers and extreme values, respectively.

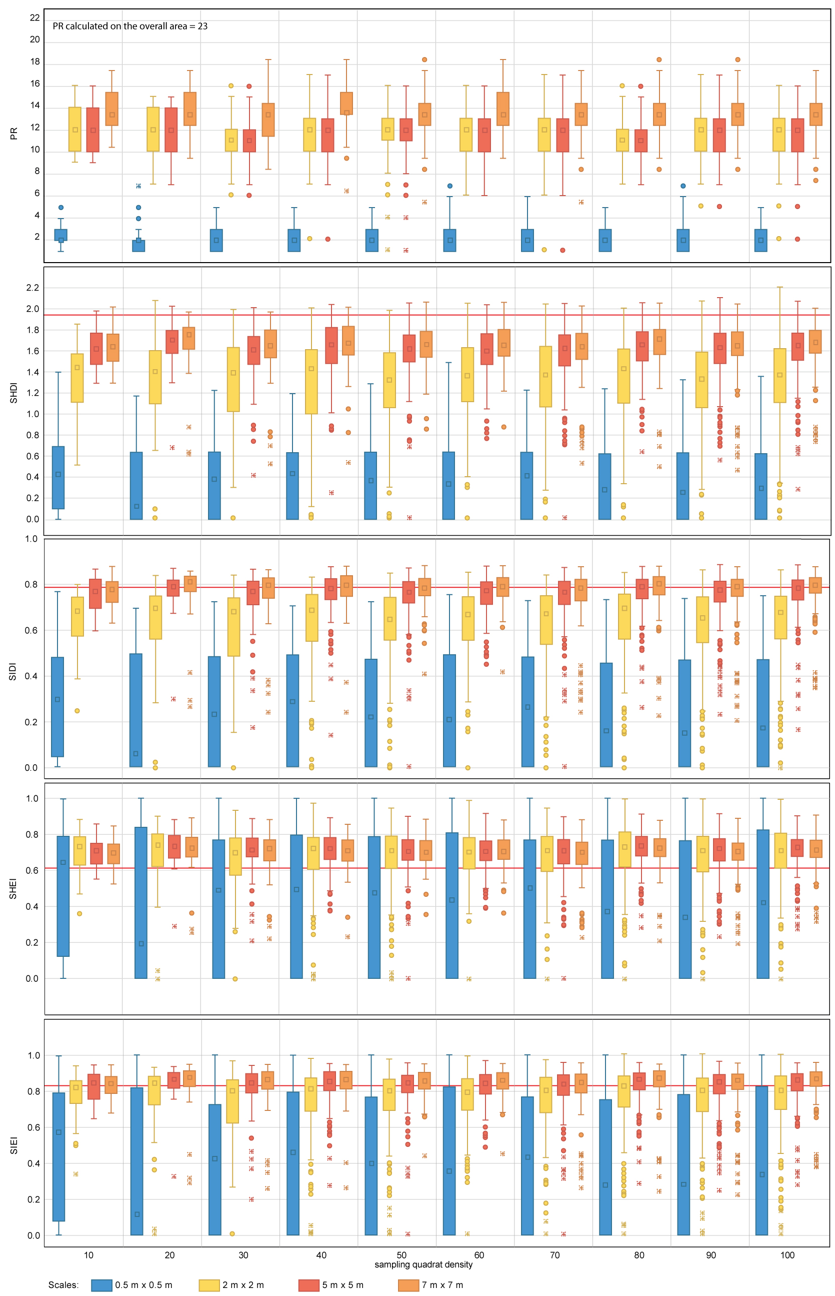

Figure 2.8: Diversity metric values obtained for the nested sampling strategy for the range of scales and quadrat densities considered. The red horizontal line indicates the metric value obtained for the total area mapped. PR, SHDI, SIDI, SHEI and SIEI stand for Patch Richness, Shannon's Diversity Index, Simpson's Diversity index, Shannon's Evenness Index and Simpson's Evenness Index, respectively. The boxplots show the first, second (median), third and fourth quartiles. Circles and crosses indicate outliers and extreme values, respectively.

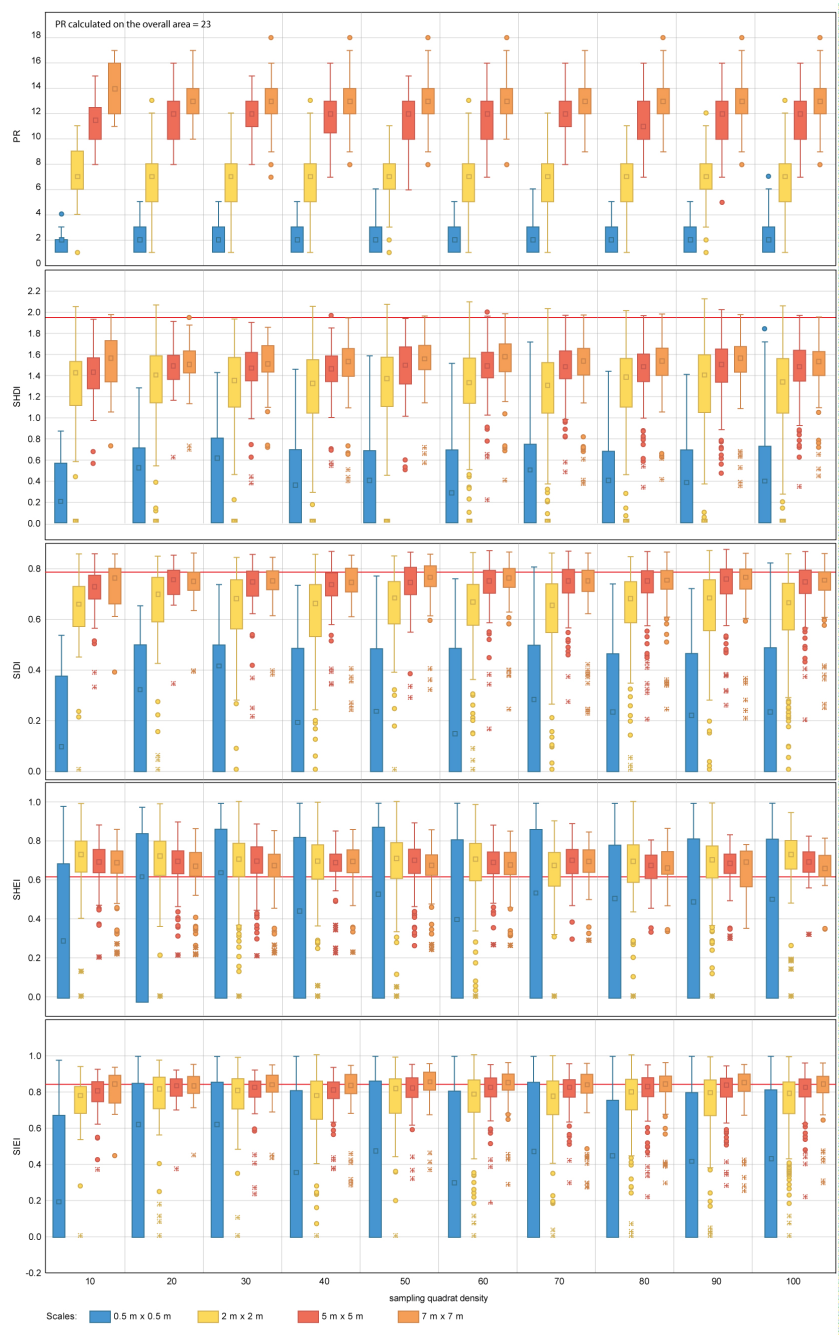

Figure 2.9: Diversity metric values obtained for the random sampling strategy for the range of scales and quadrat densities considered. The red horizontal line indicates the metric value obtained for the total area mapped. PR, SHDI, SIDI, SHEI and SIEI stand for Patch Richness, Shannon's Diversity Index, Simpson's Diversity index, Shannon's Evenness Index and Simpson's Evenness Index, respectively. The boxplots show the first, second (median), third and fourth quartiles. Circles and crosses indicate outliers and extreme values, respectively.

For SHDI and SIDI, the sampling design has a considerable effect on the estimation of the values of dispersion and central tendency, for both nested and random designs. Sampling scales equal to or finer than 5 m × 5 m for SHDI and 2 m × 2 m for SIDI fail to provide reliable metric estimates. The values of SHDI for individual quadrats oscillate between zero and two, with SIDI oscillating between zero and 0.9. SHEI and SIEI present a similar pattern to that described for SHDI and SIDI. However, for both metrics, sampling scales equal to or finer than 2 m × 2 m fail to provide close estimates of central tendency.

2.4 Discussion

The results herein presented inform about the effect that sampling scale, quadrat density and strategy have on the estimation of specific seascape metrics and address the following objectives: (1) to quantify the trade-offs between sample scale and robustness in seascape metric estimation; (2) to quantify the trade-offs between sample quadrat density and robustness in seascape metric estimation; and (3) to develop a set of guidelines for seascape metric estimation based on the findings from (1) and (2). We acknowledge that other authors (Garrabou et al., 1998; Hawkins and Hartnoll, 1980; Sleeman et al., 2005; Teixido et al., 2002) successfully estimated those seascape metrics, and their experience has been fundamental for the selection of parameters in this study. For example, Hawkins and Hartnoll (1980) estimated the species richness in intertidal benthic communities and highlighted the importance of calibrating the sample area based on the organism dimensions. They showed the effect that sample area had on different communities with different abundance and richness in species. Teixido et al. (2002) estimated a set of FRAGSTAT metrics for the characterization of the Antarctic mega-benthic communities across six stations. In their study, only one picture with a 1 m^2 footprint was taken at each station. The results indicated that the set of metrics used to characterize a coral reef must be defined and tailored to the case study area. Sleeman et al. (2005) tested several metrics on seagrass meadow and reported the importance of defining a standard area for a meaningful interpretation of the ecological relevance of the metric. Garrabou et al. (1998) investigated the spatial and temporal dynamics on rocky bottom benthic communities and successfully introduced the novel used of a set of area-perimeter-edge, shape, contagion interspersion and diversity metrics. However, none of these studies have assessed the combined effect of sampling scale, quadrat density and sampling strategy for the estimation of seascape metrics for high resolution coral reef sampling and SfM analysis.

Within the scope of Objectives (1) and (2), the area-density-edge seascape metrics obtained for the case study area of Ponta Do Ouro describe a coral reef that is disaggregated (LSI values around three) with low morphological class dominance (LPI = 0.47%). This is consistent with the cover value registered (69.52%), which indicates that the patches are dispersed within the rocky matrix. The LSI and LPI metrics also indicate that the sessile organisms within the surveyed area are present in a variety of dimensions. Based on the work by Schleyer et al. (2008), this could be the result of abrasion, caused by the combined effect of re-suspended sediments and waves energy, affecting the growth of both soft and hard corals. As a reference, in (Teixido et al., 2002), the Antarctic benthic communities analyzed scored LSI values between 2.88 and 7.47. These communities are characterized by multistoreyed assemblages, intermediate to high species richness (Starmans and Gutt, 2002) and patchy distributions (Starmans et al., 1999).

The description for the case study area of Ponta do Ouro may change depending on the sampling design implemented. For the area-density-edge metrics, quadrat densities below 70 for nested approaches and 40 for random would have failed to capture the spatial heterogeneity of LSI within the landscape (Table 2.5). For LPI, a similar pattern is encountered for quadrat densities below 40 and 30 for nested and random strategies, respectively. As a result, the seascape would have been assumed to have a homogeneous distribution of colonies, aggregation, clumpiness and dominance values based on the configuration described by the few quadrats sampled. Similarly, the finest sampling scales tested would have failed to provide representative values of area-density-edge metrics for the coral reef area. The metrics would have indicated that the reef is slightly more aggregated than observed and dominated by specific morphological classes. This would have had considerable implications in the assessment of the conservation status of the coral reef, its communities and their roles in supporting ecosystem services.

For example, an increase in habitat structural complexity generated by the presence of *Acropora austera* (ACB) has already been identified to support the diversity and abundance of the fish assemblages on South African coral reefs (Floros and Schleyer, 2017). If representative metrics of both dispersion and central tendency are to be estimated to characterize area-density-edge metrics (i.e., LSI, LPI) for the case study area, the recommended quadrat densities provided in Table 2.5 are to be applied.

Table 2.5: Suggested sampling designs for the seascape metrics considered in this study for the case study area of Ponta do Ouro (Mozambique). The metrics reported include: Landscape Shape Index (LSI), Large Patch Index (LPI), Perimeter Area Ratio (PARA), Aggregation Index (AI), Division Index (DIVISION), Patch Richness (PR), Shannon's Diversity Index (SHDI), Simpson's Diversity Index (SIDI), Shannon's Evenness Index (SHEI) and Simpson's Evenness Index (SIEI).

	Random		**Nested**	
Metric	**Scale**	**Quadrat Density**	**Scale**	**Quadrat Density**
LSI	7 × 7	40	7 × 7	70
LPI	5 × 5	30	5 × 5	40
PARA	5 × 5	30	2 × 2	40
AI	5 × 5	20	2 × 2	30
DIVISION	2 × 2	40	2 × 2	40
PR	7 × 7	10	7 × 7	10
SHDI	7 × 7	10	7 × 7	10
SIDI	5 × 5	10	5 × 5	10
SHEI	5 × 5	10	5 × 5	10
SIEI	5 × 5	10	5 × 5	10

The PARA shape metric obtained for the overall surveyed area and field observations indicates that the expected radial allometric growth of the colonies has not been disturbed and that the growth conditions within the area are suitable for all the coral colonies to settle, develop and reach typical dimensions. However, the estimation of metrics of dispersion is highly affected by the sampling scale, quadrat density and strategy selected with the maximum PARA between 1.6×10^{6} and 3×10^{6} depending on the sampling design implemented. It is difficult to argue whether this level is meaningful from an ecological perspective, as no typology exists on the expected PARA value for coral reefs. However, based on in-field observations and the results for the most comprehensive sampling design applied (7 m × 7 m and 100 quadrats), information on how PARA relates to the spatial variability of coral growth can be derived. Results are more likely to indicate that the coral reef is dominated by smaller organisms than those present when using sampling scales finer than 2 m × 2 m. This could drive the assessment of the coral reef towards a more degraded status than it is. In addition, scales finer than 2 m × 2 m provide highly variable PARA measurements between independent quadrats and, therefore, overestimate the spatial heterogeneity of PARA within the area of interest. This is probably related to the dimensions of the organisms encountered (Table 2.2); many of the morphological classes identified are larger than the sampling area covered by any of the 0.5 m × 0.5 m (total area of 0.025 m^2) and the 2 m × 2 m (total area of 4 m^2). This sampling scale fails to capture the individual organisms in full and provide a biased estimation of PARA. In addition, fine sampling scales underestimate the perimeter of the organisms. This is because the perimeter of those organisms that are not included in full within the quadrat is not accounted for. The selection of quadrat density also plays a key role in the robust estimation of the spatial heterogeneity of PARA within the area of interest. For that purpose, quadrat densities below 30 and 40 are required for nested and random strategies, respectively. The use of lower quadrat densities may result in assessments that portray the growth of colonies within the surveyed area to be more heterogeneous (i.e., degraded) than it actually is (Table 2.5).

For the contagion and dispersion seascape metrics (AI and DIVISION), the overall metrics for the area indicate that most organisms colonizing the coral reef present relatively small dimensions, are disperse across the rocky matrix and are characterized by homogeneous distributions across the area. Results show that the sampling design has an influence on the estimation of AI with different combinations of scales and quadrat densities resulting in over and underestimations of AI measures of dispersion and central tendency. AI underestimation will portray the coral reef to be more aggregated than it is, whereas overestimations will result in a more positive assessment of the overall impact within the area. He et al. (2000) demonstrated that AI is strongly dependent (non-linear relationship) on the number of patches present within the landscape, and the identification for a sampling design that optimizes AI estimation is therefore difficult. For the case study area of Ponta do Ouro, sampling designs of 20 × (7 m × 7 m) and 30 × (5 m × 5 m) quadrats, for nested and random strategies respectively, provided good approximations to the values observed for the whole surveyed area. Fine sampling scales (equal to or finer than 2 m × 2 m for nested and 0.5 m × 0.5 m for random strategies) did not provide as good estimates as coarser scales; AI and its spatial heterogeneity were systematically overestimated. This is probably due to the dimensions of the individual organisms as described for the PARA metric. If these fine scales are applied, the systematic overestimation of AI and its spatial heterogeneity will result in biased coral reef assessment. For DIVISION, fine sampling scales (finer than 2 m × 2 m) and reduced quadrat densities (<40) translate into underestimation of the measures of central tendency and dispersion. In brief, these sampling designs will portray the coral reef to be more aggregated and less spatially heterogeneous than it is.

The group of diversity metrics (PR, SHDI, SIDI, SHEI and SIEI) presents a common pattern of response to changes in sampling design. Overall, the metrics indicate that the coral reef is diverse, and its area is proportionally distributed in accordance with their presence within the seascape. For the specific case of PR, scales finer than 2 m × 2 m fail to provide a representative value of PR. As per previous metrics, this may be explained by the size configuration of organisms within the seascape. None of the scales tested reached the PR value obtained for the overall coral reef area (i.e.,23). It is therefore difficult to suggest an optimal sampling scale for the case study area and impractical to make suggestions for other coral reefs. However, from the results obtained, scales of 7 m × 7 m are the best suited from those tested for the estimation of PR. In addition, the variability of PR values between individual quadrats indicates that this metric is also highly sensitive to the presence of spatial heterogeneity within the seascape. Spatial heterogeneity can be captured through the inclusion of further quadrats within the sampling design. For the case study area of Ponta do Ouro, quadrat densities as low as 10 provided similar estimates of PR measures of dispersion and central tendency as the most comprehensive densities applied (i.e., 100). Finer scales and densities than those suggested here (Table 2.5) will result in the coral reef being portrayed as less diverse and more heterogeneous than it really is.

For the SHDI and SIDI metrics, the sampling scale is key to reliable metric characterization. For SHDI, scales equal to or finer than 2 m × 2 m would have been more likely to portray the coral reef as less diverse (i.e., more degraded) and, therefore, less suited to host multiple colonies than it is. Similar results would have been obtained if scales equal to or finer than 5 m × 5 m would have been used for SIDI. The outcomes would have indicated that the reef is dominated by specific species that are more suited to colonize the available space. For both indexes, the variation in independent quadrat values indicates that the metrics are highly susceptible to the spatial heterogeneity. In the case of SHDI, it is difficult to assess whether the variation is significant from an ecological point of view, as the index is not capped in the upper limit. The SIDI index can adopt values comprised between zero and one, where zero indicates null diversity and one maximum diversity. In the case of the studied area, where the values of SIDI for individual quadrats oscillate between zero and 0.9, it is essential to ensure that the spatial heterogeneity within the site is captured with the sampling design implemented. The same rational applies to SHEI and SIEI, which are derived calculations from SHDI and SIDI. For both SHEI and SIEI, the recommended sampling scales should be equal to or coarser than 5 m × 5 m. This is consistent with the results shown in Weinberg (1978), where for coral reef benthic communities, the number of observed species increases by less than 10% when the sampling scale is doubled. Similarly, Bianchi et al. (2004) points out the need for selecting a suitable sample size based on the dimensions of the organisms and the composition of the community and recognizes the fact that a priori standard reference sampling scales have not yet been defined. Other authors have shown that species richness is strongly dependent on sample size Drakare et al. (2006) and sampling quadrat densities Walther and MARTIN (2001); Condit et al. (1996); Gotelli and Colwell (2001), as well as indicating that comparing assemblages using different sample sizes may produce erroneous conclusions Stout and Vandermeer (1975). This is key for the interpretation of ancillary metrics, such as the Species Area Ratio (SAR) (i.e., the relationship between species richness and scale), which inform about the change in biodiversity in response to global environmental change Thomas et al. (2004).

Regarding Objective (3), results herein reported indicate that different sampling scales and quadrat densities should be considered when designing the sampling strategy depending on the metrics to be estimated. Special attention needs to be dedicated to the initial stages of the design of coral reef monitoring protocols with decisions being based on the metrics, as well as the type of statistical measures (i.e., central tendency or dispersion) being estimated. This should be coupled with the ecological relevance of these metrics and the spatio-temporal characteristics of the communities present within the sampling area. Failure to do so will result in biased estimates of the overall values.

Further work should focus on assessing the transferability of the framework presented here to other study areas. The shallow coral reef selected for the scope of the study is representative of the eastern South Africa coral reefs for this depth range (Riegl, 1993; Riegl et al., 1995; Jordan and Samways, 2001; Schleyer et al., 2008), with the overall composition of the benthic community showing a preferential abundance for soft corals. These South African coral reefs are primarily characterized by soft coral communities growing on fossil dunes outcrops (i.e., Sodwana Bay) (Schleyer and Celliers, 2004; Ramsay, 1994, 1996). In particular, the site characterizes the Delagoa Bioregion, which constitutes the southernmost coral reef in the Western Indian Ocean (Porter et al., 2013). These benthic communities have been monitored for the last 20 years along four fixed transects in Sodwana Bay (South Africa) (Porter and Schleyer, 2017) and have shown a shift in community composition due to changes in temperatures. The results herein presented are expected to be transferable to areas with similar characteristics and propose a sampling framework for wide-area (>1500 m^2) coral reef characterization that contributes to overcoming some limitations in coral reef sampling. Based on the work by previous authors (Porter and Schleyer, 2017; Schleyer and Celliers, 2004; Schleyer et al., 2008), the SfM methodology presented in this paper should be directly transferable to the coral reefs of KwaZulu-Natal province in Mozambique and the southern South African coral reefs, which present similar geomorphological characteristics (Jordan and Samways, 2001).

This study quantifies the effect of sampling protocols on coral reef seascape metric estimation using high resolution underwater imagery coupled with the photogrammetry image processing technique for the case study area of Ponta do Ouro. A set of metrics derived from FRAGSTATS that inform about the overall quality of the coral reef area surveyed have been selected for the study. However, the framework can be expanded to assess the effect that sampling protocols have on other metrics (available or not within FRAGSTATS). For example, further work could explore the effect of sampling protocols on more classic metrics that are key for coral reef characterization (e.g., rugosity) or focus on the development of new metrics that can be derived from multiple geomatic products (e.g., point cloud, DEM and orthoimage). This will require the end user to develop scripts that can automatically derive the metrics within a GIS environment. The results herein presented are a step forward and contribute to improving current practice in coral reef monitoring protocols.

2.5 Conclusions

Current efforts on coral reef monitoring have focused on the estimation of the composition and health status. Seascape metrics can be also used to assess the quality of coral reefs. However, little effort has yet been dedicated to developing robust monitoring strategies for the accurate estimation of such metrics. This paper evaluates the effects that different sampling scales, quadrat density and sampling strategy have on seascape metric estimation when relying on SfM techniques. The SfM framework herein presented generates high resolution information that is useful for the characterization of the benthic communities down to single colonies. Results show that each of the seascape metrics considered in this study has different optimal sampling scales, quadrat densities and sampling strategies for the case study area of Ponta do Ouro. Overall, sampling designs with over 30 (5 m × 5 m or 7 m × 7 m) quadrats provide representative results for most metrics considered here. Failure to select the appropriate monitoring strategy will result in biased estimates of these seascape metrics. The SfM framework has the potential to be transferred to similar coral reefs, specifically those of the KwaZulu-Natal province in Mozambique and the South African Republic. This paper contributes to improving current practice in high resolution coral reef monitoring protocols. The comparison of the metrics presented here with descriptive statistics limits the transferability of the outcomes to other coral reefs. Further work should focus on the validation of the proposed framework in other coral reefs. In addition, multiple sites need to be compared using a hierarchical modelling technique to account for a nested sampling design, with findings being used to determine the optimal sub-sampling area (quadrats) and intensity (number of quadrats) to accurately characterize this type of environment. This information would be very helpful in directing the design of future reef survey techniques.

Acknowledgements

This work was supported by the PhD scholarship " EUREKA; European Social Funds (FSE), Programma Operativo Regionale (POR) 2014/2020 Regione Marche (Italy) ; the Marie Sklodowska-Curie Action, Horizon2020 within the project Green-Bubbles (Grant Number 643712); the company UBICA srl. The authors would like to thank Miguel Goncalves, Director of Ponta do Ouro Partial Marine Reserve (Mozambique). Special thanks go to Jenny Stromvoll (Back to Basic Adventures Diving Center) for contributing to Figure 2.2. Thanks also to Dr. Fabrizio Torsani for his support in species identification. Thank you to Nicola Castelnuovo as UBICA srl co-supervisor of my research. We thank four very helpful reviewers and the Editor for providing extremely useful comments, direction and constructive criticism. We will always be grateful.

Chapter 3

Application of Structure from Motion photogrammetry to coral reefs for characterizing their spatial composition and pressures.

Abstract

Coral reefs are dynamic ecosystems subjected to environmental and human pressures varying in intensity and in duration. Recreational diving has been documented having negative effects on coral habitats and organisms, however its impacts on the composition, diversity, and fractality of coral communities at seascape scale are unknown. This study combines high-resolution ortho-mosaic generated with Structure from Motion photogrammetry and data mining techniques (X-Means clustering), to investigate the spatial composition of benthic communities at seascape scale (25 m^2) and identify potential diving impacts and environmental conditions across dive sites for marine monitoring.

The classification showed substantial to excellent agreement with expert opinion, and indicated differences in the benthic composition between diving sites in terms of (i) patches surface, perimeter, abundance, and (ii) functional groups categories (e.g. resistant, moderately resistant, fragile). Resistant-to-physical-impact categories (i.e. sponges and algae) were abundant at small diving sites and highly visited by divers. These sites were characterized by big organisms and with complex shapes, low taxa diversity and density. Fragile-to-physical-impact categories (i.e. *Acropora* spp.) were abundant at diving sites low or moderately visited by divers. These sites are characterized by complex geomorphology and moderate hydrodynamic conditions. The highest taxa diversity and density, and the lowest abundance of resistant-to-physical-impact FGs were recorded at rarely and larger dived sites. The sites exhibited different seascape

metrics (i.e. patch density, patch richness, Shannon Diversity Index, Perimeter-Area Fractal Index), with general patterns emerging in terms of responses to diving pressure and environmental conditions.

Our results suggest that site- specific human pressures, history and site geomorphology, increase understanding of impacts associated with scuba diving and therefore should be considered in conservation programs looking forward its sustainability.

3.1 Introduction

World's coral reefs are facing several threats from many directions, and people are playing a big role in this picture. Threats from local sources such as overfishing, coastal development and pollution, constitute the major peril for over the 60 % of coral reefs worldwide, and operate in combination with the global threats of climate change (i.e. raising temperature, carbon dioxide) (Hughes et al., 2003; Burke et al., 2012). Among local threats, scuba diving can have negative effects on coral ecosystems (Buckley, 2012). Previous ecological studies on tropical reefs, have documented that scuba diving directly impacts on reef benthic habitat and organisms through its effects on sedimentation, breaks and diseases (Hawkins et al., 1999; Zakai and Chadwick-Furman, 2002; Chabanet et al., 2005; Luna et al., 2009; Lyons et al., 2015), but evidences of its ecological effects at seascape scale remain rare.

Scuba diving tourism has experienced growing levels of participation worldwide since 1960s (Richardson, 1999) and is considered an example of sustainable growth (Buckley, 2012). Whilst it favours economic activities in many developing coastal communities (Dimmock and Musa, 2015), research studies suggest it can have negative indirect and direct effects over short-term and high intensity ("pulse" effect, e.g. seasonal tourism, (Bravo et al., 2015)), or over long-term and at constant intensity ("press" effect, e.g. all year tourism (Lyons et al., 2015)) on benthic reef communities. Both indirect and direct impacts constitute a concern at heavily dived sites (Roche et al., 2016). Indirect impacts on benthic habitats and organisms in coral reefs include secondary effects of scuba diving activities such as urban development, land management and sewage disposal (Lucrezi and Saayman, 2017). Processes driven by changes in coastal urbanization, result in diverse distribution and composition of corals taxa than in places where this impact is absent or low (Wongthong and Harvey, 2014). Several studies suggest that reefs affected for example by terrestrial runoff (i.e. high level of sedimentation from coastal erosion), result in changed benthic population structure, reduced size and altered structural forms (Rogers, 1990; Fabricius et al., 2005). Additionally, turbidity-related light limitation decreases gross photosynthesis and causes severe reduction of phototrophic coral recruits survival (Dikou and Van Woesik, 2006). Indirect impacts are often considered as inevitable costs of doing business (Schuhmann et al., 2013), though undermining the conditions for a long-term sustainable growth (Musa, 2002; Donner and Potere, 2007; Lucrezi and Saayman, 2017). In contrast, direct impacts refer to physical scuba divers- contact with the seabed (Lyons et al., 2015). Damages often result in tissue abrasion, skeleton breakage (Hawkins and Roberts, 1992; Chadwick-Furman, 1995), dislodging (Zakai and Chadwick-Furman, 2002), burring (Erftemeijer et al., 2012), and diseases (Lamb et al., 2014) of benthic organisms. The response of benthic corals to direct impacts is different across taxonomic groups because of taxa-specific mophological, physiological, and behavioural characteristics reflecting adaptations to physical-disturbance (Lyons et al., 2015). For example, branched and stony colonies have little resistance to breakage and sensitive to abrasion, diseases, dislodging than soft corals (Lyons et al., 2015). Massive and meandroid stony corals are unlikely to be dislodged and fragmented but can still be abraded (Meesters et al., 1992). Soft corals show low resilience to sedimentation and therefore are often distributed at sites where water hydrodynamism allows to cope with sediment loads (Schleyer and Celliers, 2003).

Most of the research have investigated direct impacts of scuba diving focusing on reef benthic community composition (i.e. taxonomic richness, organisms abundance) at high resolution and over small surfaces (Bravo et al., 2015), or on wide areas at lower resolution (Wilkinson et al., 2003; Hill and Wilkinson, 2004; Lyons et al., 2015). Whilst these small-scale studies have further our understanding on the impact of recreational diving on reef organisms, substantial gaps remain in our understanding and ability to predict interactions among scuba diving and reef benthic communities at seascape scale. Few research studies conducted at seascape scale have reported that coral reefs subjected to direct impacts by scuba diving undergo physical deterioration (Lyons et al., 2015), biodiversity loss (Hasler and Ott, 2008), changes in reproductive cycles and trophic interactions at coral ecosystem scale (Hawkins and Roberts, 1992). As large and representative areas of the seascape include the main benthic groups of the reef, a better scientific understanding of the effects of scuba diving on benthic reef communities at seascape scale is necessary to unravel changes in its structure and functions, and identify the processes affecting its health.

The composition of coral reef varies also with respect to local environmental conditions. For example, reef that are larger in area and deeper would be less affected by severe weather events (Cheal et al., 2017), and local morphological structure variability (i.e. gullets, canyons, plateau) would support different coral communities (Riegl et al., 1995). Structure from Motion (SfM) photogrammetry is an optical based technology to estimate the 3D structure of a scene from 2D overlapping images acquired from a moving sensor (Westoby et al., 2012). The camera positions and orientation are automatically calculated by the algorithms processing the images (Micheletti et al., 2015b).

In recent years, SfM has received particular attention in marine research because it is a low-cost technology, time efficient, requires low budgets, and little technical expertise to apply at sea (Westoby et al., 2012). SfM has been applied to study the ecology of coral reefs and showed to be a versatile, repeatable, and accurate technology for data collection and high-resolution analysis (Figueira et al., 2015; Storlazzi et al., 2016; Ferrari et al., 2016; Palma et al., 2017; Coro et al., 2018). For example, highly detailed ortho-mosaics were realized for the African coral reefs using SfM to investigate the spatial composition of benthic reef communities across multiple spatial scales (4 m^2 to 48 m^2), and to define the minimal sample size for representative sampling of coral reefs ecosystems (Palma et al., 2017). The potential of SfM to provide a detail picture of coral reefs health, has been demonstrated for single organisms (Ferrari et al., 2017) and habitat complexity (Storlazzi et al., 2016). Yet, this technology has not been applied at seascape scale to study the effect of scuba diving on benthic reef structural composition, diversity and fractality metrics.

This study combines high-resolution ortho-mosaics generated with SfM photogrammetry and data mining techniques, to investigate the composition of benthic reef communities at seascape scale (25 m^2), and identify potential diving impacts and environmental conditions across dive sites for marine monitoring. The benthic composition of coral reef is expected to differ across diving sites, taking into account scuba-diving pressures (i.e. number of dives per year) and the site environmental conditions (i.e. depth and reef area). Specifically we expect that: (i) specific composition metrics at seascape scale would differ across sites, as in Table 3.1, and (ii) the contribution of resistant-to -physical impact organisms to the composition of coral reefs would differ across sites, with large contribution of resistant organisms to highly dove sites and to small and shallow reefs.

Table 3.1: Metrics predicted to be significantly different across coral reefs with respect to site human pressures and environmental conditions. “Patch” indicates the single organisms in a digitized polygon (Section 3.2.2.3).

Metric responses	Number of dives/ yr			Site Area		Site Depth	
	High	Medium	Low	Small	Large	Shallow	Deep
Patch surface	medium to large	small-large	small - large	large	small - large	large	small - large
Patch perimeter	complex	simple-complex	simple - complex	simple	simple - complex	complex	simple - complex
Patch Density (PD). Informs on the complexity of the seascape with no reference to the diversity of classes and the size of the patches.	low	medium-high	high	low	high	low-medium	high
Simpson Diversity index (SIDI). Informs on the probability that two entities, (i.e., pixels) taken at random from the same seascape, belong to different patch types. Big values indicate high probability that two pixels are fromd ifferent patch types (Somerfield et al., 2008).	low	medium-high	high	low	high	low-medium	high
Patch Richness (PR) Informs about the number of patch classes present within the seascape.	low	medium-high	high	low	high	low-medium	high
Shannon Diversity Index (SHDI) Informs about the number of different patch types within the seascape and their eveness. Big SHDI values indicate high evenness amongst patch types within the seascape (Spellerberg and Fedor, 2003).	low	medium-high	high	low	high	low-medium	high
Perimeter-Area Fractal Dimension (PAFRAC). Informs about the complexity of the organisms across spatial scapes. E.g. if small and large patches have similar and simple geometric shapes, the index will be small, indicating that as the patch area increases, the patch perimeter increases too but by small increment (McGarigal, 2014).	high to medium	medium-low	medium-low	high-medium	medium-low	high-medium	medium-low
Mean Patch Fractal Dimension (FRAC_MN). Balances the PAFRAC results when the patch frequency is <20 (McGarigal, 2014) by calculating an average fractal dimension of each patch.	low	medium-high	high	low	high	low	high

3.2 Material and methods

3.2.1 Study area and experimental design

The study was conducted between April and June 2015 at the Ponta do Ouro Partial Marine Reserve (PPMR), Mozambique (Figure 3.1). Since the end of the civil war in 1994, Ponta do Ouro has grown as international scuba diving destination, rapidly registering high intensity of use: 30k -40k dives/year (1995, (Robertson et al., 1996)), 80k - 90k dives/year (1998, (Motta, 2000)), 42.5k - 62k dives/year (2001 -2002, (Costa et al., 2005)), and 26k (± 3k) dives/year (2011 2015, PPMR report) Table A.1). Seven dive sites were selected with different diving use across the PPMR (Figure 3.1, Table 3.2). The sites are characterized by "coral carpets" constituted by the unique combination of numerous endemic species covering Late Pleistocene fossils dunes and forming typical morphological structures low in profile (Robertson et al., 1996; Celliers and Schleyer, 2008; Jordan and Samways, 2001).

Imagery data were collected at each site in one single dive and covering the entire coral reef area, or in larger reef, surveying the areas most visited by dive operators (i.e. Table 3.2). Dive sites were mapped by a semi-autonomous underwater vehicle equipped with action cameras, tablet, illumination system and GPS buoy Palma et al. (2017).

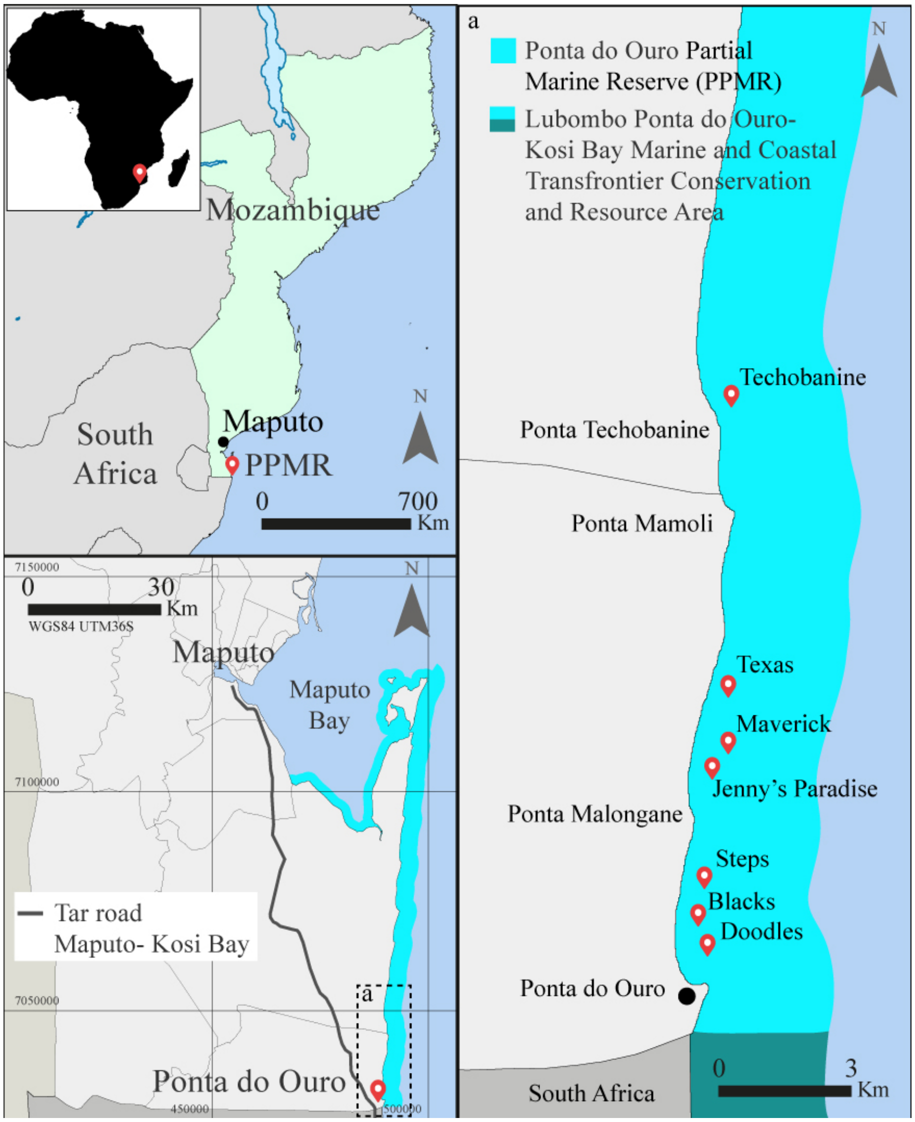

Figure 3.1: The figure shows the seven surveyed diving sites across the PPMR in Mozambique.

Table 3.2: Surveyed dive sites. Location of sites (WGS84), distance from launch point (km), average depth (m), surveyed area (m^2), and number of divers per year (2001-2002 and 2011-2016 from PPMR report). The asterisk indicates diving sites that were not sampled for their total area.

PPMR Bays	Dive sites	Long, Lat (WGS84)	Distance from launch (km)	Average depth (m)	Area (m2)	Average dives/year (2001-2002, ref)	Average dives/year (2011-2016, PPMR report)
Ponta do Ouro	Doodles	W 32.896103, N -26.830669	1.7	17	850	10350	7374
	Blacks	W 32.897408, N -26.824883	2.5	19	425	-	985
	Steps	W 32.894828, N -26.813275	3.6	16	950	3125	3462
Ponta Malongane	Maverick	W 32.904875, N -26.775608	7.9	25	2550	-	20
	Paradise ledge	W 32.903339, N -26.780397	7.1	22	2250	2403	365
	Texas*	W 32.902742, N -26.763153	9.5	15	2150	3248	280
Ponta Techobanine	Techobanine*	W 32.903397, N -26.677103	19.6	12	3500	-	35

3.2.2 Data processing

3.2.2.1 Photogrammetric processing and seascape composition analysis

For each site, high resolution ortho-mosaics (pixel size <0.01 m) were obtained by processing the geo-tagged images of the underwater surveys (Palma et al., 2017). The images were projected into the Universal Transverse Mercator (UTM) fuse 36 Southern Hemisphere coordinate system, defined by the World Geodetic System (WGS84) and processes by Photoscan (Agisoft LLC., St. Petersburg, Russia) (Palma et al., 2017). To study the composition of the coral reefs at seascape scale, virtual random quadrat of 5 m x 5 m were selected and replicated 3 times over each ortho-mosaic (Palma et al., 2017). The quadrat size 5 m x 5 m is proved representative of the coral reefs at the PPMR (Palma et al., 2017). Within each quadrat, the benthic organisms were identified in taxonomic and morphological classes, digitalised using ArcGIS 10.1 software, and finally rasterized to obtain categorical maps (Redlands, CA, USA) (Table 3.3). The classes were summarized in functional groups (FGs) and for each class, abundance and the summary statistics of surface, perimeter were calculated.

Table 3.3: Taxonomic and morphological classes identified from the ortho-mosaics for each site. The table reports also the classes of resistance obtained from the analysis of the quadrats.

Resistant- to- physical- impacts categories	Functional groups (FGs)	Classes	Code
Fragile	Acropora spp.	Acropora branched	ACB
		Acropora	ACC
		Acropora digitate	ACD
		Acropora stout branched	ACS
	Non Acropora branched coral	Non Acropora branched coral	CB
	Free living fungiid	Free living fungiid	CMR
	Tabular coral	Tabular coral	CTA
Moderately fragile	Encrusting coral	Encrusting coral	CE
	Folious coral	Folious coral	CF
	Massive coral	Massive coral	CM
	Soft corals	Soft crested coral	SCR
		Soft digitate coral	SCD
		Soft mushroom coral	SCF
		Soft plane coral	SCP
		Soft radiate coral	SCR
Resistant	Other invertebrate	Other invertebrate	OI
	Sponges	Sponge	SP
		Sponge encrusting	SPE
		Sponge massive	SPM
	Algal turf	Algal turf	TA

3.2.2.2 Clustering analysis

Data on FGs (i.e. diversity, surfaces and perimeter, average, maximal, minimal, standard deviation, count), and reef sites (i.e. depth, extension) was analysed using a principal component analysis (PCA (Jolliffe, 2005)) and the distance- based clustering X-Means (Pelleg et al., 2000) to look for similarities in community composition between diving sites and possible diving impacts. The approach, which involves a series of steps performed sequentially to the harmonized data (Figure 1 in Magliozzi et al. (2018), was applied at seascape scale and carried out by using the e-Infrastructure D4Science services (Candela et al., 2009; Magliozzi et al., 2018). First, a PCA was performed to reduce the dimensionality of the dataset and explore the patterns in data variability among diving sites (Jolliffe, 2005; Magliozzi et al., 2018). Secondly, X-Means was applied to the PCA-transformed vectors associated with largest variance, to identify the variables indicating similarities of benthic composition between sites (Magliozzi et al., 2018). In this study, we searched for a number of clusters between 1 and 10. The resulting clusters contain equally distributed variables and are characterized by a centroid which is a summary of the characteristics of the cluster. The clusters were evaluated with respect to expert opinion (Table A.2-A.5). Two experts (Pantaleo and Fernandez) evaluated independently the clusters by assigning the clusters' results to each diving sites, based on their expert opinion. Then, a confusion matrix was used to assess the agreement between the experts assignment and X-means clusters as the percentage of matching assignments (absolute percentage of agreement). The Cohen's Kappa (Cohen, 1960) was calculated to estimate the agreement between the experts and the model compared to purely random assignments (Coro et al., 2015). To look at patterns of taxonomic and morphological benthic composition over the clusters and among broad taxonomic groups, the FGs were grouped into three categories based on a series of taxa mophological, physiological, and behavioural characteristics identified in the literature as reflecting adaptations to physical-disturbance (Schleyer and Celliers, 2003), Table 3.3)."Resistant" organisms include sponges (SP), algal patches (TA) and "other invertebrates" (OI) (e.g. gasterops, tunicates, echinoderms, hexacorals such as *Stichodactyla* spp., *Atriolum* sp.). These taxa show high regenerative physiological resistance to physical damages because of their skeleton structure, and have been often reported in relation to ecological shifts in coral reefs communities (Hughes et al., 2003; Wulff, 2006; Norström et al., 2009; Lyons et al., 2015). " Moderately resistant" organisms include soft corals (SCD, SCP, SCC, SCR, SCF) (e.g. *Sarcophyton* sp., *Sinularia* sp., *Lobophyton* spp.), massive corals (CM) (e.g. *Platygyra* spp., *Montastrea* spp., *Galaxea* spp., *Favites* spp., *Favia* spp. and *Turbinaria* sp.), folios corals (CF) (e.g. *Montipora* spp., *Echinopora* spp.), and encrusting corals (CE) (e. g. *Porites* spp). Soft corals are often described as sensitive organisms to sediment burying and wave actions (Riegl et al., 1995) but their flexibility of the colonies, their low profile suggest they are resistant animals to hydrodynamic condition (Schleyer and Celliers, 2003). Massive, encrusting and folios corals show resistance to physical impacts due to a stout or flat morphological growth. However, they can be dislodged or more commonly scratched by accidental impact with divers equipment (Schleyer and Tomalin, 2000; Zakai and Chadwick-Furman, 2002; Lyons et al., 2015). Finally, the "fragile" "group includes *Acropora* spp. (AC), branched corals (CB) (e.g. *Pocillopora* spp.), free living fungiid (CMR), and tabular corals (CTA) (i.e. *Turbinaria* sp.). *Acropora* spp. and branched-corals taxa have tree- shaped carbonate skeletons that increase the structural complexity of reefs but, as erected forms are also the most exposed to breaks and fragmentation (Hawkins and Roberts, 1992; Rouphael and Inglis, 1995; Chadwick-Furman, 1995; Schleyer and Tomalin, 2000; Lyons et al., 2015; Floros and Schleyer, 2017). Among the fragile group, tabular corals and free living fungiid colonies are most the most subjected to breaks, for example during severe weather conditions entire colonies might be tipped over (Hughes and Connell, 1999)

3.2.2.3 Calculation of seascape metrics

The composition of the reefs was investigated by calculating seascape metrics such as diversity, aggregation and shape on the categorical maps using the FRAGSRATS v4 software (Amherst, MA, USA) (McGarigal, 2014). The set of metrics was selected based on their relevance to seascape ecology composition (Table 3.4). FRAGSTATS v4 computes a variety of metrics for categorical maps, and has been applied in a wide range of disciplines including seascape ecology (Garrabou et al., 1998; Teixido et al., 2002; Kendall and Miller, 2008; Wedding et al., 2011b; Palma et al., 2017). In this study, the categorical maps were processed at patch (the single individual digitized in a polygon), class (taxonomical and morphological FGs, Table 3.3) and seascape level (denotes all the patches of different classes within the quadrats) by considering the disposition, the size and the shape of the patches within the quadrats. PD, SIDI, PR, SHDI, PAFRAC, FRACMN at seascape level were compared between reef sites by applying a One-Way ANOVA test using the *aov* function in the R "stats" v3.5.1 package (Chambers et al., 1992) (Table A.1-.6). In order to solve heterogeneity in the residuals, PD, PR, SHDI, PAFRAC were log-transformed, but this was not necessary for the rest of responses. Validation of underlying assumptions of normality and homoscedasticity of tests residuals was applied following Zuur et al. (2009) (*shapiro.test* function from the R "stats" v3.5.1 package (Stats et al., 2013) and *leveneTest* in R "car" v3.0-2 package

(Fox et al., 2018) and, subsequently, post-hoc Tukey tests were applied to compare which specific treatments differ significantly using the *TukeyHSD* function from the R "stats" v3.5.1 package (Stats et al., 2013).

Table 3.4: List of landscape indices calculated on the virtual random quadrats using FRAGSTATS v4 and their description.

Metrics class	Index	Description
Aggregation metrics	PD (Patch density)	PD is the number of patch counted within the landscape.
Diversity metrics	SIDI (Simpson Diversity Index)	SIDI is the proportional abundance of each patch type squared. SIDI approaches 1 as the number of different patch types (i.e., patch richness, PR) increases and the proportional distribution of area among patch types becomes more equitable.
	PR (Patch Richness)	PR is the count of the patch variety within the landscape
	SHDI (Shannon's Diversity Index)	SHDI is calculate the probability that any two pixels selected at random would correspond to different patch types; the larger the values the greater the likelihood than any two randomly drawn pixels would be different patch types
Shape metrics	FRAC_MN (Mean patch fractal dimension)	FRAC_MN based on the fractal dimension of each patch at landscape levels by weighting patches according to their size.
	PAFRAC (Perimeter-area fractal dimension)	PAFRAC of a patch mosaic provides an index of patch shape complexity across the landscape describing the power relationship between patch area and perimeter.

3.3 Results

3.3.1 Evaluation of clusters and agreement with the experts

The reefs were classified in three clusters (Table 3.5) and their reliability evaluated with respect to expert opinion (Table 3.6, Tables A.2-.5). The clusters results showed moderate to substantial agreement with experts opinion, indicating reliable semantic interpretations of the vectors identified in the clusters variations (Table 3.5). Marginal agreement is recorded between the two experts due to Expert 2 who classified most of the sites as moderately impacted.

Table 3.5: X-Means clusters, labelled and semantically described.

Clusters	Label	Description
Cluster 1	Very impacted	Distribution of organism patches with big average surfaces and perimeter in relation with the total abundance. High abundance of algal patches with large perimeter. Abundant average sponge patches with large maximal perimeter length and high variability among patches. No Acropora corals, branched corals and massive corals patches. Folios coral patches with large perimeter. Low abundance of tabular coral patches. Rare soft crested coral patches with small maximal surface and perimeter. Very low abundance of soft digitate coral patches. Rare and soft mushroom coral with small average areas and medium average perimeter.
Cluster 2	Moderately impacted	Distribution of organism patches with small average surface and perimeter in relation with the total abundance. Medium abundance of algal patches with medium perimeter. Abundant average sponge patches with medium maximal perimeter and low variability among patches. Medium abundance of Acropora patches with medium average perimeter. Large average branched coral patches surface with large perimeter. Folios coral patches with medium perimeter. Massive coral with medium patch areas and perimeters. Medium abundance of tabular coral patches. Medium soft crested coral patches maximal surface with large maximal perimeter. Medium abundance of soft digitate coral patches. Soft mushroom coral with large average areas and large average perimeter.
Cluster 3	Low impacted	Distribution of organism patches with very small average surface and perimeter in relation with the total abundance. Low abundance of algal patches with small perimeter. Rare sponges with very small perimeter length. High abundance of Acropora coral patches with medium average perimeter. Small average branched coral patches surface with small perimeter. Folios coral patches with small perimeter. Massive coral with medium patch areas and perimeters. High abundance of tabular coral patches. Large soft crested coral patches maximal surface with medium maximal perimeter. High abundanceof soft digitate coral patches. Soft mushroom coral with medium average areas and medium average perimeter.

Table 3.6: Absolute percentage of agreement and Kappa statistic between the Experts and the Experts vs the X-Means classification across sites.

	Expert 2	**Clustering**
Kappa values on comm./non-comm. classes		
Expert 1	0.36	**0.78**
Expert 2		0.57
Kappa interpretation Fleiss/LandisKoch		
Expert 1	Marginal	**Excellent / substantial**
Expert 2		Good/Moderate
Absolute percentage of agreement		
Expert 1	57%	**86%**
Expert 2		71%

3.3.2 Seascape composition of diving sites

A total of 2102 images were processed for generating the ortho-mosaic from the dive site Doodle, whereas for the site Blacks the images processed were 1165. The sites Steps, Maverick, Paradise Ledge and Texas from Ponta Malongane bay counted 2108 images, 1758 images, 2444 images and 1490 images respectively. For the site Techobanine the images processed were 3662. From the ortho-mosaics analysis and digitalization, a total of eleven functional groups were identified (Table 3.3). The sites Doodles and Blacks showed the higher frequencies of sponges and algal patches among the selected sites for the study and the lower abundances of organisms with <0.5 individual/m^2. The site Steps is characterized by the presence of massive sponges and algal patches as well as by the presence of soft corals digitate (SCD) and Soft corals crested (SCC). Coral branched (i.e. *Pocillopora* sp.) and Acropora are described also in the site. The average organisms density is 0.75 individual/m^2. In Paradise ledge and Maverick the frequencies of soft corals classes (SCD, SCC, SCF, SCR) is higher and characterize the seascape. The classes of Acropora (ACS, ACD), non-Acropora branched corals, folios corals and massive hard corals are presents. The organism densities count for 1.7 individual/m^2 and 1.5 individual/m^2 in Paradise Ledge and Maverick, respectively. In the site Texas the organisms density is the highest among the selected sites with 2.1 individual/m^2.

The site shows a lower diversity of classes with the presences of sponges (SP), Acropora spp (ACC), branched corals (CB), Tabular corals (CTU) and all the classes of soft corals (SCD, SCC, SCR, SCF). In the site Techobanine, the branched corals (ACD, ACC, ACS and CB) shown the higher frequencies with the folios corals (CF), massive corals (CM) and the tabular corals (CTU) and the smaller frequencies in soft corals with the classes SCD, SCF, SCR. The organisms density counted for 1.2 individual/m^2. The clusters were labelled in terms of ecological stability, and semantically described (Table 3.5). The cluster very impacted (Cluster number 1) contains 23 vectors and corresponds to two sites (Doodles and Blacks). It indicates the whole set of benthic taxa that are very resistant and resilient to physical pressures (i.e algae, sponges), with low density and diversity, and generally more complex morphological shapes per organism. The moderately impacted cluster (cluster number 2) contains 33 vectors and three sites (Steps, Techobanine and Texas). It represents the set of taxa that are low resistant but high resilient to pressures (i.e. branched hard coral are sensitive to breaks but high growth rates (Gladfelter et al., 1978) and show higher density and diversity, and lower morphological complexity per organism and higher fractal complexity at seascape scale than the cluster number 1. Finally, low impacted cluster (cluster number 3) describes 32 vectors and two sites (Paradise ledge and Maverick). It refers to taxa that are moderately resistant and low resilient to physical pressures (i.e. soft corals that have low growth rate and low recruitment rate but high resistance to high energy hydrodynamic conditions (Schleyer and Celliers, 2004)), show the highest level taxa diversity and density, and high level of fractal complexity at seascape scale. Very impacted sites showed the greatest patches areas, and similar distribution to moderately impacted sites (cluster 2, Figure 3.2a). Doodles and Blacks were also described by patches with bigger perimeters and higher variability in the first and third quartile than Steps, Techobanine, Texas, Paradise ledge and Maverick (Figure 3.2b). In fact, sites in cluster 2 and 3 were characterized by patches with smaller perimeters and low variabilities (Figure 3.2b). Low impacted sites showed the highest abundance of benthic organisms and high variability among the two sites (Figure 3.2c). Conversely, in very and moderately impacted sites, organisms abundances have overall similar distributions among sites (cluster 1 and 2, Figure 3.2ac).

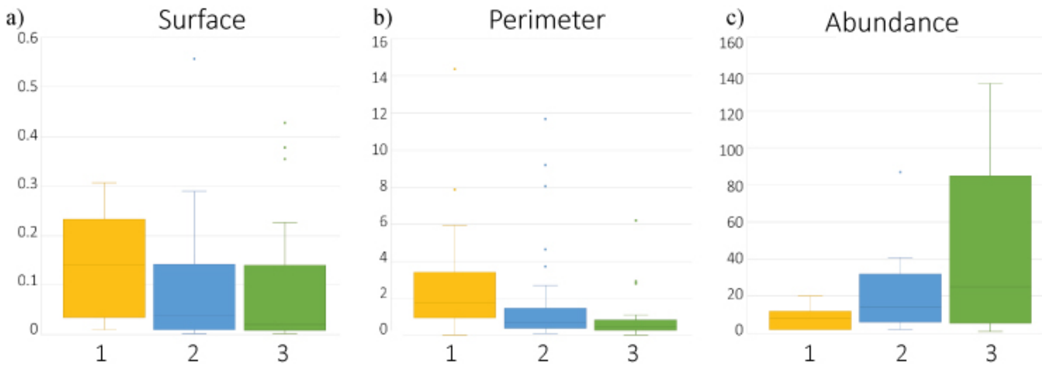

Figure 3.2: Distribution of surface, perimeter and count across the clusters. Axis "x" indicates clusters 1, 2, and 3.

Ten FGs were distributed across the clusters (Figure 3.3) and reflected different adaptations to physical disturbance (Figure 3.4).

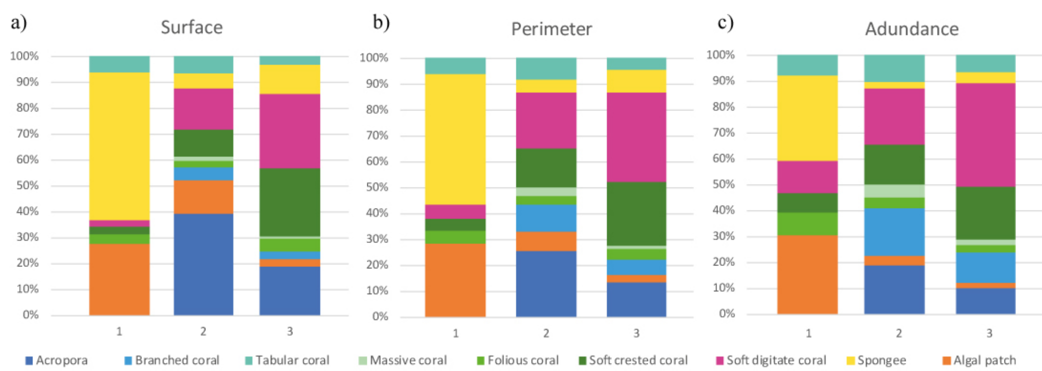

Figure 3.3: Relative frequency distribution of the functional groups across the clusters. Axis "x" indicates clusters 1, 2, and 3.

The resistant group accounted for >85% of the patches surface, the 80% of their perimeter and more than >60% in abundances in the very impacted cluster (Figure 3.4a, b). Moderately resistant organisms, constituted only the 10% of the patches surface at very impacted cluster, while contributed >30% in moderately and more than 60% in low impacted clusters (Figure 3.4a). The moderately resistant group had a similar pattern also for patches perimeter and abundances (Figure 3.4b, c).

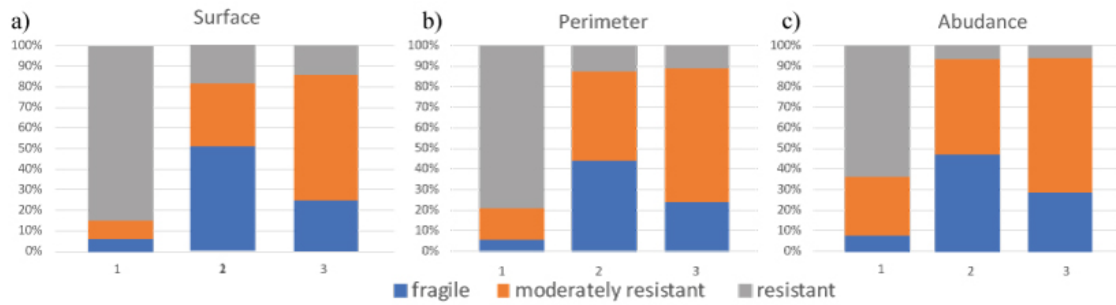

Figure 3.4: Relative frequency distribution of the three categories indicating resistance to physical-disturbance across the clusters. Axis "x" indicates clusters 1, 2, and 3.

Among sites, the resistant group had the highest contribution in percentage to mean patch areas and abundances to Blacks (95%) Doodle (>75%), and Steps (>50%) (Figure A.2, A.4). The moderately fragile group mostly accounted in percentage to mean patch areas and abundances to Paradise Ledge (50%), Maverick (70%), and Texas (60%) (Figure A.2, A.4). Finally, Paradise ledge and Techobanine showed the highest contribution in percentage to mean patch areas (45% in Paradise Ledge, 70% in Techobanine) of the fragile organisms group (Figure A.2, A.4).

3.3.3 Seascape metrics

Most of the seascape metrics significantly differed across reefs, only the Mean Patch Fractal Dimension and the Simpson Diversity indeces did not show significant differences suggesting low planar complexity of the seascape (Figure 3.5). PD, PR and SHDI declined at very impacted sites (cluster 1, Blacks and Doodle) and these differences were significant (Figure 3.5). The PD index showed significant differences ($F(6,14)= 23.04$, $p < 0.01$) between sites, with larger seascape complexity at Paradise ledge (52 ±1.8 organisms) and the lowest at Black (6 ±1.0 patches) and Doodles diving sites (6 ±1.5 patches) (Figure 4.3). PR showed that the number of classes of organisms is also significantly different ($F(6,14)= 37.40$, $p < 0.01$) between sites: only 5 classes at Black 5 (±0.4) and Doodle 6 (±0.4) and over 10 at the other diving sites (Figure 3.3). To this end, SDHI index suggests that Maverick and Techobanine have higher number of classes of organisms, equally distributed within the sites, than other sites (Figure 3.3,

Figure A1). Finally, higher morphological complexity of the patches in the seascape (PAFRAC index F(6,14)= 3.54, p =0.02) is recorded at Doodle (2.23 ± 0.54) (Figure 3.3).

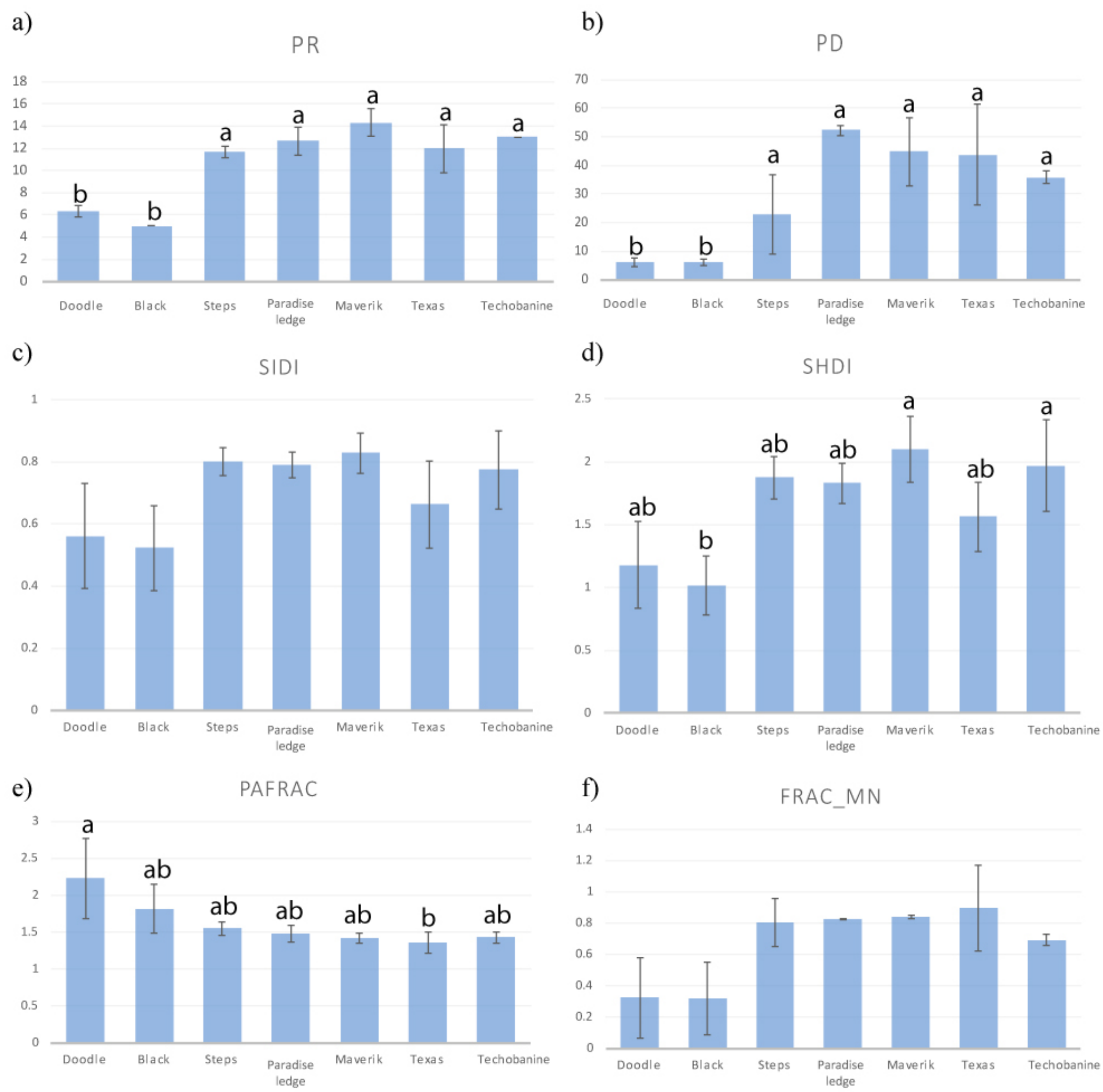

Figure 3.5: Patch Richness, Patch Density, Simpson Diversity Index, Shannons Diversity Index, Perimeter-Area Fractal Dimension, Mean Patch Fractal dimension (mean $\pm SD).Siteswheretheresponsesarenotsignificantlydifferentareindicatedwiththesameletter(95\%CI)$.

3.4 Discussions

This study is, to the authors' knowledge, the first attempt to assess benthic composition of coral reef using SfM ortho-mosaics and seascape ecology index over wide areas (25 m^2) and in relation to scuba diving and environmental conditions for marine monitoring. The result of the classification showed substantial to excellent agreement with expert opinion, and indicated differences in the benthic composition between diving sites in terms of (i) patches surface, perimeter, abundance, and (ii) FGs categories (e.g. resistant, moderately resistant, fragile). The sites exhibited different seascape metrics (i.e. PD, PR, SHDI, PAFRAC), with general patterns emerging in terms of responses to diving pressure and environmental conditions. In this section we discuss the result of the classification against diving pressure and environmental conditions.

Our study found that the benthic composition differed between reef sites, suggesting a functional relationship to diving in the PPMR, and upholding our first hypothesis that scuba diving and environmental conditions would affect the composition of coral reefs. Cluster results show groups of FGs and their metrics (i.e. surface, perimeter, abundance) that suggest differences between sites in relation to benthic communities resilience and resistance, indicating that scuba diving and environmental conditions reflects on reef composition at seascape scale. The calculation of the seascape indices did not show significant variability within sites suggesting that the selected sampling unit and the number of replicates were adequate for describing the communities of the selected coral reefs. The resistant- to- physical- impacts categories provide further insights into seascape composition, and partialy support our second hypothesis that the contribution of resistant organism would reflect highly dove sites and small and shallow reefs. Dimensional factors, such as patch surface and perimeter inform the benthic assemblage composition and complexity observing the organisms sizes and planar shape. The shape of bigger size organisms is expected to show higher complexity in results of intra- and inter-specific competition and is related with the organisms' densities populating the seascape. The seascape composition factors (i.e. functional groups and organisms abundance), inform about benthic taxa diversity and organisms density. Lower values in taxa diversity are related to more homogeneous seascapes, whereas higher values of organisms densities suggested lower human (i.e. low number of dives per year) and environmental pressures (i.e. deeper and larger coral reefs). Low organisms densities with large and complex shapes were recorded in Doodle and Blacks which were grouped in the very impacted cluster. These sites are characterized by lower taxa diversity and by the highest number of dives per year and are the closest sites to lauching point at Ponta do Ouro beach. Doodle is highly frequented since 1995 while Blacks has been dove since 2011 with moderately intensities (Table 3.2). Both sites are subjected to strong environmental pressures due to small surface areas (450 m^2 to 850 m^2) and moderatly shallow average depth (-17m to -19m); the waves and the abrasive action of resuspended sediment, limit the settlement and growth of resistant to physical impact organism as sponges and algae. Previous studies related the presence of the organisms to scuba diving pressures (Lyons et al., 2015). Higher FGs diversity and high presence of Acropora colonies were recorded on the moderately impacted cluster. This cluster included three sites very distant one another (Figure 3.1): Techobanine is at 19.6 km, Steps at 3.6 km and Texas at 9.6 km from Ponta do Ouro launching point. Steps, is characterized by lowest organisms density while Texas by the highest. Both sites present high variability which suggests that there are spatial differences in the benthic community composition (PR and PD) over the sampled seascapes (Figure 3.5). Texas also shows smaller average organisms surface and higher fractal dimension than the other two sites suggesting greater variabilities in organisms' shapes and dimensions which could be related to local recovering to environmental extreme events (i.e. cyclones storms) or to intense scuba diving use of the dive site in the past (Table A.1). Techobanine shows highest frequencies in hard branched corals and Acroporas' colonies probably favoured by the lower average depth of the site (-12 m) and by the very low number of dives per years recorded in the last decade. The low density and large dimensions of the organisms is explained by the higher grow rate of these hard corals ((Lirman, 2000)) which compensate the impacts caused by the high energy hydrodynamic conditions of the area. Among sites, Steps is the only highly visited by scuba divers since 1995 (>3000 dives/yr), while Texas has less than 300 dives/yr in the last decade and Techobanine is annually rarely visited (Table 3.2 Table A.1). Steps is smaller than Techobanine and Texas but it develops along a rocky edge; small canyons and cracks in the rocky substrate provide sheltered areas to waves action and scuba diving direct impacts, likely favouring the presence of branched corals (Schleyer et al., 2008).

Cluster 3 shows higher level of taxa diversity and organisms density in results of the low scuba diving pressure and the low Environmental conditions. Paradise ledge and Maverick are the deeper (-18m to -20 m) and extended sites with maximal of 2852 dives/yr recorded in Paradise Ledge 2002 and an average of 365 dive/yr for the same site in the last decade. Maverick is located in the close proximity and it has been rarely visited. The high taxa diversity observed in the sites has correspondence with the high organisms' abundance composing the seascape which is more variable in Maverick. Soft corals classes which mainly represent the moderately resistant organisms shown low growth rate and low larval recruitment (Schleyer et al., 2008) compose in the sites the more characteristic "coral carpet" described in literature (Jordan and Samways, 2001). The three clusters described with organisms' classes of resistance to physical impacts showed the agreements with the scuba diving pressure intensity and duration and environmental pressures defined with site extension and average depth. Recreational diving appears to elicit a press on benthic assemblages' composition effecting more on small size and shallow sites. Doodles and Blacks presented the higher frequencies of organisms resistant- to- physical- impacts (i.e. sponges, algal patches), the lower patch classes diversity and organisms' density. The few fragile organisms identified in the cluster 1 sites are tabular corals which have a limited three-dimensional complexity shape and are potentially more resistant- to- physical- impacts to scuba diving activities than Acroporas and other branched corals. In Steps, resistant organisms are relatively higher than in Techobanine. The reef morphology (i.e. edges and canyons) could influence the abundance and dimension of fragile organisms (i.e. Acropora corals) favouring a more heterogeneous community with moderately fragile and resistant organisms. Steps and Texas present higher frequencies in resistant organisms especially sponges, and the relatively low frequencies in fragile organisms. Cluster 3 grouped the sites Paradise ledge and Maverick. Both are large sites and the most deeper (-18 m to

-20 m) therefore environmental pressure were considered low. Benthic communities in both sites are well represented by soft corals and moderately resistant organisms. Organisms abundance is the higher which includes several size organisms with is reflected in a smaller perimeter variability of the second and third quartiles and in a lower fractality of the patches within the landscape. The lowest number of dives registered in these sites suggest a low to null scuba diving impacts. As reported in literature the southernmost African coral reef areas are frequently kicked by seasonal cyclones which may cause extensive damages (Ramsay, 1996) but on a long term are do not exceed human damages recorded on benthic habitat (Schleyer and Tomalin, 2000). In these hydrodynamic high energy habitats where coral reefs morphological complexity is low, the role of branched coral colonies has been descried as very important for protecting fish species juveniles (Floros and Schleyer, 2017). Physical damages on these particular coral reef population where soft and low in profile corals are dominant in seascape are not easy to identify by visual census even if Schleyer and Tomalin (2000) studying the coral reef communities of Sodwana Bay quantify damages on both hard and soft corals caused by scuba diving activities and recreational fishing. The method here proposed does not focus on the damages observed on organisms but described the resulting effect of the human pressures combined with environmental conditions on the spatial composition of benthic functional groups and their interaction in the seascape (Lamb et al., 2014; Bravo et al., 2015). Traditional tools for establishing management programmes for recreational SCUBA diving estimate the sites carry capacity as the maximal amount of disturbances that communities can cope without showing degradation effects and losing their aesthetic value (Davis, 1993; Hawkins and Roberts, 1997). The calculation based on the vulnerability of the site, therefore consider the species composition and their conservation status (Hawkins and Roberts, 1997). However, this approach does not consider if the community composition is already the result of human driven changes or the community composition is the results of environmental conditions. Despite, our study looked at the benthic habitat composition as the result of the specific history of each site and consider all the site equally able to support similar benthic communities in order to the similar geology, geomorphology, exposition and depth range, long-term monitoring program are required for a correct interpretation of natural trend in the coral reef composition. Porter and Schleyer (2017) describing the results of a 20 years long monitoring program at Sodwana bay highlighting the decreasing trend in soft corals and the positive increment of hard corals with inter annual positive temperature increment. These information, when available should be considered in the definition of the new descriptors related to the fragility of the studied sites.

3.5 Acknowledgments

This work was supported by the PhD scholarship EUREKA, the European Social Funds (FSE), Programma Operativo Regionale (POR) 2014/2020 Regione Marche (Italy), the Marie Sklodowska-Curie Action, Horizon2020 within the project GreenBubbles (Grant Number 643712) and UBICA srl.

Chapter 4

SfM-Based Method to Assess Gorgonian Forests (*Paramuricea clavata* (Cnidaria, Octocorallia))

[1]

Abstract

Animal forests promote marine habitats morphological complexity and functioning. The red gorgonian, *Paramuricea clavata*, is a key structuring species of the Mediterranean coralligenous habitat and an indicator species of climate effects on habitat functioning. *P. clavata* metrics such as population structure, morphology and biomass inform on the overall health of coralligenous habitats, but the estimation of these metrics is time and cost consuming, and often requires destructive sampling. As a consequence, the implementation of long-term and wide-area monitoring programmes is limited. This study proposes a novel and transferable Structure from Motion (SfM) based method for the estimation of gorgonian population structure (i.e., maximal height, density, abundance), morphometries (i.e., maximal width, fan surface) and biomass (i.e., coenenchymal Dry Weight, Ash Free Dried Weight). The method includes the estimation of a novel metric (3D canopy surface) describing the gorgonian forest as a mosaic of planes generated by fitting multiple 5 cm × 5 cm facets to a SfM generated point cloud. The performance of the method is assessed for two different cameras (GoPro Hero4 and Sony NEX7). Results showed that for highly dense populations (17 colonies/m^2), the SfM-method had lower accuracies in estimating the gorgonians density for both cam-

[1]Palma, M., Rivas Casado, M., Pantaleo, U., Pavoni, G., Pica, D. and Cerrano, C., 2018. SfM-Based Method to Assess Gorgonian Forests (*Paramuricea clavata* (Cnidaria, Octocorallia)). Remote Sensing, 10(7), p.1154.
The spelling of the original published manuscript has been adjusted to fit the format of this thesis.

eras (60% to 89%) than for medium to low density populations (14 and 7 colonies/m^2) (71% to 100%). Results for the validation of the method showed that the correlation between ground truth and SfM estimates for maximal height, maximal width and fan surface were between $R^2 = 0.63$ and $R^2 = 0.9$, and $R^2 = 0.99$ for coenenchymal surface estimation. The methodological approach was used to estimate the biomass of the gorgonian population within the study area and across the coralligenous habitat between −25 to −40 m depth in the Portofino Marine Protected Area. For that purpose, the coenenchymal surface of sampled colonies was obtained and used for the calculations. Results showed biomass values of dry weight and ash free dry weight of 220 g and 32 g for the studied area and to 365 kg and 55 Kg for the coralligenous habitat in the Marine Protected Area. This study highlighted the feasibility of the methodology for the quantification of *P. clavata* metrics as well as the potential of the SfM-method to improve current predictions of the status of the coralligenous habitat in the Mediterranean sea and overall management of threatened ecosystems.

Keywords: animal forest; point cloud classification; Good Environmental Status; environmental accounting; conservation

4.1 Introduction

The term animal forest refers to the underwater population of suspension feeders mainly represented by sponges, cnidarians and bivalves which are well known for enhancing the morphological complexity of the seascape and structuring the habitat of the communities, thus promoting their functionalities Sánchez (2015). In the Mediterranean Sea, animal forests are well represented by several octocoral species such as the gorgonian *Paramuricea clavata* (Risso, 1826). This is a slow-growing, long-lived and low fecundity species which forms dense forests along outcrops, cliffs and biogenic substrates (Ballesteros, 2006) from −15 m to −200 m depth (Rossi, 2013; Gori et al., 2017). *P. clavata* is of special interest in coralligenous habitats because its canopy reduces the range of environmental variability and supports key associated biota (Rossi, 2013; Valisano et al., 2016; Ponti et al., 2016). The annual linear growth rate for the species ranges between 2.7 cm and 3.0 cm, with larger rates observed for smaller colonies (Mistri and Ceccherelli, 1994). The shape of the fan, its growth and orientation adapt to local water current regimes, with the maximal filtration surface always opposing the water flow to maximize feeding efficiency (Grigg, 1972). In return, the drag effect of the fans promotes particle retention, this supporting both invertebrate and vertebrate and favoring the trophic energy transfer between benthos and plankton (Gili and Coma, 1998). As cold-affinity species, *P. clavata* has a high sensitivity to thermal stress (Previati et al., 2010; Vezzulli et al., 2013) and is therefore considered an indicator species of climate effects on benthic assemblages (Linares et al., 2008b). In the last decades, the gorgonian forests in the Mediterranean Sea have been affected by mass mortality events triggered by water temperature anomalies that have led to functional changes in the coralligenous habitat, and to local extinctions of the species in shallow waters (Cerrano et al., 2000; Linares et al., 2008c; Cerrano and Bavestrello, 2008, 2009; Garrabou et al., 2009; Vezzulli et al., 2010; Huete-Stauffer et al., 2011; Santangelo et al., 2015; Ponti et al., 2016). Moreover, the short larval dispersion of *P. clavata* could inhibit genetic exchanges between populations increasing their genetic isolation and limit the species recovery to mass mortality events (Mokahtar-Jamaï et al., 2011).

Multiple structural, morphological and biomass metrics have been used to describe the status (or quality) of gorgonian forests (Coma et al., 1995; Mistri and Ceccherelli, 1994; Coma et al., 1998; Cerrano et al., 2005). For example, the linear growth and density of colonies, the basal diameter, and the coenenchymal ash free dry weight inform about the population's structure, the secondary production and the growth, which in combination with the sex ratio and the characteristics of the gonads (number, dimension and dry weight) provides insight into the population's conservation status and the state of evolution (Mistri and Ceccherelli, 1994; Coma et al., 1995; Mistri, 1995; Cerrano et al., 2005). The rectangular fan surface, calculated as the product of the maximal height and the maximal width of the fan, informs about the age of the colony (Weinbauer and Velimirov, 1995), whereas the epibiosis typology and coverage of the colonies highlight the intensity of the mechanical impacts that the colonies have been exposed to (Cerrano et al., 2005). These metrics are therefore critical to (i) monitor changes in the population structure over time (Linares et al., 2008b; Rossi, 2013), (ii) quantify the magnitude of environmental disturbances (Deter et al., 2012) and (iii) assess the recovery capacity of the populations (Santangelo et al., 2015).

In recent years, the up-take of new technologies has supported researchers and surveyors with the collection of in-situ data. Structure from Motion (SfM) photogrammetry based methods are perhaps the most successful example within the context of benthic community mapping (Figueira et al., 2015; Ferrari et al., 2017; Palma et al., 2017). SfM is a topographic survey technique for the reconstruction of real scale three dimensional models of subjects or scenarios, using imagery collected at unknown camera positions (James and Robson, 2012). It enables non-destructive, repeatable measurements and facilitates rapid sampling (Figueira et al., 2015). Applications of SfM surveying methods in terrestrial and seascape environments have provided accuracies and resolutions comparable to more sophisticated technologies (e.g., laser scanning) (Wallace et al., 2016; Palma et al., 2017) and therefore, show great potential for the estimation of gorgonian structural and morphological metrics. The accuracy of SfM in estimating habitat complexity and morphometries of massive organisms and branched hard corals has been recently assessed by other authorsm (Ferrari et al., 2017; Raoult et al., 2017; Bryson et al., 2017; Royer et al., 2018) but none previously characterized erected and branched soft corals such as gorgonian species, even though SfM could provide an effective way forward towards assessing colonies' sizes and density, as well as biomass across habitats. With an increasing need to rapidly characterize gorgonian size, density and biomass being more prominent than ever under an economically constrained scenario and increased antrophogenic and climate pressures, the potential of SfM methods to fill this gap in knowledge cannot be left unexplored.

In Palma et al. (2017), we developed an SfM based framework for the design of robust monitoring programmes of African coral reefs. Here, we propose a method for the estimation of density, abundance and key *P. clavata* morphometrics in gorgonian forests through segmentation and analysis of scaled point clouds generated by SfM photogrammetry. This is achieved through the following objectives: 1—To develop a SfM based framework for the automated and accurate estimation of *P. clavata* density, abundance, maximal height, maximal width, fan surface and biomass; 2—To assess the performance of the SfM method using two cameras representative of different market segments. 3—To demonstrate the usefulness of the method for the estimation of the gorgonian forests biomass within the Marine Protected Area of Portofino (Punta del Faro, Italy); 4—To discuss the relevance of the proposed method in line with current practice in gorgonian forest monitoring and its implications for future *P. clavata* research and management.

4.2 Materials and Methods

4.2.1 Study Site

The study site is located in the Marine Protected Area of Portofino (Punta del Faro, Italy) (44.298414N, 9.218549E, WGS84) and extends along 52 m^2. The sampling was carried out between −32 m to −36 m along the West-East oriented cliff of Punta del Faro (Figure 4.1). In the area, the gorgonian forest underwent four consecutive mass mortality episodes in 1999, 2003, 2008 and 2013 that led to a progressively fragmented distribution of the colonies with increasing depth and the species extinction above −20 m (Cerrano and Bavestrello, 2008; Garrabou et al., 2009; Huete-Stauffer et al., 2013).

Figure 4.1: The study site in the Marine Protected Area of Portofino (Punta del Faro, Italy). (**a**) The border of the Marine Protected Area; (**b**) a detailed view of the benthic biocenosis mapped in the location of the study site using shape files available from Diviacco (2009); (**c**) 3D view of the seabed around the study site at Punta del Faro (white polyline) generated via SfM using imagery collected on site.

4.2.2 Data Collection

4.2.2.1 Pilot Study on Gorgonian Population Structure

A pilot study was carried out to characterize the gorgonian population structure within the case study area and inform on whether further survey campaigns should consider stratification of the sampling within the study site. Standard sampling quadrats ($n = 14$, 0.5 m × 0.5 m) were used to record (i) the density of the colonies per quadrat, (ii) the maximal colony height, and (iii) the maximal colony width (Pergent, 2011; Lepareur, 2011). The survey showed that *P. clavata* had an heterogeneous spatial distribution in the study site and that three different density areas could be identified for the species: high, medium, low. Each density area will be referred to as stratum and the analysis will be performed for all strata.

4.2.2.2 Underwater Imagery Collection

Photogrammetric surveys were performed using two different cameras: (i) a Gopro Hero4 Black Edition (Woodman Labs, Inc., San Mateo, CA, US) and (ii) a Sony NEX7 alpha digital camera (Sony Corporation, Minato, Tokyo, Japan). The two cameras were chosen as they were considered representative of the range of action cameras (Gopro Hero4) and mirror-less cameras (Sony NEX7) currently available on the market. The proposed methodology was validated with respect to both cameras. Both the Gopro Hero4 and the Sony NEX7 cameras recorded nadiral imagery, at a constant ground sampling distance, along four parallel transects traveling from the deeper to the shallower area of the cliff (Figure 4.2a). The cameras were placed at a maximal standard distance of 1.5 m from the substrate and moved along parallel transects.

The Gopro Hero4 had a CMOS sensor and recorded 4000 × 3000 pixels images with the imagery being automatically recorded every second. The Sony NEX7, also equipped with a CMOS sensor, recorded in video format at 50 frames per second, with progressive mode and frame size of 1920 × 1080 pixels (Figure 4.3 and Table B.1). The cameras were equipped with two RGBlue (AOI Japan Co., Ltd, Yokohama, Japan) System01-2 video LED torches with total luminous flux of 5000 lm.

A total of three 3D ground control points were systematically distributed every three metres along the rocky cliff, from West to East, at −34 m. The ground control points consisted of plastic tripods with a calibrated chessboard extension (Figures 4.2a and 4.3). The dimension of each of the ground control points was 22 cm × 22 cm × 22 cm. The chessboard extension was 21 cm long by 8 cm wide. The 52 m^2 study site was sampled within six minutes under clear and steady sea water conditions.

4.2.2.3 Gorgonian Colony Density and Morphometry Measurement

In each stratum, the colonies larger than 15 cm falling within three randomly distributed 1 m × 1 m quadrats, were counted in-situ. This count data constituted the "abundance" ground-truth dataset (Section 4.2.4) which was used to validate the SfM-estimated density and abundance (Section 4.2.5). In each quadrat, two colonies were photographed with a dimensional reference (Figure 4.2b) and the morphometries measured by photo analysis. This data represented the "morphometric" ground truth dataset which was used to validate the SfM- estimated colonies morphometries (maximal height, maximal width and fan planar surface) (Section 4.2.5). The images taken for that purpose were not used in the SfM processing.

4.2.2.4 Relationship between Planar Surface Area and Weight

Nine colonies of various sizes were collected outside of the study area but as close as possible to the Marine Protected Area borders and at the same depth as the study area. The colonies were dried, photographed in a cubelite following the SfM approach (Figures 4.2c and Figure B.1) and the coenenchymal surface area (A) measured. This constituted the laboratory ground truth and was used to validate the coenenchymal surface estimated through SfM (Section 4.2.5).

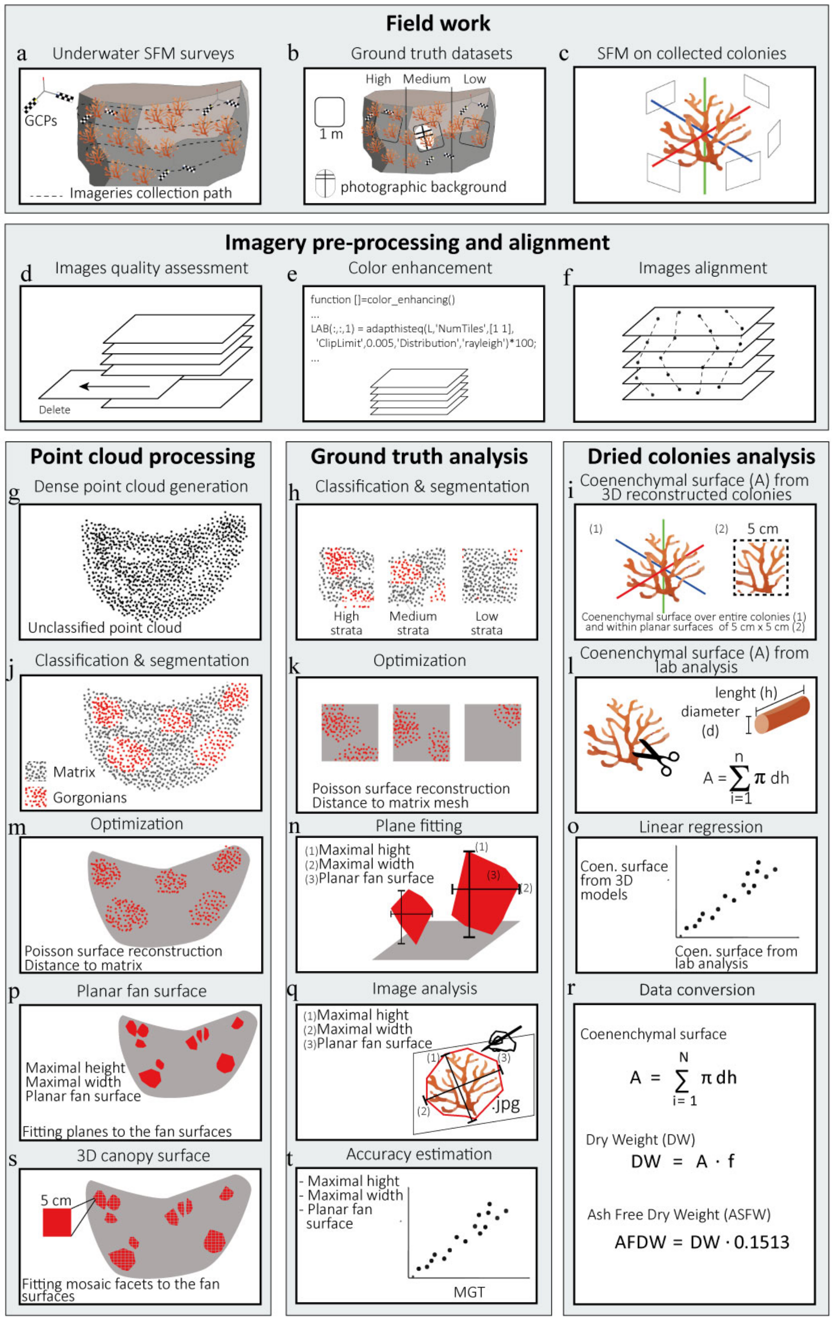

Figure 4.2: Schematic diagram summarizing the workflow including data collection, imagery pre-processing and alignment, point cloud processing, ground truth data analysis and the analysis of the dried colonies (i.e., biomass).

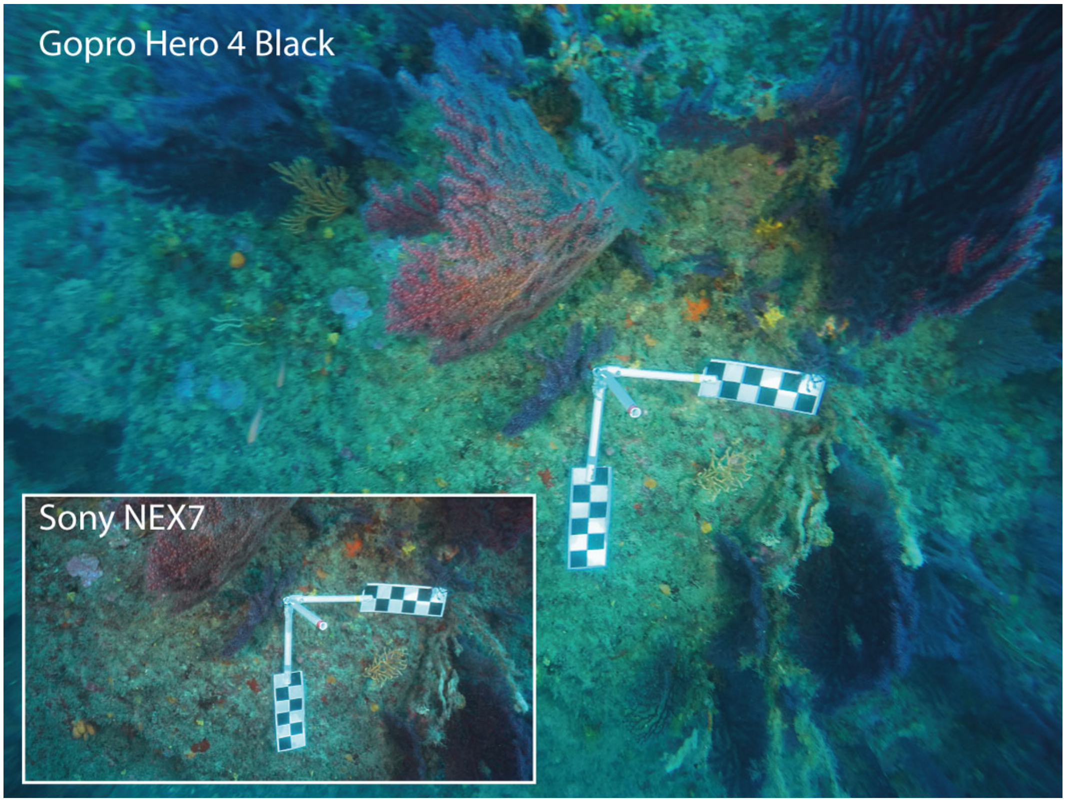

Figure 4.3: Image footprint obtained with the Gopro Hero4 Black Edition (Woodman Labs, Inc., San Mateo, CA, USA) and the Sony NEX7 alpha (Sony Corporation, Minato, Tokyo, Japan) with both cameras being triggered at the same point over a ground control point. The image depicts the difference in frame size and in extent covered by each frame. The dimension of each of the ground control points was 22 cm × 22 cm × 22 cm. The chessboard extension was 21 cm long by 8 cm wide.

The branches were divided into fragments and the height and the diameter of each fragment were measured (Mitchell et al., 1992; Mistri and Ceccherelli, 1994). The total A of each colony was estimated as:

$$A = \pi \sum_{i=1}^{N} (d_{\mathrm{i}} h_{\mathrm{i}}) \tag{4.1}$$

where i is a given fragment from 1 to the total number of segments (N) for the target colony, d is the diameter and h is the length of the fragments. The dry weight (DW) was calculated as the product of A by a conversion factor (f) specific for *P. clavata* (Mistri and Ceccherelli, 1994) (Table 4.1):

$$DW = A \cdot f \tag{4.2}$$

where f is equal to 0.0047 g cm^{-2} (±0.0020 SD).

The ash free dry weight ($AFDW$) represents the biomass weight remaining after oxidation of the organic component at high temperature.

$$AFDW = DW \cdot 0.1513 \tag{4.3}$$

The resulting dry weight and ash free dry weight values per m^2 were directly used to derive their content overall to the whole study site (52 m^2) and the full extent of the coralligeneous habitat along the Marine Protected Area of Portofino (Punta del Faro, Italy) (86,300 m^2) (Figure B.2 a,b).

Table 4.1: Description of the metrics calculated from the Structure from Motion (SfM) based approach presented in this paper. A dash line separator is used for "Maximal height" because it is a metric used both in structural and morphological metric categories.

Categories	Metrics	Tool	Unit	Description
Structural	Abundance	CloudCompare, Facet	count	Number of colonies within the study area
	Density	CloudCompare, Facet	count	Number of colonies per square metre
Morphology	Maximal height	CloudCompare, Facet	cm	Maximal vertical extension of the segmented colony.
	Maximal width	CloudCompare, Facet	cm	Maximal horizontal extension of the segmented colony.
	Planar fan surface	CloudCompare, Facet	cm^2	Surface of the polygon generated by fitting a single plane to the colony's point cloud.
	3D canopy surface	CloudCompare, Facet	cm^2	Mosaic of planes generated by fitting multiple facets dimensioned 5 cm × 5 cm within the point cloud.
	Coenenchymal surface (A)	Meshlab, Screened Poisson Surface Reconstruction	cm^2	Total tissue surface of the gorgonian calculated through the generation of the 3D model of the colony.
Biomass	Dry weight (DW)	Conversion factor	g	Weight of the dry coenenhymal tissue of the gorgonian estimated through the conversion from surface unit (cm^2) to weight per surface unit (g cm^{-2}) (Mistri and Ceccherelli, 1994)
	Ash Fee Dry Weight (AFDW)	Conversion factor	g	Weight of the inorganic component of the coenenchymal tissue estimated through the conversion from DW (g) to Ash Free Dry Weight (AFDW) (g) (Mistri and Ceccherelli, 1994)

4.2.3 Image Processing

All the imagery collected underwater was screened and chosen for photogrammetric processing when having suitable image quality and consecutive spatial coverage (Palma et al., 2017) (Figure 4.2d–f and Table 4.2). The selected images were processed within Matlab (Mathworks, Natick, MA, USA) using the Contrast Limited Adaptive Histogram Equalization (CLAHE) algorithm (Zuiderveld, 1994) to enhance the luminosity, sharpness and contrast of the images (Figure 4.2e). The uncalibrated images were then processed using AgiSoft Photoscan software (Agisoft LLC., St. Petersburg, Russia) to estimate the relative camera poses and generate dense clouds. For consistency and comparability purposes, both Gopro Hero4 and Sony NEX7 datasets were aligned together generating a sparse point cloud and then separated to create the dense point cloud under the same settings (Figure 4.2f). The photogrammetric processing was performed with an Asus laptop (Beitou District, Taipei, Taiwan) with an Intel Core i7-3630QM 2.40-GPz processor (Intel Corporation, Santa Clara, CA, USA), 16 Gb RAM and NVIDIA Geoforce GTX 670M (NVIDIA Corporation, Santa Clara, CA, USA) graphic card. The overall procedure for the two cameras combined required a total of 10 h (Figure 4.2g). The resulting dense point clouds were sub-sampled at 1 mm, scaled using the ground control point and cleaned of extremes and outliers using the software CloudCompare (Girardeau-Montaut, 2014). Then, the clouds were clipped using a polygon mask to a common surface of 52 m^2. The dense point clouds (and derived population structure and morphometry) obtained by processing the imagery of each camera, were compared to determine the sensitivity of the proposed SfM method to the equipment used. For that purpose, the closest point distance between the two clouds was calculated. For each point of the second point cloud, the closest point from the first point cloud and the distance between them was recorded (Lague et al., 2013). Similarly, the point frequency per distance class (1 cm) and the average value were also calculated. The imagery collected in the cubelite from the dried colonies was also processed to generate dense point clouds. The Screened Poisson Reconstruction filter in Meshlab, ref. (Kazhdan and Hoppe, 2013) was applied to the cleaned and scaled dense point cloud to generate an accurate coenenchymal surface model of each colony

(Figures 4.2i and 4.4).

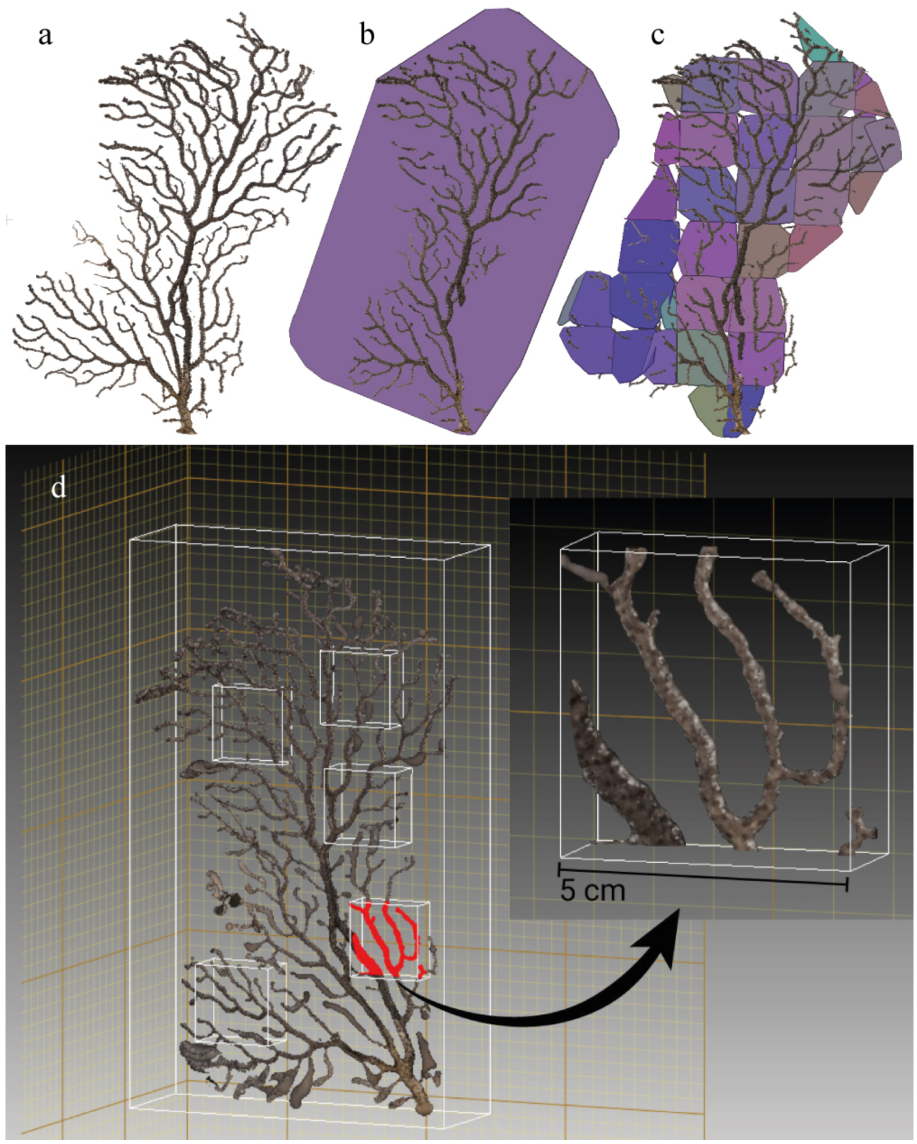

Figure 4.4: (**a**) the point cloud generated from SfM on one of the dried colonies; (**b**) the planar fan surface interpolated over the colony; (**c**) the mosaic of planes representing the filtering gorgonian surface; (**d**) the 3D reconstruction of the colony's coenenchymal surface with the detail of one quadrat sample of 5 cm × 5 cm.

Table 4.2: Summary of key image processing outcomes using the Gopro Hero4 Black Edition (GP) and the Sony NEX7 alpha (SN).

	GP	**SN**
Number of collected images	365	333
Number of processed images	325	321
Processing time (h)	5	5
Colonies detected	103	71
Point cloud density (pts m^{-2})	120,442	209,269
Nominal pixel dimension (mm)	0.558	0.741

4.2.4 Data Analysis

4.2.4.1 SfM Estimation of Gorgonian Density Colony and Morphometry

Classification and segmentation techniques were used to estimate the population structure (density, maximal height) and morphometries (maximal height, maximal width, planar fan surface, 3D canopy surface) (Table 4.1). These methods were applied to the generated point clouds to distinguish the background matrix and the gorgonians point clouds. The classification was performed using the CANUPO classifier (Brodu and Lague, 2012) available as a plugin for CloudCompare (Girardeau-Montaut, 2014), with the algorithms trained through the manual selection of points that represented both the "matrix" and the "gorgonian" classes (Figure 4.2h,j).

The classifier used a multi-scale calculation around each point analysing the 1D (points set along a line), 2D (points forming a plane) and 3D (volume relation) between each point within the cloud (Figure 4.2h,j). The segmentation of the "gorgonian" point cloud was carried out in Meshlab (Cignoni et al., 2008) directly after classification by selecting and deleting from the unclassified point cloud, all the points closer than 5 cm to the mesh fused from the "matrix" point cloud (Figures 4.2m and 4.5a,b). Colony abundance, density and morphometries were calculated from the "gorgonian" point cloud using the Facet Plugin (Dewez et al., 2016) of CloudCompare (Girardeau-Montaut, 2014). This plugin, developed to study the geological planar facets (Figure 4.4) of rock out-crops, processed the point cloud twice. The first time, to count the gorgonian's fans by approximating them to elementary planar objects (Figures 4.2p and 4.5c) and to calculate the maximal height, maximal width and planar fan surface (Table 4.1). The second time, to divide the point cloud into a mosaic of facets with maximal dimension of 5 cm × 5 cm (Figure 4.2s) from which the 3D canopy surface (Table 4.1, Figures 4.4c and 4.5d) of the population was estimated as the sum of the individual facet surfaces.The facet dimensions (5 cm × 5 cm) were determined based on the size of the smallest colonies considered in the study site.

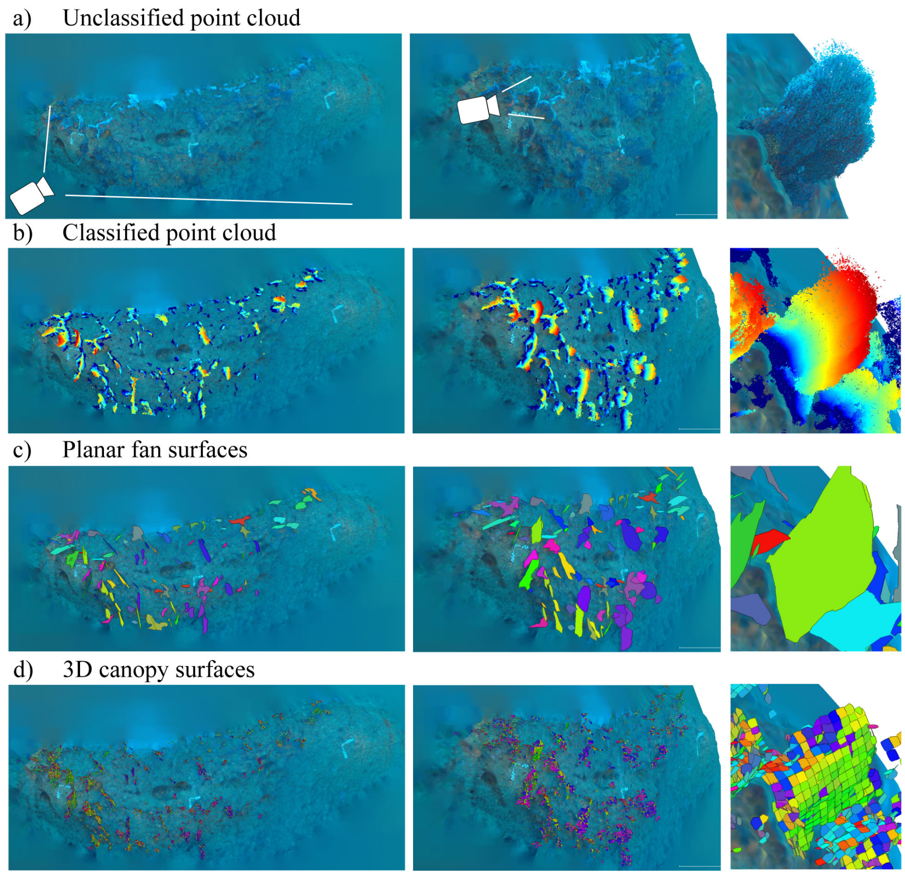

Figure 4.5: Three spatial representations of: (**a**) The unclassified point cloud (blue); (**b**) the point cloud segmented into matrix (blue background) and gorgonians (other colours); (**c**) the planar surfaces fitted to the point cloud and representing the colonies (matrix in blue and gorgonians in multiple colours); (**d**) the 3D canopy surface generated by fitting facets with a maximal dimension of 5 cm × 5 cm to the point cloud. The three spatial representations include (from left to right): the orthoimage, a prospective view from the Western point of the case study area and a close-up view of a gorgonian.

4.2.4.2 Dried Colonies Analysis

The morphometries of the morphological ground truth dataset and of the dried colonies, with the exception for the filtering fan surface, were estimated from the images collected with the dimensional reference (Figure 4.2q) and manually measured using the software ImageJ (Schneider et al., 2012). The coenenchymal surface area (A) was calculated as the sum of the surface area within each facet composing the 3D canopy surface. Within each facet, the average coenenchymal surface area was obtained from the nine dried colonies 3D-reconstructed that were randomly sampled using 56 quadrats (5 cm × 5 cm) (Figure 4.2i). According to the colony size, the sampling was replicated from three to nine times. The coenenchymal surface was then computed using the geometry filter in Meshlab software (Figure 4.4). The average colonies DW and the average AFDW were estimated using Equations (2) and (5).

4.2.5 Validation

Colony density and abundance estimated by the SfM were compared against the abundance ground truth dataset by counting the identified colonies within the 1 m × 1 m quadrats across the three density strata. The SfM-estimated morphometries were validated against the morphological ground truth dataset and a linear regression model performed to assess the accuracy of morphometries estimation (Figure 4.2t). The SfM-estimated coenenchymal surface estimation (A) was compared against the laboratory ground truth dataset and its accuracy calculated by applying a linear regression model. A residual analysis was carried out for all linear regression models to assess the validity of the normality, homoscedasticity and independence assumptions (Figure 4.2o).

4.3 Results

A total of 325 and 321 images were processed respectively by the Gopro Hero4 and Sony NEX7 cameras. Tables 4.2 and Table B.2 summarize the total number of frames included in the photogrammetric processing pipeline. The point clouds generated over the study area contained 10.9 million and 6.2 million points each and the cloud to cloud distance was on average 3 cm ± 1.8 SD. Over 98% of the points presented a cloud to cloud distance smaller than 8 cm with an average distance between the two point clouds representing the gorgonians of 1.6 cm ± 5.3 SD.

4.3.1 SfM-Population Structure Estimates and Validation

The gorgonian population had a mean density of 12.4 colonies m^{-2} (Table 4.3, pilot study). The densities ranged between 6.4 colonies m^{-2} to 16.8 colonies m^{-2} across the three strata (Table 4.3). The species distribution was denser along the Western side of the cliff and sparser towards the Eastern side. The SfM estimated higher abundance of *P. clavata* using the Gopro Hero4 (103 colonies) than the Sony NEX7 camera (71 colonies) (Table 4.2). The density estimated by SfM-method ranged between 3.3 colonies m^{-2} to 14.0 colonies m^{-2} across the three strata (Table 4.3). The Gopro Hero4 showed higher accuracies (89%, 81%, 100% in high, medium and low density strata respectively) than the Sony NEX7 camera (60%, 71%, 77% in high, medium and low density strata respectively) across strata (Figure B.2). When compared to the abundance ground truth dataset, the SfM-density estimates demonstrated an overall systematical underestimation for both cameras and across strata. The Gopro Hero4 showed lower departures from the abundance ground truth dataset values, <2.0 colonies m^{-2}, whereas the Sony NEX7 camera presented larger departures, <6.4 colonies m^{-2} (Table 4.3).

Table 4.3: Mean gorgonian density (colonies m^{-2}), density range (minimum to maximum in number of colonies per quadrat) and abundance (number of colonies) within each stratum in the study area. Note that all the quadrats are 1 m × 1 m, except for the pilot study where the quadrats are 0.5 m × 0.5 m. Values in brackets denote the standard deviation. SfM stands for Structure from Motion. GP and SN stand for Gopro Hero4 and Sony NEX7, respectively. AGT stands for abundance ground truth dataset.

	Metrics	**High Density**	**Strata Medium Density**	**Low Density**
Pilot study 0.5 m × 0.5 m	Average Range	16.8 (±7.6) 1–7	14.0 (±4.0) 1–4	6.4 (±9.2) –3
AGT 1 m × 1 m	Average Range	15.7 (±1.9) 13–17	10.3 (±1.2) 7–12	4.3 (±1.2) 3–6
SfM-GP 1 m × 1 m	Average Range	14.0 (±1.4) 13–16	8.3 (±0.9) 7–9	4.3 (±1.2) 3–6
SfM-SN 1 m × 1 m	Average Range	9.3 (±1.2) 8–11	7.3 (±2.1) 5–10	3.3 (±0.5) 3–4

The study site was dominated by colonies of small/ medium sizes (Figure 4.6). The colonies recorded by the Gopro Hero4 and the Sony NEX7 cameras ranged between 10–58 cm in maximal height, 7–55 cm in maximal width and 60–1770 cm^2 in planar surface (Table 5). The comparison of the SfM estimates with the morphological ground truth dataset values showed that both cameras underestimated maximal height measures by 2.6 cm (Gopro Hero4) and 1.9 cm (Sony NEX7). The difference between the morphological ground truth dataset and the SfM cameras ranged between −11.1 cm and 12.6 cm for the Gopro Hero4 and between −7.9 cm and 9.1 cm for the Sony NEX7, where negative values indicated underestimation. The mean maximal width was also underestimated by 3.6 cm (Gopro Hero4) and 2.5 cm (Sony NEX7). The difference between the morphological ground truth and the SfM estimates ranged from −9.2 cm to 13.0 cm (Gopro Hero4) and −14.7 cm and 14.7 cm (Sony NEX7).

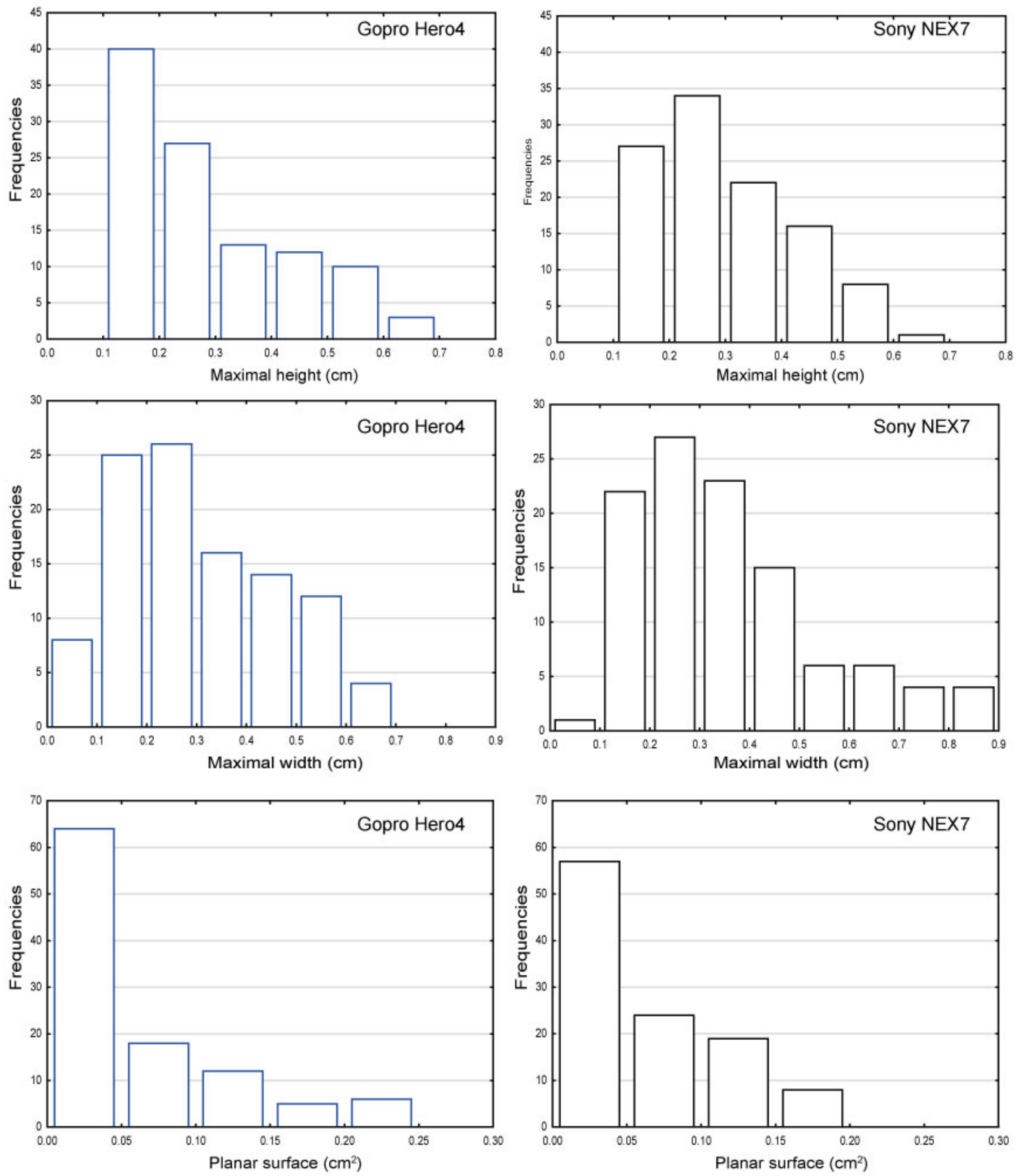

Figure 4.6: Histogram of the morphometric values obtained for the SfM method across the study site of Punta del Faro (Portofino, Italy).

The value for the mean planar fan surface was underestimated by 153 cm^2 (Gopro Hero4) and 53 cm^2 (Sony NEX7). The difference between the morphological ground truth and the cameras ranged between −276 cm^2 and 533 cm^2 (Gopro Hero4) and

−552 cm^2 and 420 cm^2 (Sony NEX7). Finally, the results of the linear regression analysis between the estimated SfM morphometric and the morphological ground truth showed that the Gopro Hero4 camera was more accurate than the Sony NEX7 in estimating the maximal width and planar fan surface (R^2 = 0.8, R^2 = 0.9) whereas the Sony NEX7 provided better estimations of maximal height measures (R^2 = 0.8) (Figure 4.7).

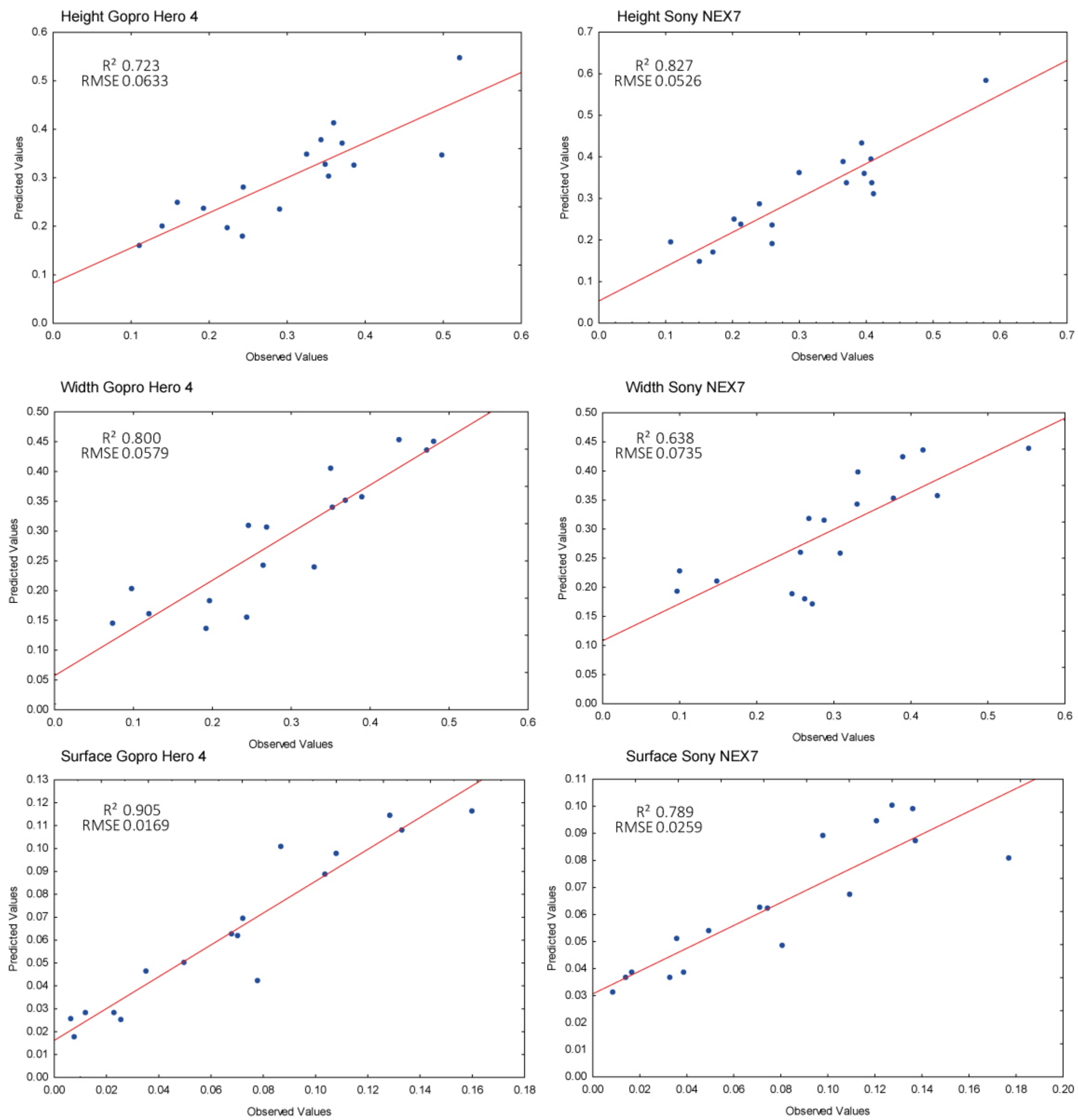

Figure 4.7: Correlation between the SfM method vs. the ground truth data for each of the morphometrics calculated and cameras considered: (**a**) Gopro Hero4 and (**b**) Sony NEX7. Height refers to maximal height (m), width refers to maximal width (m) and surface refers to planar fan surface area (m^2).

4.3.2 SfM-Biomass Estimation and Validation

The mean coenenchymal surface obtained from the 56 sampling quadrats (5 cm × 5 cm) was 23.24 cm^2 (±0.06 SD) and corresponded to a coenenchymal dry weight of 0.109 g (±0.0750 SD) per facet. The total coenenchymal surface, derived from the 3D canopy surface estimated across the study site, was 4.74 m^2 (Gopro Hero4) corresponding to 1896 facets and 4.61 m^2 (Sony NEX7) for a total of 1844 facets (Figure 4.5d). Lower estimates of 3D canopy surface were obtained with the Sony NEX7.

The linear regression analysis showed a strong correlation between the laboratory ground truth dataset and SfM R^2= 0.99 (Figure 4.8). SfM overestimated the calculation of the coenenchymal surface (Table 4.4): the differences with respect to the laboratory ground truth dataset varied between 24.6 cm^2 and 341.2 cm^2. The nine colonies used for dry weight estimation showed sizes comprised between the small colonies dimensions (15.1 maximal height, 9.9 cm maximal width, 115.6 cm^2 planar fan surface) to the big dimensions (55.6 cm in maximal height, 30.3 cm maximal width, 729.8 cm^2 planar fan surface) (Table 4.5).

The dry weight values calculated from the coenenchymal surfaces, are reported in Table 4.4. For the laboratory analysis, the mean dry weight content per colony corresponded to 1.56 g, whereas for the SfM method the value was 2.27 g. The calculated mean adh free dry weight did not differ by more than 0.24 g per colony between the two methods.

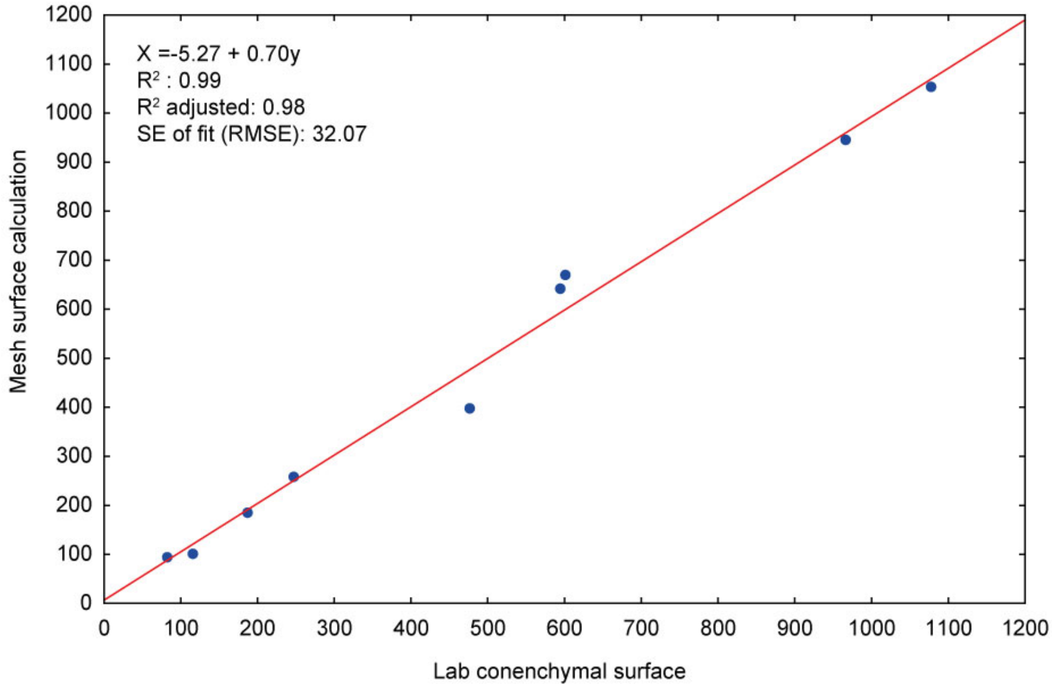

Figure 4.8: Correlation between the coenenchymal surface estimated through the SfM method and the laboratory measurements over the nine dried gorgonian colonies.

Table 4.5: Mean and range of the estimated morphometrics for the colonies sampled in-situ with a dimensional background for each of the approaches considered. Height and width stand for maximal height and maximal width, respectively. N stands for the number of colonies used for the morphometric estimation. MGT stands for Morphometry Ground Truth data set. Within the table, difference refers to the difference between MGT and SfM outcomes. Positive differences represent overestimations.

Study	Metric	N	Mean	Range	Mean Difference	Difference Range
MGT	Height (cm)	17	32.63	14.3–64.7	–	–
SfM-GP		17	30.0	11.1–52.1	−2.63	−11.12–12.57
SfM-SN		17	30.7	10.7–57.8	−1.93	−7.95–9.09
Dry colony analysis		9	30.6	15.1–55.6	–	–
MGT	Width (cm)	17	32.3	12.5–54.3	–	–
SfM-GP		17	28.7	7.3–48.1	−3.63	−9.20–13.04
SfM-SN		17	29.8	9.7–55.2	−2.47	−14.70–14.69
Dry colony analysis		9	18.9	9.89–30.3	–	–
MGT	Plannar fan surface (cm^2)	17	833	120–1640	–	–
SfM-GP		17	680	60–1590	−153.0	−276.4–533.0
SfM-SN		17	780	80–1770	−52.8	−552.2–420.4
Dry colony analysis		9	330	116–730	–	–

4.4 Discussion

The SfM method was developed and applied to *P. clavata* to showcase the direct estimation of population and colony metrics at a large scale. The comparison between both cameras showed high to moderate accuracy between results and ground-truth data, thus supporting the suitability of the presented method for the estimation of the gorgonian metrics by the SfM data processing. A good agreement between Gopro Hero4 and Sony NEX7 (30% approximately as per Table 4.4) was also observed for dry weight and ash free dry weight, thus indicating that the SfM method can be a suitable tool for estimating the indirect contribution of *P. clavata* to local and regional carbon budgets. In this section we discuss the results of the SfM framework on the estimation of *P. clavata* metrics (Section 4.4.1) and the domain of application of the method (Section 4.4.2).

Table 4.4: Summary of morphometric results for the study site. The abbreviations used correspond to: Structure-from-Motion (SfM), laboratory (lab), coenenchymal (coen), Dry Weight (DW) based on (Mistri, 1995), Ash Free Dry Weight (AFDW) and difference (diff). Positive differences represent overestimations.

Colonies	**Units**	**1**	**2**	**3**	**4**	**5**	**6**	**7**	**8**	**9**
Maximal height	cm	24.43	15.07	39.31	19.78	24.12	24.56	38.09	55.65	38.26
Maximal width		12.82	11.53	21.49	9.89	16.02	20.30	30.33	15.74	22.63
Fan surface	cm^2	196.95	115.66	667.76	124.05	226.10	428.86	729.88	609.41	566.55
Coen. surface SfM analysis		186.48	82.72	600.56	115.57	246.48	475.77	966.34	1078.17	601.43
Coen. surface lab analysis	cm^2	121.30	58.13	465.82	61.98	172.88	273.61	660.46	736.99	445.65
Diff. between SfM and lab coen surfaces		65.18	24.59	134.76	53.59	73.6	202.16	305.88	341.18	149.78
Coen. DW SfM analysis		0.876	0.388	2.822	0.543	1.158	2.236	4.541	5.067	2.798
Coen. DW lab analysis	g	0.570	0.273	2.189	0.291	0.812	1.285	3.104	3.463	2.094
Diff. between SfM and lab DW		0.306	0.115	0.633	0.252	0.346	0.951	1.437	1.604	0.704
AFDW SfM analysis		0.133	0.059	0.427	0.082	0.175	0.338	0.687	0.767	0.423
AFDW lab analysis	g	0.086	0.041	0.331	0.044	0.123	0.194	0.470	0.524	0.317
Diff. between SfM and lab AFDW		0.046	0.017	0.096	0.038	0.052	0.144	0.217	0.243	0.107

4.4.1 Estimated Metrics of *P. clavata*

The SfM method (Figure 4.6) showed promising results when estimating *P. clavata* population structure, colonies morphometries and biomass suggesting that the method would be transferable for application on similar erected, plane shaped corals. Across all the sampled quadrats and strata, the accuracy on mean colonies density was greater or equal to 60%. The two cameras performed differently on estimating the morphometries although both showed good to moderate agreement with the morphological ground truth data. The error reported for these metrics accounted for the arbitrary decision on the selection of a 5 cm threshold to segment the "gorgonian" point cloud from the "matrix" point cloud. Lower errors would be expected for a more refined estimation of such a threshold.

The Gopro Hero4 showed higher accuracy than the Sony NEX7 for abundance and density, maximal width and planar fan surface. These results could be explained by the small frame dimension provided by the Sony NEX7 camera when in recording mode (Figure 4.3 and Table B.1), which resulted in clouds with lower number of points. The use of the Sony NEX7 in video recording mode was obliged to ensure an automatic and continuous imagery collection and effective data sampling. The accuracy of the overall method could be improved through the use of cameras in video recording mode that allow for the extraction of frames at frequencies higher than those here presented. The approach will however be limited by the size of the video imagery files collected.

The SfM method allowed for the calculation of the gorgonian planar fan surface based on the planar shape of the gorgonian point cloud. This approach presents an advantage over traditional methods, which usually rely on the product between the maximal height and the maximal width of the colony (Weinbauer and Velimirov, 1995). In this study, we estimated the *Paramuricea clavata* 3D canopy surface using SfM; this is a novel approach that for the first time provides accurate approximation of the gorgonian population surface by interpolating the species point cloud with a mosaic facets of standard maximal dimension (5 cm × 5 cm). The metric provides complementary information to those traditionally used in gorgonian population structure studies (i.e., abundance, density, maximal height, maximal width, fan surface) and further insights about the characteristics of the entire population. The accuracy of the coenenchymal surface achieved by the SfM method and validated through the laboratory analysis was promising, supporting the use of virtual sampling for calculating the colony geometry. The calculations are subject to the inherent error associated with water loss of the interbranches fan surface when drying the individual gorgonian samples. Further research should focus on increasing the accuracy of the proposed method by taking into account the loss in volume of the tissues between coral arms.

The average coenenchymal surface per surface unit was converted into DW and AFDW to obtain the biomass of the gorgonian population in the study area. The two cameras showed similar results (223 g for the Gopro Hero4 and 217 g for the Sony NEX7), this suggesting that biomass estimation is not affected by the camera characteristics and that the Gopro Hero4 and the Sony NEX7 have similar performances in the estimation of the 3D canopy surface.

The SfM method described a mixed-size gorgonian population; few big colonies (maximal height > 40 cm), indicative of greater reproductive organisms, were depicted by both cameras whereas the higher frequencies were identified around small/medium size colonies (maximal height < 30 cm). These results are indicative of populations that are recovering after mass mortality events. Similar findings were reported by previous studies on *P. clavata* population structure that have observed an unimodal and bell-shaped distribution of species size in years following mortality episodes (Linares et al., 2008a; Santangelo et al., 2015; Bramanti et al., 2015). The Sony NEX7 showed higher frequencies for the wider colonies classes (from 50 cm to 90 cm in maximal width) with respect to the smaller number of colonies counted. Regarding the laboratory analysis, the SfM method overestimated the size of the colonies (discrepancy range 24.6–341.2 cm^2) probably in return of the lower accuracy showed in abundance ground truth dataset comparison.

Finally, field SfM sampling required less than 6 m for data collection including deployment and retrieval of ground control points, thus ensuring safe scuba diving condition and high-quality data. The sampling approach did not require the manipulation of gorgonians, thus minimizing the risk of seabed contact and as a consequence damage to other benthic organisms (Milazzo et al., 2002). The time required for images alignment was ¡ 5 h whereas only 4 h of post-processing time were required to extract the morphometry values. Overall, the operational times were suitable for a fast estimation of the required values, with the times provided improving as the user gets acquainted with data and software manipulation.

Although the point clouds generated with the imagery from both cameras were highly dense (over 6 million points) and only differed an average distance of 1.6 cm (±5.3 cm SD) for the points representing the gorgonians. This discrepancy propagated in the calculation of the population structure and morphometries. The uncertainties associated to the species population structure and morphometry likely affected the estimation of the biomass (dry weight and ash free dry weight). Overall, the SfM framework can provide accuracies suitable for traditional population structure, morphometric and biomass studies (Rossi et al., 2011; Linares et al., 2008a), and is flexible to support finer gorgonian measurements based on the projection of images over point cloud fitted planes (Pavoni et al., 2018).

4.4.2 Domain of Application

This study proposes a SfM-based method which allows the estimation of gorgonian population structure, morphometries and biomass, and supports scientist and marine managers in fulfilling the requirements of national and European policies (Commission, 2011; Franzese et al., 2015) on ecosystem functioning assessments (i.e., Environmental accounting). *P. clavata* was chosen as the species because of its role in structuring the coralligenous habitat and being an indicator of climate change effect, thus an assessment of its conservation status and its contribution for environmental accounting is of key relevance to managers and scientists alike. Several studies have reported that gorgonian populations, recovering after mass mortalities events, tend to reach a new state of equilibrium with lower density and trophic energy (Linares et al., 2008a; Coma et al., 2009; Cerrano et al., 2010; Santangelo et al., 2015), this implying that the ecological and the economic value of coralligenous habitat can be negatively affected. In the selected areas across the Portofino MPA (Figures B.2,B.3), the contribution of *P. clavata* was calculated to be between 370.4 kg (Gopro Hero4) and 360.5 kg (Sony NEX7) of DW and 56 kg and 54 kg of AFDW, not a negligible contribution in terms of trapped organic matter. As highlighted by studies on ecosystem functions, heterotrophic habitat dominated by corals can contribute to carbon turnover and nutrient recycling (White et al., 2012; Cathalot et al., 2015; Le et al., 2017) and our approach provides a way forward towards the accurate estimation of the turned organic carbon by animal forests in the Mediterranean Sea. However, the contribution of the phylum Cnidaria in environmental accounting approaches has not been calculated yet (Franzese et al., 2015, 2017; Picone et al., 2017). Our approach is transferable and can therefore assist scientists and managers by providing a method to quantify the essential gorgonian forest metrics and to prioritize actions over spatial scales relevant for the MPAs management even supporting existing conservation indexes on coralligenous habitat (see Sartoretto et al. (2017)). Finally, existing scientific literature suggests that knowing the structure and morphometry at population level is fundamental to assess the conservation status of marine habitats and their ecosystem functions. There is an increasing emphasis on addressing innovative technologies to monitor marine habitats to allow overcoming spatial resolution and temporal data limitations; our SfM framework can support scientists and marine managers as a tool to target key-habitat species and thus provide the greatest benefit to prioritization plans.

4.5 Conclusions

The methodology here presented highlights the potential of SfM based methods for fast and reliable monitoring of demography and morphometry of gorgonian forests. Of particular relevance is the development of the method for very slow growing and threatened species such as gorgonian colonies that are indicators of the effects of climatic anomalies on the coralligeneous community. Results show that the method could complement traditional sampling methods by enabling effective long-frequency wide-area monitoring of gorgonian forests, enhancing current management practices of and compliance with legislative requirements for coralligeneous areas (including MPAs).

Acknowledgments

This research was funded through the scolarship EUREKA; European Social Funds (FSE), Programma Operativo Regionale (POR) 2014/2020 Regione Marche (Italy) grant number 0020404 and Cranfield University. We thank the Visual Computing Laboratory, Research laboratory of ISTI-CNR (Italy), for providing full support for the development of this research. Special thanks go to Ilaria delle Mura and Fabio Benelli for the underwater support during the surveys and to Carlos Gomez for the photographic support. We also thank the reviewers that helped shape and improve the final version of this manuscript with their useful comments.

Chapter 5

Discussion and Conclusion

5.1 Introduction

Previous chapters have described the application of SfM-based methods to marine habitats and their advantages. SfM demonstrated to be a flexible, affordable and reliable technology for rapid surveys, providing informative data to support spatial analysis of ecological communities and to investigate the effects of natural and human stressors. Considering SfM-based approaches in management plans could bring a major benefit to assess pressures on marine ecosystems. But, to develop adequate management strategies, advancing standard SfM-methods to marine environments, are required to improve data collection and analysis at relevant spatial scale for conservation.

To this end, a novel and transferable approach was developed to assess the spatial composition of benthic communities using SfM ortho-mosaics and uncover the scale-specific effects that determine sample representativeness (Objective 1) and applied on coral reefs to investigate the effects of human and environmental pressures (Objective 2). Finally, a new method is implemented to investigate the population structure (e.g. maximal height, abundance) and biomass of benthic tree-shaped species (i.e. gorgonians) in coralligenous habitat and to support environmental accounting calculation (Objective 3). This last chapter of the thesis will reflect on how SfM-based approaches can support marine management in coral reefs and coralligenous systems through the implementation of standardised methods for assessing benthic composition and organisms morphometrics at seascape scale.

5.2 Marine management plans and SfM

Internationally, there are several strategies adopted to provide general knowledge of distribution, species composition and functioning of calcareous bio-concretions UNEP-MAP-RAC (2008). However, most actions regard individual-national-based efforts limited in spatial and temporal resolution and extent, or lack of coordinated standard method. Reasons for this are technology limitation on high-resolution ecological information and costs, complicating our ability to formulate guidelines that can be universally applied. Only when we are able to capture spatial and temporal variations of the benthic community, it is possible to effectively allocate resources for conservation and human-impact prevention UNEP-MAP-RAC (2008).

By assessing the spatial composition of benthic marine communities and associated morphometrics at representative spatial scales using standardized SfM-based approaches, potential issues can be identified that require management interventions (Sections 5.2.1, 5.2.2).

A starting point for management to use the SfM methods developed in this thesis is considering the prioritization of sites with a seascape approach. By focusing on strengthening the resilience of marine ecosystems at seascape scale, marine management can optimise its good and services as new environmental challenges arise Magris et al. (2014); Bellwood et al. (2004). This means collecting quantitative, georeferenced and representative samples (Chapter 2) and including compositional data providing a functional perspective (Chapter 3). The SfM-based seascape approach leads to a more inclusive understanding of the short, medium and long-term implications of benthic changes to management actions, overcoming technical limitations (i.e. decompression time and diver performances in deep waters).

At the regional scale, SfM approaches can be included into the current monitoring activities required by the European Marine Strategy Framework Directive (MSFD 2008/56/EC) and the Barcelona Convention Decision (IG.21/9, 2016; Parliament and the Council, 2008). The basic scheme of data collection, in fact, includes periodic monitoring of reference parameters or indicators. To this end, data collected using SfM will provide per se information on structural and functional parameters (i.e. the degree of complexity of coralligenous habitats, Chapters 3 and 4), and impacts of disturbances (i.e. fishing nets).

In this context, marine management would be an opportunity for marine research to access information-rich data being collected in time. Marine management, whose design is informed by a scientific understanding of ecological processes at the seascape, can provide to science a wide range of fine resolution data with more intensive sampling at a local scale to evaluate human and natural factors driving community changes. Also, temporal data so obtained could facilitate the development of indicators for the monitoring of the Good Environmental Status (GES) within the Marine Strategy Framework Directive and COP18 EcAp Decision (IG.21/9, 2016; Parliament and the Council, 2008).

To this end, community involvement could take many different forms (i.e. recent started 4Dive, Section 5.3.2), promote awareness and actions across broad geographic scales. Especially at this stage that interdisciplinary collaboration with the academic institutions would be beneficial to understand the extent at which marine management actions promote habitat conservation.

5.2.1 Scuba diving

Scuba diving at Ponta do Ouro Partial Marine Reserve (Mozambique) may have major impacts on the ecological status of local reefs in the near future. Research has demonstrated that scuba diving might have different effects on coral reefs, this is to be considered for determining management guidelines to limit the access upon individual reefs (Hawkins and Roberts, 1997; Lyons et al., 2015; Roche et al., 2016). Based on the results of the SfM framework, coral communities at PPMR show different characteristics reflecting organisms resistance and benthic communities resilience to scuba diving and environmental conditions. The study is the first providing relevant information for studying changes in composition and functionality across reefs at PPMR and constitute the starting point for conservation actions and long-term data collection programs.

Recently, the village of Ponta do Ouro has been connected with an high speed road to Maputo. The new road allows to cover the distance in less than two hours by car or buses while previously 7 hours were needed by all-terrain vehicles. Managers of the PPMR are expecting great changes on the touristic offer with possible negative influences on natural habitats including coral reefs.

Managers of the PPMR can benefit from the combined SfM-approach and statistical classification at any stage of the analysis. First looking at the clusters that describe: i) taxonomic and morphologic composition of the benthic communities, ii) seascape spatial composition and organisms' shape complexity, iii) classes of fragility to physical impacts. Second by looking at the final confusion matrices which embeds the summary of related ecological data and provide insights into the spatial variability of the coral reef benthic communities in the protected area.

Considering the above information, managers of the PPMR can prioritise conservation measures at each site. Different types of management actions could be experimented on coral reef sites, given the possible negative impacts (Figure 5.1). For example, strategic policies could favor visiting sites with more resistant community to beginner divers while limiting the access to sites with more fragile organisms to more expert divers and when environmental conditions are favourable. This approach might minimize accidental impacts with the seafloor. To this end, the methodological SfM-based approach combining high-resolution orthomosaics and data mining technique (Chapter 2 and Chapter 3) will support future surveys in the PPMR.

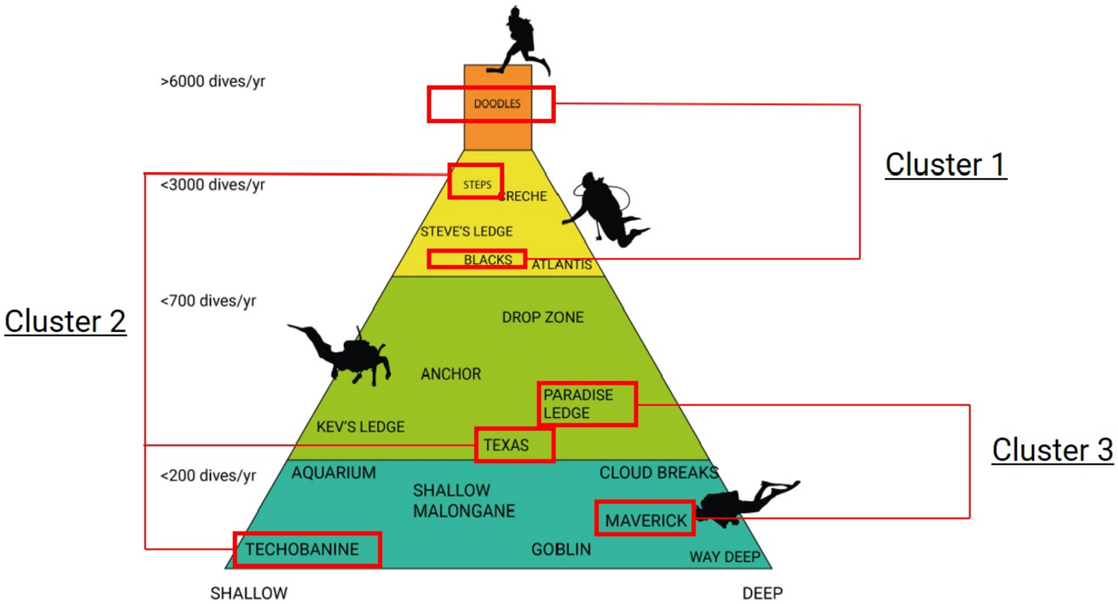

Figure 5.1: The distribution of the clusters of the seven dive sites analysed at PPMR highlights the deep and the diver frequencies variabilities.

5.2.2 Climate change

In the last 20 years, mass mortality events of benthic species have become more frequent. Coralligenous sessile invertebrates (i.e. red gorgonian) are particularly sensitive to seawater temperature anomalies which trigger rapid tissues necrosis and pathogens across populations. Many events has been registered at the Portofino MPA (Italy) causing a shift in benthic assemblages composition with negative consequences on the goods and services the ecosystem provides. In recent years, several authors proposed the emergetic approach for quantifying ecosystem services (ES) provided by natural habitats. The calculations of the emergetic accounting (Odum, 1988, 1996), consider the distribution, the abundance and the health status (e.g. epibiosis) of key species. The emergetic approach is therefore a powerful tool for assessing the Good Environmental Status (GES) as required by the European Commission through the Biodiversity Convention and the Marine Strategy Framework Directive. However, very often emergetic studies lack of quantitative and spatially significant and up-to-date data regarding species distribution and abundances, resulting in general approximation of habitat status (Franzese et al., 2015, 2017; Picone et al., 2017; Paoli et al., 2018). As a result, these studies do not reflect the intrinsic variability of ecological communities and of their responses to environmental changes. The method of Chapter 4 is transferable and can complement emergetic approaches by providing quantitative metrics of key-habitat species. In our study (Chapter 4) the estimated contribution of *P.clavata* across the Portofino MPA was of 1.51 GJ of Energy, considering the bathymetric range and the habitat map layer across the studied area (Figure B.3). This is a significant contribution calling for further investigations to support the development of conservation indexes on coralligenous habitat (Sartoretto et al., 2017) and tailored natural capital calculations (Paoli et al., 2018).

5.3 Implication for future research

It is important to acknowledge that the results of this research and associated interpretation in terms of underlying processes, are constrained by high quality data. Therefore, implications and recommendations for further research are formulated here in terms of (i) data collection and (ii) availability.

5.3.1 Data collection of benthic communities

While technological advancements have made it easier to collect large amounts of samples using SfM, implementation of specific measuring are often constrained.

For example in this study, field campaigns were limited by weather conditions (i.e. seawater visibility) and seasonal mucilages. This means a restricted temporal sampling in some geographic areas (i.e. winter and spring seasons in the North Mediterranean Sea; summer until late autumn in Southern Mozambique). The environmental conditions during which the sampling is performed have consequences on the quality and resolution of the resulting point cloud as well as on the sharpness of the generated ortho-mosaic and the number of faces of the 3D model. Surveys should be therefore performed in calm sea-weather condition with good visibility during the central hours of the day. For example, in Chapter 3, data collected under low visibility conditions were not analyzed because affecting the sharpness and blurriness of the images and reducing the quality of the orthomosaic. The horizontal underwater visibility at PPMR varied between 20 meters in April to 5 meters in June as a result of the seasonal changes of the current direction and regime (Ramsay, 1996).

In this study, sampling has been carried out at the same distance to the seafloor to guarantee a similar pixel size of the generated ortho-mosaics. It was not possible to collect SfM imageries at different distances from the object and to then select only the images in proximity to the target to generate the dense cloud points as often implemented in terrestrial surveys. This is an approach that ensures high accuracy but it is not very efficient underwater due to reflectance and colour problems.

Future research should explore the possibility of implementing oblique SfM data collection underwater with multiple cameras today limited to terrestrial environments. This is technique provides high accuracy of altimetric information and corrected geometrical edges of complex scenarios (i.e. metropolitan areas) but requires high performance computing and costly cameras. This approach could have offered the possibility of having a more accurate estimate of organisms morphometries (Chapter 4).

To this end, the success of using SfM-approaches in marine management plans lies in the ability of providing methods easy to implement, suitable to the scale of assessment, and responding to impacts in an interpretable way.

5.3.2 Availability of photogrammetric data

More studies are required that apply SfM at a high temporal and spatial resolution to improve scientific understandings on how changes in benthic communities relate to environmental and human processes. Towards that, there is the need to explore alternative possibilities to increase the availability of underwater quality information e.g. working with scuba divers. Online repositories already exist to access to photogrammetric datasets for terrestrial environments (i.e. Open Aerial Map web portal), while have not been implemented yet underwater. In this context, ongoing citizen and science initiatives, such as 4Dive have opened new strategies to promote the use of

SfM-methods for conservation by involving scuba volunteers collecting data on cultural heritage (i.e. shipwrecks) at Malta Island and providing an e- infrastructure for image processing. Hopefully this initiative could be used to coordinate standardize sampling approaches and provide benchmark data to complement routine monitoring in MPAs.

Finally, application of SfM-based method, and reliably quantify the effects of scuba diving, it is recommended to collect environmental data potentially relevant to the aim of the study. For example, the method testing presented in Chapter 3 suggested that environmental conditions mediate the effect of diving at some coral reefs sites. Due to time constraints, it was not possible to collect data about current velocity, topography and test the correlation with benthic composition and seascape metrics.

5.4 Conclusion

This research aimed to improve the characterization of benthic marine communities by using SfM, and to support the development of targeted marine management strategies by providing standardised methods for assessing benthic composition and organisms' morphometrics in tropical and mediterranean environments. By using ortho-mosaics and point clouds from SfM, there are three main ways in which this research will improve methodologies to investigate and quantify benthic communities changes.

First, a novel framework, statistical investigation based on empirical evidences on spatial composition of reef communities demonstrated the importance of sample representativeness in order to evaluate and select high resolution ortho-mosaics to investigate benthos. The benthic community of Ponta do Ouro Partial Marine Reserve (Mozambique) is disaggregated within a rocky matrix. The organism are often characterized by small sizes and regular shapes and and the population is highly represented by soft corals. Common metrics (i.e. diversity index, shape index, fractal index) have specific requirements of sampling scale and quadrat density to be robust but, overall accurately identified by sampling scales of 25 m^2. The results confirmed the need of selecting the appropriate sampling strategy when accounting for community metrics, the lack of which result in biased estimate of population structure and functions.

Second, by combining high resolution ortho-mosaics and data mining techniques to reef communities, the potential impact of scuba diving could be assessed (Chapter 3). The findings confirmed hypotheses made in previous research about scuba diving having negative direct (i.e breaks, sedimentation) and indirect effects (i.e. diseases) over reef habitats, and provided baseline information for the reefs at PPMR. However, it is essential to establish further knowledge on how scuba diving affect benthic communities in different reefs types and over multiple spatial and temporal scales, so that marine management can account for heterogeneity of seascapes and specific processes (Sections 5.2.1).

Third, a method based on empirical evidences on density and morphometrics of gorgonian forests demonstrated the high accuracy of metrics quantifications in order to evaluate and select scaled point clouds to indirect estimates of biomass. This type of approach has not been applied before to tree-shaped organisms, and it clearly demonstrates the potential of the method to improve predictions coralligenous status in the Mediterranean sea. The findings provide important empirical evidence that highlights the need to further application to others species and protected area.

In conclusion, through new methodological approaches and empirical evidence, this research highlights that SfM-based method are a flexible, affordable and reliable technology to improved survey of ecological communities. Further development of this avenue of research will aid better-resolved scientific understanding of benthic communities and management to safeguard marine habitats.

References

Assessment, M. E., 2003. Ecosystems and human well-being.

Ballesteros, E., 2006. Mediterranean coralligenous assemblages: a synthesis of present knowledge. Oceanography and marine biology: an annual review 44, 123–195.

Barbier, E. B., Hacker, S. D., Kennedy, C., Koch, E. W., Stier, A. C., Silliman, B. R., 2011. The value of estuarine and coastal ecosystem services. Ecol Monogr 81 (2), 169–193.

Barnes, B. B., Hallock, P., Hu, C., Muller-Karger, F., Palandro, D., Walter, C., Zepp, R., 2015. Prediction of coral bleaching in the Florida Keys using remotely sensed data. Coral Reefs 34 (2), 491–503.

Beijbom, O., Edmunds, P. J., Kline, D. I., Mitchell, B. G., Kriegman, D., 2012. Automated annotation of coral reef survey images. In: Computer Vision and Pattern Recognition (CVPR), 2012 IEEE Conference on. IEEE, pp. 1170–1177.

Bellwood, D. R., Hughes, T. P., Folke, C., Nyström, M., 2004. Confronting the coral reef crisis. Nature 429 (6994), 827.

Bianchi, C., Pronzato, R., Cattaneo-Vietti, R., Benedetti-Cecchi, L., Morri, C., Pansini, M., Chemello, R., Milazzo, M., Fraschetti, S., Terlizzi, A., et al., 2004. Hard bottoms. Biol Mar Mediterr 11 (1), 185–215.

Boström, C., Pittman, S. J., Simenstad, C., Kneib, R. T., 2011. Seascape ecology of coastal biogenic habitats: advances, gaps, and challenges. Mar Ecol Prog Ser 427, 191–217.

Bramanti, L., Benedetti, M. C., Cupido, R., Cocito, S., Priori, C., Erra, F., Iannelli, M., Santangelo, G., 2015. Demography of Animal Forests: The Example of Mediterranean Gorgonians. Springer International Publishing, Cham, pp. 1–20.

Bravo, G., Márquez, F., Marzinelli, E. M., Mendez, M. M., Bigatti, G., 2015. Effect of recreational diving on patagonian rocky reefs. Marine environmental research 104, 31–36.

Brodu, N., Lague, D., 2012. 3d point cloud classification of complex natural scenes using a multi-scale dimensionality criterion: applications in geomorphology. In: EGU General Assembly Conference Abstracts. Vol. 14. p. 4368.

Brown, C. J., Smith, S. J., Lawton, P., Ander-son, J. T., 2011. Benthic habitat mapping: A review of progress towards improved un-derstanding of the spatial ecology of the seafloor using acoustic tech-niques. Estuarine, Coastal and Shelf Science 92 (3), 502–520.

Bryson, M., Ferrari, R., Figueira, W., Pizarro, O., Madin, J., Williams, S., Byrne, M., 2017. Characterization of measurement errors using structure-from-motion and photogrammetry to measure marine habitat structural complexity. Ecology and Evolution 7 (15), 5669–5681.

Buckley, R., 2012. Sustainable tourism: Research and reality. Annals of Tourism Research 39 (2), 528–546.

Buhl-Mortensen, L., Buhl-Mortensen, P., Dolan, M. F., Holte, B., 2015. The mareano programme–a full coverage mapping of the norwegian off-shore benthic environment and fauna. Marine Biology Research 11 (1), 4–17.

Burke, L., Reytar, K., Spalding, M., Perry, A., 2012. Reefs at risk revisited in the coral triangle: World resources institute. In: The Nature Conservancy. World-Fish Center, International Coral Reef Action Network. UNEP World Conservation Monitoring Centre and Global Coral Reef Monitoring Network Washington, DC.

Burns, J., Delparte, D., Kapono, L., Belt, M., Gates, R., Takabayashi, M., 2016. Assessing the impact of acute disturbances on the structure and composition of a coral community using innovative 3D reconstruction techniques. Method Oceanogr 15, 49–59.

Candela, L., Castelli, D., Pagano, P., 2009. D4science: an e-infrastructure for supporting virtual research en-vironments. In: IRCDL. pp. 166–169.

Carrivick, J. L., Smith, M. W., Quincey, D. J., 2016. Structure from Motion in the Geosciences. John Wiley & Sons.

Casella, E., Collin, A., Harris, D., Ferse, S., Bejarano, S., Parravicini, V., Hench, J. L., Rovere, A., 2016. Mapping coral reefs using consumer-grade drones and structure from motion photogrammetry techniques. Coral Reefs, 1–7.

Cathalot, C., Van Oevelen, D., Cox, T. J., Kutti, T., Lavaleye, M., Duineveld, G., Meysman, F. J., 2015. Cold-water coral reefs and adjacent sponge grounds: Hotspots of benthic respiration and organic carbon cycling in the deep sea. Frontiers in Marine Science 2, 37.

Celliers, L., Schleyer, M. H., 2008. Coral community structure and risk assessment of high-latitude reefs at sodwana bay, south africa. Biodiversity and Conservation 17 (13), 3097–3117.

Cerrano, C., Arillo, A., Azzini, F., Calcinai, B., Castellano, L., Muti, C., Valisano, L., Zega, G., Bavestrello, G., 2005. Gorgonian population recovery after a mass mortality event. Aquatic Conservation: Marine and Freshwater Ecosystems 15 (2), 147–157.

Cerrano, C., Bavestrello, G., 2008. Medium-term effects of die-off of rocky benthos in the Ligurian Sea. What can we learn from gorgonians? Chemistry and Ecology 24 (sup1), 73–82.

Cerrano, C., Bavestrello, G., 2009. Mass mortalities and extinctions. In: Marine Hard Bottom Communities. Springer, pp. 295–307.

Cerrano, C., Bavestrello, G., Bianchi, C. N., Cattaneo-Vietti, R., Bava, S., Morganti, C., Morri, C., Picco, P., Sara, G., Schiaparelli, S., et al., 2000. A catastrophic mass-mortality episode of gorgonians and other organisms in the Ligurian Sea (North-western Mediterranean), summer 1999. Ecology letters 3 (4), 284–293.

Cerrano, C., Danovaro, R., Gambi, C., Pusceddu, A., Riva, A., Schiaparelli, S., 2010. Gold coral (*Savalia savaglia*) and gorgonian forests enhance benthic biodiversity and ecosystem functioning in the mesophotic zone. Biodiversity and Conservation 19 (1), 153–167.

Chabanet, P., Adjeroud, M., Andréfouët, S., Bozec, Y.-M., Ferraris, J., Garcìa-Charton, J.-A., Schrimm, M., 2005. Human-induced physical disturbances and their indicators on coral reef habitats: A multi-scale approach. Aquatic Living Resources 18 (3), 215–230.

Chadwick-Furman, N., 1995. Effects of scuba diving on coral reef invertebrates in the us virgin islands: implications for the management of diving. In: Proceedings of the 6th International Conference on Coelenterate Biology. Vol. 91. pp. 1–5.

Chambers, J. M., Hastie, T. J., et al., 1992. Statistical models in S. Vol. 251. Wadsworth & Brooks/Cole Advanced Books & Software Pacific Grove, CA.

Cheal, A. J., MacNeil, M. A., Emslie, M. J., Sweatman, H., 2017. The threat to coral reefs from more intense cyclones under climate change. Glob Change Biol.

Chirayath, V., Earle, S. A., 2016. Drones that see through waves–preliminary results from airborne fluid lensing for centimetre-scale aquatic conservation. Aquatic Conservation: Marine and Freshwater Ecosystems 26, 237–250.

Cignoni, P., Callieri, M., Corsini, M., Dellepiane, M., Ganovelli, F., Ranzuglia, G., 2008. MeshLab: an Open-Source Mesh Processing Tool. In: Scarano, V., Chiara, R. D., Erra, U. (Eds.), Eurographics Italian Chapter Conference. The Eurographics Association.

Cohen, J., 1960. A coefficient of agreement for nominal scales. Educational and psychological measurement 20 (1), 37–46.

Coma, R., Ribes, M., Serrano, E., Jiménez, E., Salat, J., Pascual, J., 2009. Global warming-enhanced stratification and mass mortality events in the Mediterranean. Proceedings of the National Academy of Sciences 106 (15), 6176–6181.

Coma, R., Ribes, M., Zabala, M., Gili, J.-M., 1998. Growth in a modular colonial marine invertebrate. Estuarine, Coastal and Shelf Science 47 (4), 459–470.

Coma, R., Zabala, M., Gili, J.-M., 1995. Sexual reproductive effort in the Mediterranean gorgonian paramuricea clavata. Marine ecology progress series. Oldendorf 117 (1), 185–192.

Commission, E., 2011. Communication from the commission to the European Parliament, the Council, the Economic and Social Committee and the Committee of the Regions. Brussels.

Condit, R., Hubbell, S. P., Lafrankie, J. V., Sukumar, R., Manokaran, N., Foster, R. B., Ashton, P. S., 1996. Species-area and species-individual relationships for tropical trees: a comparison of three 50-ha plots. J Ecol, 549–562.

Coro, G., Palma, M., Ellenbroek, A., Panichi, G., Nair, T., Pagano, P., 2018. Reconstructing 3d virtual environments within a collaborative e-infrastructure. Concurrency and Computation: Practice and Experience, e5028.

Coro, G., Webb, T. J., Appeltans, W., Bailly, N., Cattrijsse, A., Pagano, P., 2015. Classifying degrees of species commonness: North sea fish as a case study. Ecological modelling 312, 272–280.

Costa, A., Pereira, M. A., Motta, H., Schleyer, M., 2005. Status of coral reefs of mozambique: 2004. Coral reef degradation in the Indian Ocean: status report, 54–60.

Costa, B., Battista, T., Pittman, S., 2009. Comparative evaluation of airborne LiDAR and ship-based multibeam SoNAR bathymetry and intensity for mapping coral reef ecosystems. Remote Sens Environ 113 (5), 1082–1100.

Cowen, R. K., Sponaugle, S., 2009. Larval dispersal and marine population connectivity. Annu Rev Mar Sci 1, 443–466.

Currier, K., 2015. Mapping with strings attached: Kite aerial photography of durai island, anambas islands, indonesia. Journal of Maps 11 (4), 589–597.

Dai, C.-f., 1990. Interspecific competition in Taiwanese corals with special reference to interactions between alcyonaceans and scleractinians. Mar Ecol Prog Ser 60 (3), 291–297.

Dandois, J. P., Olano, M., Ellis, E. C., 2015. Optimal altitude, overlap, and weather conditions for computer vision uav estimates of forest structure. Remote Sensing 7 (10), 13895–13920.

Davis, D., 1993. Scuba diving: Conflicts in marine protected area. Australian Journal of Leisure and Recreation 3 (4), 65–71.

De'ath, G., Fabricius, K. E., Sweatman, H., Puotinen, M., 2012. The 27–year decline of coral cover on the Great Barrier Reef and its causes. P Natl A Sci USA 109 (44), 17995–17999.

Deter, J., Descamp, P., Ballesta, L., Boissery, P., Holon, F., 2012. A preliminary study toward an index based on coralligenous assemblages for the ecological status assessment of Mediterranean French coastal waters. Ecological indicators 20, 345–352.

Dewez, T. J. B., Girardeau-Montaut, D., Allanic, C., Rohmer, J., 2016. Facets: a CloudCompare plugin to extract geological planes from unstructured 3d point clouds. ISPRS - International Archives of the Photogrammetry, Remote Sensing and Spatial Information Sciences XLI-B5, 799–804.

Dikou, A., Van Woesik, R., 2006. Survival under chronic stress from sediment load: spatial patterns of hard coral communities in the southern islands of singapore. Marine pollution bulletin 52 (11), 1340–1354.

Dimmock, K., Musa, G., 2015. Scuba diving tourism system: a framework for collaborative management and sustainability. Marine Policy 54, 52–58.

Diviacco, 2009. Atlante degli habitat marini sc. 1:10000 - 2009, Accessed: 2018–05–30.

Doney, S. C., 2010. The growing human footprint on coastal and open-ocean biogeochemistry. science 328 (5985), 1512–1516.

Donner, S. D., Potere, D., 2007. The inequity of the global threat to coral reefs. AIBS Bulletin 57 (3), 214–215.

Dornelas, M., Madin, J. S., Baird, A. H., Connolly, S. R., 2017. Allometric growth in reef-building corals. P Roy Soc Lond B Bio 284 (1851).
URL http://rspb.royalsocietypublishing.org/content/284/1851/20170053

Drakare, S., Lennon, J. J., Hillebrand, H., 2006. The imprint of the geographical, evolutionary and ecological context on species–area relationships. Ecol Lett 9 (2), 215–227.

Edinger, E. N., Risk, M. J., 2000. Reef classification by coral morphology predicts coral reef conservation value. Biol Conserv 92 (1), 1–13.

Erftemeijer, P. L., Riegl, B., Hoeksema, B. W., Todd, P. A., 2012. Environmental impacts of dredging and other sediment disturbances on corals: a review. Marine pollution bulletin 64 (9), 1737–1765.

Fabricius, K., Death, G., McCook, L., Turak, E., Williams, D. M., 2005. Changes in algal, coral and fish assemblages along water quality gradients on the inshore great barrier reef. Marine pollution bulletin 51 (1-4), 384–398.

Faig, W., Moniwa, H., 1973. Convergent photos for close range. Photogrammetric Engineering and Remote Sensing 39 (6), 605–610.

Ferrari, R., Bryson, M., Bridge, T., Hustache, J., Williams, S. B., Byrne, M., Figueira, W., 2016. Quantifying the response of structural complexity and community composition to environmental change in marine communities. Glob Change Biol.

Ferrari, R., Figueira, W. F., Pratchett, M. S., Boube, T., Adam, A., Kobelkowsky-Vidrio, T., Doo, S. S., Atwood, T. B., Byrne, M., 2017. 3d photogrammetry quantifies growth and external erosion of individual coral colonies and skeletons. Scientific reports 7 (1), 16737.

Ferraris, D., Palma, M., Pantaleo, U., Cerrano, C., Chiantore, M., January 2015 2017. Method and device for tracking the path of an object. WO Patent App. PCT/IB2016/053,924.
URL `https://www.google.co.uk/patents/WO2017002060A2?cl=en`

Figueira, W., Ferrari, R., Weatherby, E., Porter, A., Hawes, S., Byrne, M., 2015. Accuracy and precision of habitat structural complexity metrics derived from underwater photogrammetry. Remote Sens-Basel 7 (12), 16883–16900.

Floros, C., Schleyer, M., 2017. The functional importance of acropora austera as nursery areas for juvenile reef fish on south african coral reefs. Coral Reefs 36 (1), 139–149.

Fox, J., Weisberg, S., Friendly, M., Hong, J., Andersen, R., Firth, D., Taylor, S., Team, R. C., Fox, M. J., 2018. Package effects.

Franzese, P. P., Buonocore, E., Donnarumma, L., Russo, G. F., 2017. Natural capital accounting in marine protected areas: The case of the Islands of Ventotene and S. Stefano (Central Italy). Ecological Modelling 360, 290–299.

Franzese, P. P., Buonocore, E., Paoli, C., Massa, F., Stefano, D., Fanciulli, G., Miccio, A., Mollica, E., Navone, A., Russo, G. F., et al., 2015. Environmental accounting in marine protected areas: the eampa project. Journal of Environmental Accounting and Management 3 (4), 324–332.

Friedman, A., Pizarro, O., Williams, S. B., Johnson-Roberson, M., 2012. Multi-scale measures of rugosity, slope and aspect from benthic stereo image reconstructions. PloS one 7 (12), e50440.

Furukawa, Y., Ponce, J., 2010. Accurate, dense, and robust multiview stereopsis. IEEE transactions on pattern analysis and machine intelligence 32 (8), 1362–1376.

Garrabou, J., Ballesteros, E., Zabala, M., 2002. Structure and dynamics of north-western Mediterranean rocky benthic communities along a depth gradient. Estuar Coast Shelf S 55 (3), 493–508.

Garrabou, J., Coma, R., Bensoussan, N., Bally, M., Chevaldonné, P., Cigliano, M., Diaz, D., Harmelin, J.-G., Gambi, M., Kersting, D., et al., 2009. Mass mortality in northwestern mediterranean rocky benthic communities: effects of the 2003 heat wave. Global change biology 15 (5), 1090–1103.

Garrabou, J., Riera, J., Zabala, M., 1998. Landscape pattern indices applied to Mediterranean subtidal rocky benthic communities. Landscape Ecol 13 (4), 225–247.

Gili, J.-M., Coma, R., 1998. Benthic suspension feeders: their paramount role in littoral marine food webs. Trends in ecology & evolution 13 (8), 316–321.

Girardeau-Montaut, D., 2014. Cloudcompare (version 2.6. 0)[gpl software].

Gladfelter, E. H., Monahan, R. K., Gladfelter, W. B., 1978. Growth rates of five reef-building corals in the northeastern car-ibbean. Bulletin of Marine Science 28 (4), 728–734.

González-Rivero, M., Beijbom, O., Rodriguez-Ramirez, A., Holtrop, T., González-Marrero, Y., Ganase, A., Roelfsema, C., Phinn, S., Hoegh-Guldberg, O., 2016. Scaling up Ecological Measurements of Coral Reefs Using Semi-Automated Field Image Collection and Analysis. Remote Sens-Basel 8 (1), 30.

González-Rivero, M., Bongaerts, P., Beijbom, O., Pizarro, O., Friedman, A., Rodriguez-Ramirez, A., Upcroft, B., Laffoley, D., Kline, D., Bailhache, C., et al., 2014. The Catlin Seaview Survey–kilometre-scale seascape assessment, and monitoring of coral reef ecosystems. Aquat Conserv 24 (S2), 184–198.

Gori, A., Bavestrello, G., Grinyó, J., Dominguez-Carrió, C., Ambroso, S., Bo, M., 2017. Animal Forests in Deep Coastal Bottoms and Continental Shelf of the Mediterranean Sea. Marine Animal Forests: The Ecology of Benthic Biodiversity Hotspots, 1–27.

Gotelli, N. J., Colwell, R. K., 2001. Quantifying biodiversity: procedures and pitfalls in the measurement and comparison of species richness. Ecol Lett 4 (4), 379–391.

Graham, N., Nash, K., 2013. The importance of structural complexity in coral reef ecosystems. Coral Reefs 32 (2), 315–326.

Grigg, R. W., 1972. Orientation and growth form of sea fans. Limnology and Oceanography 17 (2), 185–192.

Guinda, X., Gracia, A., Puente, A., Juanes, J. A., Rzhanov, Y., Mayer, L., 2014. Application of landscape mosaics for the assessment of subtidal macroalgae communities using the CFR index. Deep Sea Research II: Topical Studies in Oceanography 106, 207–215.

Gutiérrez-Heredia, L., D'Helft, C., Reynaud, E., 2015. Simple methods for interactive 3D modeling, measurements, and digital databases of coral skeletons. Limnol Oceanogr: Methods 13 (4), 178–193.

Harris, P. T., 2012. Anthropogenic threats to benthic habitats. In: Seafloor Geomorphology as Benthic Habitat. Elsevier, pp. 39–60.

Harris, P. T., Baker, E. K., 2012. Why map benthic habitats? In: Seafloor geomorphology as benthic habitat. Elsevier, pp. 3–22.

Hasler, H., Ott, J. A., 2008. Diving down the reefs? intensive diving tourism threatens the reefs of the northern red sea. Marine Pollution Bulletin 56 (10), 1788–1794.

Hattori, A., Shibuno, T., 2015. Total volume of 3D small patch reefs reflected in aerial photographs can predict total species richness of coral reef damselfish assemblages on a shallow back reef. Ecol Res 30 (4), 675–682.

Hawkins, J. P., Roberts, C., 1997. Estimating the carrying capacity of coral reefs for scuba diving. In: Proceedings of the 8th international coral reef symposium. Vol. 2. Smithsonian Tropical Research Institute Panama, pp. 1923–1926.

Hawkins, J. P., Roberts, C. M., 1992. Effects of recreational scuba diving on fore-reef slope communities of coral reefs. Biological Conservation 62 (3), 171–178.

Hawkins, J. P., Roberts, C. M., Van't Hof, T., De Meyer, K., Tratalos, J., Aldam, C., 1999. Effects of recreational scuba diving on caribbean coral and fish communities. Conservation Biology 13 (4), 888–897.

Hawkins, S., Hartnoll, R., 1980. A study of the small-scale relationship between species number and area on a rocky shore. Estuar Coast Mar Sci 10 (2), 201–214.

He, H. S., DeZonia, B. E., Mladenoff, D. J., 2000. An aggregation index (AI) to quantify spatial patterns of landscapes. Landscape Ecol 15 (7), 591–601.

Hedley, J. D., Roelfsema, C. M., Chollett, I., Harborne, A. R., Heron, S. F., Weeks, S., Skirving, W. J., Strong, A. E., Eakin, C. M., Christensen, T. R., et al., 2016. Remote sensing of coral reefs for monitoring and management: A review. Remote Sens-Basel 8 (2), 118.

Hill, J., Wilkinson, C., 2004. Methods for ecological monitoring of coral reefs. Australian Institute of Marine Science, Townsville 117.

Hilmi, N., Bambridge, T., Claudet, J., David, G., Failler, P., Feral, F., Leopold, M., Pascal, N., Safa, A., 2014. Préserver la biodiversité des récifs coralliens: l'évaluation économique comme outil d'une gouvernance multi-échelle. In: Les sciences sociales dans le Pacifique Sud : terrains, questions et mthodes. Marseille : Pacific-Credo Publ., (Cahiers du Credo). ISBN 978-2-9537485-2-9, pp. 291–312.

Hong Kong Special Administrative Region, 2016. Hong Kong Biodiversity Strategy Action Plan 2016-2021
`https://www.afcd.gov.hk/tc_chi/conservation/Con_hkbsap/files/HKBSAP_ENG_2.pdf`.

Huete-Stauffer, C., Previati, M., Scinto, A., Palma, M., Pantaleo, U., Cappanera, V., Cerrano, C., Imperia, C. E. A., Portofino, M., 2013. Long-term monitoring in a multi-stresses *Paramuricea clavata* population.

Huete-Stauffer, C., Vielmini, I., Palma, M., Navone, A., Panzalis, P., Vezzulli, L., Misic, C., Cerrano, C., 2011. *Paramuricea clavata* (Anthozoa, Octocorallia) loss in the Marine Protected Area of Tavolara (Sardinia, Italy) due to a mass mortality event. Marine Ecology 32 (s1), 107–116.

Hughes, T., Connell, J., 1999. Multiple stressors on coral reefs: A long-term perspective. Limnology and oceanography 44 (3part2), 932–940.

Hughes, T. P., Baird, A. H., Bellwood, D. R., Card, M., Connolly, S. R., Folke, C., Grosberg, R., Hoegh-Guldberg, O., Jackson, J. B., Kleypas, J., et al., 2003. Climate change, human impacts, and the resilience of coral reefs. science 301 (5635), 929–933.

Hughes, T. P., Kerry, J. T., Álvarez-Noriega, M., Álvarez-Romero, J. G., Anderson, K. D., Baird, A. H., Babcock, R. C., Beger, M., Bellwood, D. R., Berkelmans, R., et al., 2017. Global warming and recurrent mass bleaching of corals. Nature 543 (7645), 373.

IG.21/9, U., 2016. Annex II Thematic Decisions. http://actionmed.eu/wp-content/uploads/2016/03/Decision-21.3-ECAP-FINAL.pdf.

Ingwer, P., Gassen, F., Püst, S., Duhn, M., Schälicke, M., Müller, K., Ruhm, H., Rettig, J., Hasche, E., Fischer, A., et al., 2015. Practical usefulness of structure from motion (sfm) point clouds obtained from different consumer cameras. In: Mobile Devices and Multimedia: Enabling Technologies, Algorithms, and Applications 2015. Vol. 9411. International Society for Optics and Photonics, p. 941102.

James, M., Robson, S., 2012. Straightforward reconstruction of 3d surfaces and topography with a camera: Accuracy and geoscience application. Journal of Geophysical Research: Earth Surface 117 (F3).

Jolliffe, I., 2005. Principal component analysis: Wiley online library. Google Scholar.

Jordan, I. E., Samways, M. J., 2001. Recent changes in coral assemblages of a south african coral reef, with recommendations for long-term monitoring. Biodiversity & Conservation 10 (7), 1027–1037.

Kazhdan, M., Hoppe, H., 2013. Screened poisson surface reconstruction. ACM Transactions on Graphics (TOG) 32 (3), 29.

Kendall, M. S., Miller, T., 2008. The influence of thematic and spatial resolution on maps of a coral reef ecosystem. Marine Geodesy 31 (2), 75–102.

Kenefick, J. F., Gyer, M. S., Harp, B. F., 1972. Analytical self-calibration. Photogrammetric Engineering 38 (11), 1117–1126.

Lague, D., Brodu, N., Leroux, J., 2013. Accurate 3d comparison of complex topography with terrestrial laser scanner: Application to the rangitikei canyon (nz). ISPRS journal of photogrammetry and remote sensing 82, 10–26.

Lamb, J. B., True, J. D., Piromvaragorn, S., Willis, B. L., 2014. Scuba diving damage and intensity of tourist activities increases coral disease prevalence. Biological Conservation 178, 88–96.

Laurans, Y., Pascal, N., Binet, T., Brander, L., Clua, E., David, G., Rojat, D., Seidl, A., 2013. Economic valuation of ecosystem services from coral reefs in the South Pacific: Taking stock of recent experience. J Environ Manage 116, 135–144.

Lavy, A., Eyal, G., Neal, B., Keren, R., Loya, Y., Ilan, M., 2015. A quick, easy and non-intrusive method for underwater volume and surface area evaluation of benthic organisms by 3D computer modelling. Methods Ecol Evol 6 (5), 521–531.

Le, J. T., Levin, L. A., Carson, R. T., 2017. Incorporating ecosystem services into environmental management of deep-seabed mining. Deep Sea Research Part II: Topical Studies in Oceanography 137, 486–503.

Lecours, V., Devillers, R., Schneider, D. C., Lucieer, V. L., Brown, C. J., Edinger, E. N., 2015. Spatial scale and geographic context in benthic habitat mapping: review and future directions. Mar Ecol Prog Ser 535, 259–284.

Leon, J. X., Roelfsema, C. M., Saunders, M. I., Phinn, S. R., 2015. Measuring coral reef terrain roughness using 'Structure-from-Motion'close-range photogrammetry. Geomorphology 242, 21–28.

Lepareur, F., 2011. Évaluation de létat de conservation des habitats naturels marins à léchelle dun site natura 2000. Guide méthodologique. Rapport SPN 3, 9.

Levy, J., Hunter, C., Lukacazyk, T., Franklin, E. C., 2018. Assessing the spatial distribution of coral bleaching using small unmanned aerial systems. Coral Reefs 37 (2), 373–387.

Liang, X., Wang, Y., Jaakkola, A., Kukko, A., Kaartinen, H., Hyyppä, J., Honkavaara, E., Liu, J., 2015. Forest data collection using terrestrial image-based point clouds from a handheld camera compared to terrestrial and personal laser scanning. IEEE transactions on geoscience and remote sensing 53 (9), 5117–5132.

Linares, C., Coma, R., Garrabou, J., Díaz, D., Zabala, M., 2008a. Size distribution, density and disturbance in two Mediterranean gorgonians: *Paramuricea clavata* and *Eunicella singularis* . Journal of Applied Ecology 45 (2), 688–699.

Linares, C., Coma, R., Mariani, S., Díaz, D., Hereu, B., Zabala, M., 2008b. Early life history of the Mediterranean gorgonian *Paramuricea clavata*: implications for population dynamics. Invertebrate Biology 127 (1), 1–11.

Linares, C., Coma, R., Zabala, M., 2008c. Restoration of threatened red gorgonian populations: An experimental and modelling approach. Biological Conservation 141 (2), 427 – 437.

Lirman, D., 2000. Fragmentation in the branching coral acropora palmata (lamarck): growth, survivorship, and reproduction of colonies and fragments. Journal of Experimental Marine Biology and Ecology 251 (1), 41–57.

Lucrezi, S., Saayman, M., 2017. Sustainable scuba diving tourism and resource use: Perspectives and experiences of operators in mozambique and italy. Journal of Cleaner Production 168, 632–644.

Luna, B., Pérez, C. V., Sánchez-Lizaso, J. L., 2009. Benthic impacts of recreational divers in a mediterranean marine protected area. ICES Journal of Marine Science 66 (3), 517–523.

Lyons, P. J., Arboleda, E., Benkwitt, C. E., Davis, B., Gleason, M., Howe, C., Mathe, J., Middleton, J., Sikowitz, N., Untersteggaber, L., et al., 2015. The effect of recreational scuba divers on the structural complexity and benthic assemblage of a caribbean coral reef. Biodiversity and conservation 24 (14), 3491–3504.

MacArthur, R. H., Wilson, E. O., 2015. Theory of Island Biogeography.(MPB-1). Vol. 1. Princeton University Press.

Magliozzi, C., Coro, G., Grabowski, R., Packman, A. I., Krause, S., 2018. A multi-scale statistical method to identify potential areas of hyporheic exchange for river restoration planning. Environmental Modelling & Software.

Magris, R. A., Pressey, R. L., Weeks, R., Ban, N. C., 2014. Integrating connectivity and climate change into marine conservation planning. Biological Conservation 170, 207–221.

McCarthy, J., Benjamin, J., 2014. Multi-image photogrammetry for underwater archaeological site recording: An accessible, diver-based approach. J Mari Arch 9 (1), 95–114.

McGarigal, K., 2014. Fragstats help. Documentation for FRAGSTATS 4.

Mcgarigal, K., Cushman, S. A., Neel, M. C., Ene, E., 2002. FRAGSTATS: Spatial pattern analysis program for categorical maps. Tech. rep.
URL `http://www.umass.edu/landeco/research/fragstats/fragstats.html`

McGarigal, K., Marks, B. J., 1995. FRAGSTATS: spatial pattern analysis program for quantifying landscape structure. Gen tech rep pnw-gtr-351, United States Department of Agriculture, Forest Service, Pacific Northwest Research Station.

Meesters, E., Bos, A., Gast, G., 1992. Effects of sedimentation and lesion position on coral tissue regeneration. In: Proc 7th Int Coral Reef Symp. Vol. 2. pp. 681–688.

Mengerink, K. J., Van Dover, C. L., Ardron, J., Baker, M., Escobar-Briones, E., Gjerde, K., Koslow, J. A., Ramirez-Llodra, E., Lara-Lopez, A., Squires, D., et al., 2014. A call for deep-ocean stewardship. Science 344 (6185), 696–698.

Micheletti, N., Chandler, J. H., Lane, S. N., 2015a. Investigating the geomorphological potential of freely available and accessible structure-from-motion photogrammetry using a smartphone. Earth Surface Processes and Landforms 40 (4), 473–486.

Micheletti, N., Chandler, J. H., Lane, S. N., 2015b. Structure from motion (sfm) photogrammetry.

Milazzo, M., Chemello, R., Badalamenti, F., Camarda, R., Riggio, S., 2002. The impact of human recreational activities in marine protected areas: what lessons should be learnt in the Mediterranean sea? Marine ecology 23 (s1), 280–290.

Mistri, M., 1995. Gross morphometric relationships and growth in the mediterranean gorgonian *Paramuricea clavata*. Italian Journal of Zoology 62 (1), 5–8.

Mistri, M., Ceccherelli, V. U., 1994. Growth and secondary production of the Mediterranean gorgonian *Paramuricea clavata*. Marine Ecology-Progress Series 103, 291–291.

Mitchell, N. D., Dardeau, M. R., Schroeder, W. W., Benke, A. C., 1992. Secondary production of gorgonian corals in the northern Gulf of Mexico. Marine Ecology Progress Series, 275–281.

Mokahtar-Jamaï, K., Pascual, M., Ledoux, J.-B., Coma, R., Féral, J.-P., Garrabou, J., Aurelle, D., 2011. From global to local genetic structuring in the red gorgonian paramuricea clavata: the interplay between oceanographic conditions and limited larval dispersal. Molecular Ecology 20 (16), 3291–3305.

Mora, C., 2015. 36 Perpetual struggle for conservation in a crowded world and the needed paradigm shift for easing ultimate burdens. In: Ecology of Fishes on Coral Reefs. Vol. 20. Cambridge University Press, p. 289.

Motta, H, R. M. S. M. H., 2000. Coral reef monitoring and management in mozambique.

Musa, G., 2002. Sipadan: a scuba-diving paradise: an analysis of tourism impact, diver satisfaction and tourism management. Tourism Geographies 4 (2), 195–209.

Norström, A. V., Nyström, M., Lokrantz, J., Folke, C., 2009. Alternative states on coral reefs: beyond coral–macroalgal phase shifts. Marine ecology progress series 376, 295–306.

Nyström, M., 2006. Redundancy and response diversity of functional groups: implications for the resilience of coral reefs. AMBIO: A Journal of the Human Environment 35 (1), 30–35.

Odum, H. T., 1988. Self-organization, transformity, and information. Science 242 (4882), 1132–1139.

Odum, H. T., 1996. Environmental accounting: emergy and environmental decision making. Wiley.

Palma, M., Rivas Casado, M., Pantaleo, U., Cerrano, C., 2017. High Resolution Orthomosaics of African Coral Reefs: A Tool for Wide-Scale Benthic Monitoring. Remote Sensing 9 (7), 705.

Palma, M., Rivas Casado, M., Pantaleo, U., Pavoni, G., Pica, D., Cerrano, C., 2018. Sfm-based method to assess gorgonian forests (paramuricea clavata (cnidaria, octocorallia)). Remote Sensing 10 (7), 1154.

Paoli, C., Povero, P., Burgos, E., Dapueto, G., Fanciulli, G., Massa, F., Scarpellini, P., Vassallo, P., 2018. Natural capital and environmental flows assessment in marine protected areas: The case study of liguria region (nw mediterranean sea). Ecological Modelling 368, 121–135.

Parliament, E., the Council, 2008. Directive 2008/56/EC. http://data.europa.eu/eli/dir/2008/56/oj.

Pascal, N., Allenbach, M., Brathwaite, A., Burke, L., Le Port, G., Clua, E., 2016. Economic valuation of coral reef ecosystem service of coastal protection: A pragmatic approach. Ecosyst Serv 21, 72–80.

Pavoni, G., Palma, M., Callieri, M., Dellepiane, M., Scopigno, R., Cerrano, C., 2018. Quasi-Orthorectified projection for the measurement of Red Gorgonian colonies. ISPRS Annals of the Photogrammetry, Remote Sensing and Spatial Information Sciences.

Pelleg, D., Moore, A. W., et al., 2000. X-means: Extending k-means with efficient estimation of the number of clusters. In: Icml. Vol. 1. pp. 727–734.

Peraira, M. A., Schleyer, M. H., 2005. A diver and diving survey in southern mozambique. Coral Reef Degradation in the Indian Ocean, 184.

Pergent, G., 2011. Proposal for the definition of standard methods for inventorying and monitoring coralligenous and maerl populations. UNEP-MAP, RAC/SPA Report. UNEP (DEPI)/MED WG 362 (4), 20.

Picone, F., Buonocore, E., DAgostaro, R., Donati, S., Chemello, R., Franzese, P., 2017. Integrating natural capital assessment and marine spatial planning: A case study in the Mediterranean sea. Ecological Modelling 361, 1–13.

Pittman, S. J., Costa, B. M., Battista, T. A., 2009. Using lidar bathymetry and boosted regression trees to predict the diversity and abundance of fish and corals. J Coastal Res, 27–38.

Ponti, M., Grech, D., Mori, M., Perlini, R. A., Ventra, V., Panzalis, P. A., Cerrano, C., 2016. The role of gorgonians on the diversity of vagile benthic fauna in Mediterranean rocky habitats. Marine Biology 163 (5), 1–14.

Porter, S., Branch, G., Sink, K., 2013. Biogeographic patterns on shallow subtidal reefs in the western Indian Ocean. Mar Biol 160 (5), 1271–1283.

Porter, S., Schleyer, M., 2017. Long-term dynamics of a high-latitude coral reef community at sodwana bay, south africa. Coral Reefs, 1–14.

Previati, M., Scinto, A., Cerrano, C., Osinga, R., 2010. Oxygen consumption in Mediterranean octocorals under different temperatures. Journal of Experimental Marine Biology and Ecology 390 (1), 39 – 48.

Purkis, S. J., Graham, N., Riegl, B., 2008. Predictability of reef fish diversity and abundance using remote sensing data in Diego Garcia (Chagos Archipelago). Coral reefs 27 (1), 167–178.

Ramsay, P., 1994. Marine geology of the Sodwana Bay shelf, southeast Africa. Mar Geol 120 (3), 225–247.

Ramsay, P., 1996. Quaternary marine geology of the Sodwana Bay continental shelf, Northern KwaZulu-Natal. Oceanograph Lit Rev 11 (43), 1103.

Raoult, V., Reid-Anderson, S., Ferri, A., Williamson, J. E., 2017. How reliable is structure from motion (sfm) over time and between observers? a case study using coral reef bommies. Remote Sensing 9 (7), 740.

Richardson, D., 1999. A brief history of recreational diving in the united states.

Riegl, B., 1993. Taxonomy and ecology of South African reef corals. Ph.D. thesis, University of Cape Town.

Riegl, B., 1995. Effects of sand deposition on scleractinian and alcyonacean corals. Marine Biology 121 (3), 517–526.

Riegl, B., Schleyer, M. H., Cook, P., Branch, G., 1995. Structure of africa's southernmost coral communities. Bulletin of Marine Science 56 (2), 676–691.

Robertson, W., Schleyer, M., Fielding, P., Tomalin, B., Beckley, L., Fennessy, S., Van der Elst, R., Bandeira, S., Macia, A., Gove, D., 1996. Inshore marine resources and associated opportunities for development of the coast of southern mozambique: Ponta do ouro to cabo de santa maria.

Roche, R. C., Harvey, C. V., Harvey, J. J., Kavanagh, A. P., McDonald, M., Stein-Rostaing, V. R., Turner, J. R., 2016. Recreational diving impacts on coral reefs and the adoption of environmentally responsible practices within the scuba diving industry. Environmental management 58 (1), 107–116.

Roelfsema, C., Phinn, S., Jupiter, S., Comley, J., Albert, S., 2013. Mapping coral reefs at reef to reef-system scales, 10s–1000s km2, using object-based image analysis. Int J Remote Sens 34 (18), 6367–6388.

Rogers, C. S., 1990. Responses of coral reefs and reef organisms to sedimentation. Marine ecology progress series. Oldendorf 62 (1), 185–202.

Rossi, S., 2013. The destruction of the animal forests in the oceans: towards an over-simplification of the benthic ecosystems. Ocean & coastal management 84, 77–85.

Rossi, S., Gili, J.-M., Garrofé, X., 2011. Net negative growth detected in a population *Leptogorgia sarmentosa*: quantifying the biomass loss in a benthic soft bottom-gravel gorgonian. Marine Biology 158 (7), 1631–1643.

Rothermel, M., Wenzel, K., Fritsch, D., Haala, N., 2012. Sure: Photogrammetric surface reconstruction from imagery. In: Proceedings LC3D Workshop, Berlin. Vol. 8. p. 2.

Rouphael, T., Inglis, G., 1995. The effects of qualified recreational scuba divers on coral reefs. Tech. Rep. CRC Reef Res. Cent. (4), 39.

Royer, J.-P., Nawaf, M. M., Merad, D., Saccone, M., Bianchimani, O., Garrabou, J., Ledoux, J.-B., Lopez-Sanz, A., Drap, P., 2018. Photogrammetric surveys and geometric processes to analyse and monitor red coral colonies. Journal of Marine Science and Engineering 6 (2), 42.

Samonte, G. P., Eisma-Osorio, R.-L., Amolo, R., White, A., 2016. Economic value of a large marine ecosystem: Danajon double barrier reef, Philippines. Ocean Coast Manage 122, 9–19.

Sánchez, J. A., 2015. Diversity and evolution of octocoral animal forests at both sides of tropical america. Marine Animal Forests: The Ecology of Benthic Biodiversity Hotspots, 1–33.

Santangelo, G., Cupido, R., Cocito, S., Bramanti, L., Priori, C., Erra, F., Iannelli, M., Oct 2015. Effects of increased mortality on gorgonian corals (cnidaria, octocorallia):

different demographic features may lead affected populations to unexpected recovery and new equilibrium points. Hydrobiologia 759 (1), 171–187.

Sartoretto, S., Schohn, T., Bianchi, C. N., Morri, C., Garrabou, J., Ballesteros, E., Ruitton, S., Verlaque, M., Daniel, B., Charbonnel, E., et al., 2017. An integrated method to evaluate and monitor the conservation state of coralligenous habitats: The INDEX-COR approach. Marine pollution bulletin 120 (1-2), 222–231.

Schleyer, M., 2000. South African coral communities. In: Coral reefs of the Indian ocean: their ecology and conservation. Oxford University Press, New York. pp. 83–105.

Schleyer, M., Celliers, L., 2003. Coral dominance at the reef–sediment interface in marginal coral communities at sodwana bay, south africa. Marine and Freshwater Research 54 (8), 967–972.

Schleyer, M., Celliers, L., 2004. Coral dominance at the reef–sediment interface in marginal coral communities at Sodwana Bay, South Africa. Mar Freshwater Res 54 (8), 967–972.

Schleyer, M. H., Kruger, A., Celliers, L., 2008. Long-term community changes on a high-latitude coral reef in the Greater St Lucia Wetland Park, South Africa. Mar Pollut Bull 56 (3), 493–502.

Schleyer, M. H., Tomalin, B. J., 2000. Damage on south african coral reefs and an assessment of their sustainable diving capacity using a fisheries approach. Bulletin of Marine Science 67 (3), 1025–1042.

Schneider, C. A., Rasband, W. S., Eliceiri, K. W., 2012. Nih image to imagej: 25 years of image analysis. Nature methods 9 (7), 671–675.

Schuhmann, P. W., Casey, J. F., Horrocks, J. A., Oxenford, H. A., 2013. Recreational scuba divers' willingness to pay for marine biodiversity in barbados. Journal of environmental management 121, 29–36.

Schumann, E., Orren, M., 1980. The physico-chemical characteristics of the south-west Indian Ocean in relation to Maputaland. Rhodes University and The Wildlife Society of Southern Africa.

Seenprachawong, U., 2016. An economic analysis of coral reefs in the Andaman Sea of Thailand. In: Marine and Coastal Ecosystem Valuation, Institutions, and Policy in Southeast Asia. Springer, pp. 31–45.

Sleeman, J. C., Kendrick, G. A., Boggs, G. S., Hegge, B. J., 2005. Measuring fragmentation of seagrass landscapes: which indices are most appropriate for detecting change? Mar Freshwater Res 56 (6), 851–864.

Snavely, N., Seitz, S. M., Szeliski, R., 2008. Modeling the world from internet photo collections. International journal of computer vision 80 (2), 189–210.

Somerfield, P., Clarke, K., Warwick, R., 2008. Simpson index. In: Encyclopedia of Ecology. Elsevier.

Spellerberg, I. F., Fedor, P. J., 2003. A tribute to claude shannon (1916–2001) and a plea for more rigorous use of species richness, species diversity and the shannon–wienerindex. Global Ecol Biogeogr 12 (3), 177–179.

Starmans, A., Gutt, J., 2002. Mega-epibenthic diversity: a polar comparison. Mar Ecol Prog Ser 225, 45–52.

Starmans, A., Gutt, J., Arntz, W., 1999. Mega-epibenthic communities in arctic and antarctic shelf areas. Mar Biol 135 (2), 269–280.

Stats, R. C., et al., 2013. R: A language and environment for statistical computing.

Storlazzi, C. D., Dartnell, P., Hatcher, G. A., Gibbs, A. E., 2016. End of the chain? rugosity and fine-scale bathymetry from existing underwater digital imagery using structure-from-motion (sfm) technology. Coral Reefs 35 (3), 889–894.

Stout, J., Vandermeer, J., 1975. Comparison of species richness for stream-inhabiting insects in tropical and mid-latitude streams. The American Naturalist 109 (967), 263–280.

Teixido, N., Garrabou, J., Arntz, W., 2002. Spatial pattern quantification of Antarctic benthic communities using landscape indices. Mar Ecol Prog Ser 242, 1–14.

Thakur, M., Schättin, E. W., McShea, W. J., 2018. Globally common, locally rare: revisiting disregarded genetic diversity for conservation planning of widespread species. Biodiversity and Conservation, 1–5.

Thomas, C. D., Cameron, A., Green, R. E., Bakkenes, M., Beaumont, L. J., Collingham, Y. C., Erasmus, B. F., De Siqueira, M. F., Grainger, A., Hannah, L., et al., 2004. Extinction risk from climate change. Nature 427 (6970), 145–148.

Turner, M. G., 1989. Landscape Ecol: the effect of pattern on process. Annu Rev Ecol Syst, 171–197.

UNEP-MAP-RAC, S., 2008. Action plan for the conservation of the coralligenous and other calcareous bio-concretions in the mediterranean sea. UNEP MAP RAC-SPA publ., Tunis.

Valisano, L., Notari, F., Mori, M., Cerrano, C., 2016. Temporal variability of sedimentation rates and mobile fauna inside and outside a gorgonian garden. Marine Ecology 37 (6), 1303–1314.

Van Dover, C., Ardron, J., Escobar, E., Gianni, M., Gjerde, K., Jaeckel, A., Jones, D., Levin, L., Niner, H., Pendleton, L., et al., 2017. Biodiversity loss from deep-sea mining. Nature Geoscience 10 (7), 464.

Vezzulli, L., Colwell, R. R., Pruzzo, C., 2013. Ocean warming and spread of pathogenic vibrios in the aquatic environment. Microbial ecology 65 (4), 817–825.

Vezzulli, L., Previati, M., Pruzzo, C., Marchese, A., Bourne, D. G., Cerrano, C., 2010. Vibrio infections triggering mass mortality events in a warming Mediterranean Sea. Environmental microbiology 12 (7), 2007–2019.

Wallace, L., Lucieer, A., Malenovskỳ, Z., Turner, D., Vopěnka, P., 2016. Assessment of forest structure using two uav techniques: A comparison of airborne laser scanning and structure from motion (sfm) point clouds. Forests 7 (3), 62.

Walther, B. A., MARTIN, J.-L., 2001. Species richness estimation of bird communities: how to control for sampling effort? Ibis 143 (4), 413–419.

Wedding, L. M., Friedlander, A. M., McGranaghan, M., Yost, R. S., Monaco, M. E., 2008. Using bathymetric lidar to define nearshore benthic habitat complexity: Implications for management of reef fish assemblages in Hawaii. Remote Sens Environ 112 (11), 4159–4165.

Wedding, L. M., Lepczyk, C. A., Pittman, S. J., Friedlander, A. M., Jorgensen, S., 2011a. Quantifying seascape structure: extending terrestrial spatial pattern metrics to the marine realm. Mar Ecol Prog Ser 427, 219–232.

Wedding, L. M., Lepczyk, C. A., Pittman, S. J., Friedlander, A. M., Jorgensen, S., 2011b. Quantifying seascape structure: extending terrestrial spatial pattern metrics to the marine realm. Marine Ecology Progress Series 427, 219–232.

Weinbauer, M. G., Velimirov, B., 1995. Biomass and secondary production of the temperate gorgonian coral *Eunicella cavolini* (coelenterata: Octocorallia). Marine Ecology Progress Series, 211–216.

Weinberg, S., 1978. The minimal area problem in invertebrate communities of Mediterranean rocky substrata. Mar Biol 49 (1), 33–40.

Weinberg, S., 1981. A comparison of coral reef survey methods. Bijdragen tot de Dierkunde 51 (2), 199–218.

Westoby, M., Brasington, J., Glasser, N., Hambrey, M., Reynolds, J., 2012. 'Structure-from-Motion' photogrammetry: A low-cost, effective tool for geoscience applications. Geomorphology 179, 300–314.

White, M., Wolff, G. A., Lundälv, T., Guihen, D., Kiriakoulakis, K., Lavaleye, M., Duineveld, G., 2012. Cold-water coral ecosystem (Tisler Reef, Norwegian Shelf) may be a hotspot for carbon cycling. Marine Ecology Progress Series 465, 11–23.

Wilkinson, C. R., Green, A., Almany, J., Dionne, S., 2003. Monitoring coral reef marine protected areas: A practical guide on how monitoring can support effective management of mpas.

Wilkinson, C. R., Souter, D. N., 2008. Status of Caribbean coral reefs after bleaching and hurricanes in 2005. Global Coral Reef Monitoring Network.

Williams, S. B., Pizarro, O. R., Jakuba, M. V., Johnson, C. R., Barrett, N. S., Babcock, R. C., Kendrick, G. A., Steinberg, P. D., Heyward, A. J., Doherty, P. J., et al., 2012. Monitoring of benthic reference sites: using an autonomous underwater vehicle. IEEE IEEE Robot Autom Mag 19 (1), 73–84.

Wongthong, P., Harvey, N., 2014. Integrated coastal management and sustainable tourism: A case study of the reef-based scuba dive industry from thailand. Ocean & Coastal Management 95, 138–146.

Wright, D. J., Heyman, W. D., 2008. Introduction to the special issue: marine and coastal gis for geomorphology, habitat mapping, and marine reserves. Marine Geodesy 31 (4), 223–230.

Wulff, J., 2006. Resistance vs recovery: morphological strategies of coral reef sponges. Functional Ecology 20 (4), 699–708.

Zakai, D., Chadwick-Furman, N. E., 2002. Impacts of intensive recreational diving on reef corals at eilat, northern red sea. Biological Conservation 105 (2), 179–187.

Zhang, C., Selch, D., Xie, Z., Roberts, C., Cooper, H., Chen, G., 2013. Object-based benthic habitat mapping in the Florida Keys from hyperspectral imagery. Estuar Coast Shelf S 134, 88–97.

Zuiderveld, K., 1994. Contrast limited adaptive histogram equalization. Graphics gems, 474–485.

Zuur, A., Ieno, E., Walker, N., Saveliev, A., Smith, G., 2009. Mixed effects models and extensions in ecology with r. springer science+.

Appendix A

Application of Structure from Motion photogrammetry to coral reefs for characterizing their spatial composition and pressures.

Table A.1: Dives per year. “*” data provided by Peraira and Schleyer (2005).“ **” data provided by the management authority of the Ponta do Ouro Partial Marine Reserve (Mozambique).

year	BLACK’S	DOODLES	MAVERIEK	PARADISE LEDGE	STEPS	TECHOBANINE	TEXAS
2001*		8419		1955	2542		2286
2002*		12282		2852	3708		4210
2011**	761	5644		187	3213		407
2012**	1257	9737	34	366	3957		305
2013**	869	8474		388	4369		127
2014**	668	7117	14	176	3477		222
2015**	1174	6105		563	3042	35	305
2016**	1184	7168	14	512	2714		318

Table A.2: Confusion matrix Pantaleo

	Clustering			
Pantaleo	Cluster1	Cluster2	Cluster3	total
Cluster1	2.00	0.00	0.00	2.00
Cluster2	0.00	2.00	0.00	2.00
Cluster3	0.00	1.00	2.00	3.00
total	2.00	3.00	2.00	7.00
Agreement	2.00	2.00	2.00	6.00
By Chance	0.57	0.86	0.86	2.29
		Intepretation acc. to Fleiss	Interpretation acc to Landis-Koch	
Kappa	0.79	“**Excellent**”	“**Substantial**”	
Absolute Perc. Of Agreement	**86%**			

Table A.3: Confusion matrix Fernandez

	Clustering			
Fernandez	Cluster1	Cluster2	Cluster3	total
Cluster1	2.00	0.00	0.00	2.00
Cluster2	0.00	2.00	1.00	3.00
Cluster3	0.00	1.00	1.00	2.00
total	2.00	3.00	2.00	7.00
Agreement	2.00	2.00	1.00	5.00
By Chance	0.57	0.86	0.86	2.29
		Intepretation acc. to Fleiss	Interpretation acc to Landis-Koch	
Kappa	0.58	"**Good**"	"**Moderate**"	
Absolute Perc. Of Agreement	**71%**			

Table A.4: Confusion matrix Fernandez-Pantaleo

	Fernandez			
Pantaleo	Cluster1	Cluster2	Cluster3	total
Cluster1	2.00	0.00	0.00	2.00
Cluster2	0.00	1.00	1.00	2.00
Cluster3	0.00	2.00	1.00	3.00
total	2.00	3.00	2.00	7.00
Agreement	2.00	1.00	1.00	4.00
By Chance	0.57	0.86	0.86	2.29
		Intepretation acc. to Fleiss	Interpretation acc to Landis-Koch	
Kappa	0.36	**"Marginal"**	**"Fair"**	
Absolute Perc. Of Agreement	**57%**			

Table A.5: Expert opinion on the clusters and across sites

Sites	**Pantaleo**	**Fernandez**	**Clustering**
Doodle	1	1	1
Blacks	1	1	1
Steps	2	2	2
Techo	3	2	2
Texas	2	3	2
Jenny	3	3	3
Maverick	3	2	3

Response: Patch Richness (PR)					
	Df	Sum Sq	Mean Sq	F value	Pr (>F)
Sites	6.00	0.56	0.09	37.40	0.00
Residuals	14.00	0.04	0.00		

Shapiro-Wilk normality test : p-value = 0.14
Levene test of homogeneity of variances: p-value = 0.50

Response: Patch Density (PD)					
	Df	Sum Sq	Mean Sq	F value	Pr (>F)
Sites	6.00	2.98	0.50	23.04	0.00
Residuals	14.00	0.30	0.02		

Shapiro-Wilk normality test : p-value = 0.91
Levene test of homogeneity of variances: p-value = 0.17

Response: Landscape Shannon Diversity Index (SHDI)					
	Df	Sum Sq	Mean Sq	F value	Pr (>F)
Sites	6.00	0.28	0.05	4.55	0.01
Residuals	14.00	0.14	0.01		

Shapiro-Wilk normality test : p-value = 0.35
Levene test of homogeneity of variances: p-value = 0.87

Response: Landscape Simpson Diversity Index (SIDI)					
	Df	Sum Sq	Mean Sq	F value	Pr (>F)
Sites	6.00	0.14	0.02	2.14	0.11
Residuals	14.00	0.15	0.01		

Shapiro-Wilk normality test : p-value = 0.47
Levene test of homogeneity of variances: p-value = 0.77

Response: Mean patch fractal dimension (FRAC_MN)					
	Df	Sum Sq	Mean Sq	F value	Pr (>F)
Sites	6.00	1.09	0.18	1.19	0.36
Residuals	14.00	2.13	0.15		

Shapiro-Wilk normality test : p-value = 0.06
Levene test of homogeneity of variances: p-value = 0.56

Response: Perimeter-area fractal dimension (PAFRAC)					
	Df	Sum Sq	Mean Sq	F value	Pr (>F)
Sites	6.00	0.51	0.08	3.54	0.02
Residuals	14.00	0.34	0.02		

Shapiro-Wilk normality test : p-value = 0.33
Levene test of homogeneity of variances: p-value = 0.77

Figure A.1: One-way ANOVA tables for seascape metrics.

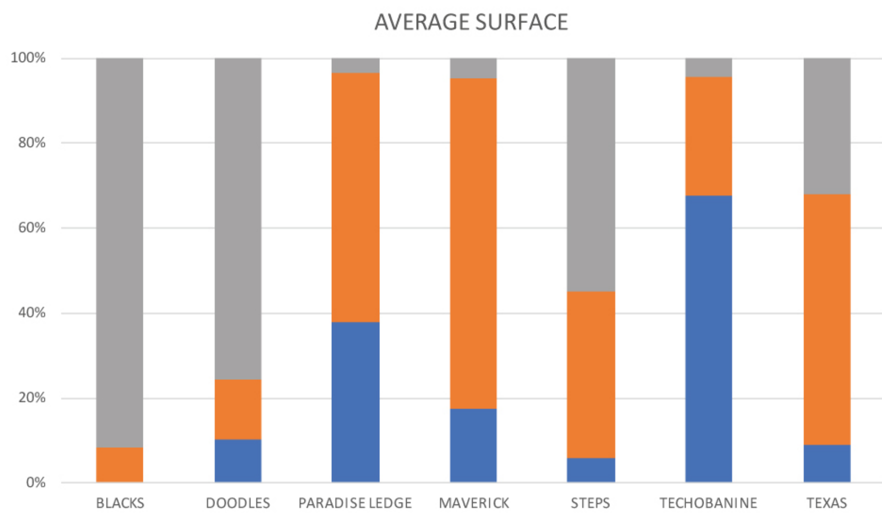

Figure A.2: Relative contribution in percentage of the classes of fragility to physical impacts of the average organisms' surface, across the sites

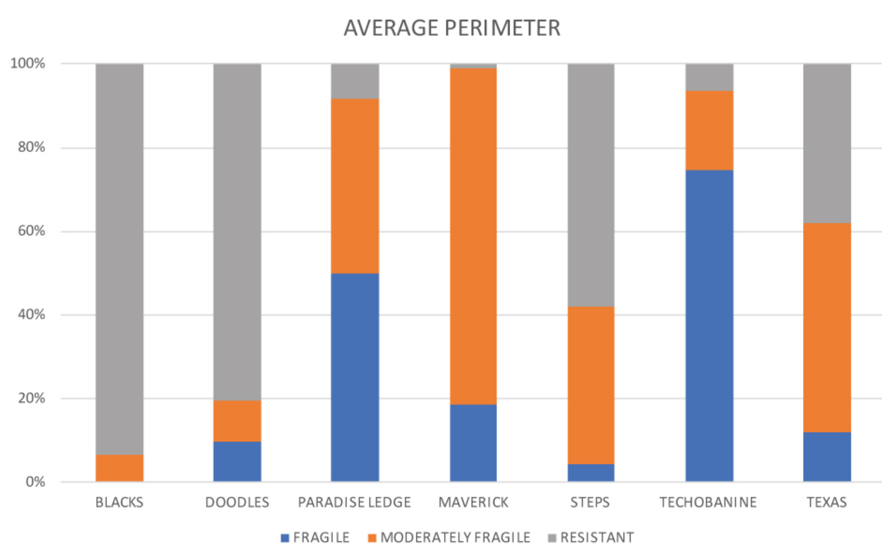

Figure A.3: Relative contribution in percentage of the classes of fragility to physical impacts of the average organisms' perimeter, across the sites

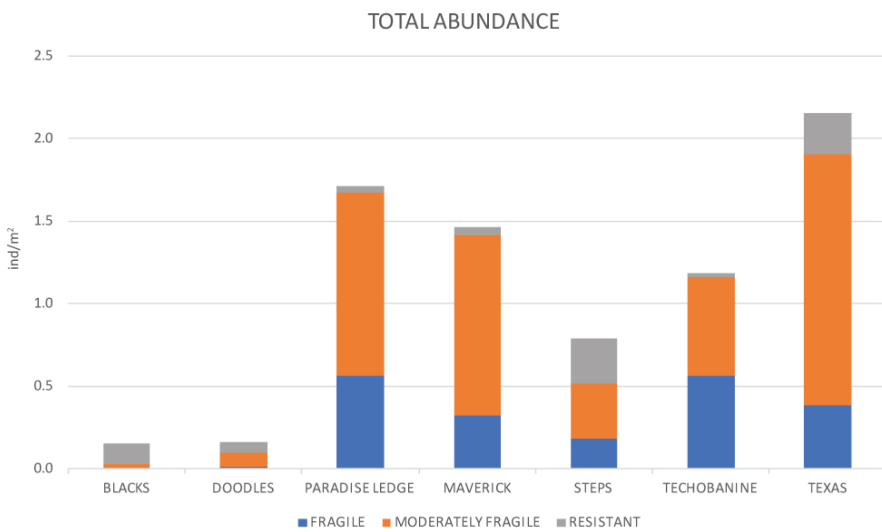

Figure A.4: Total organisms' abundance across sites expressed in class of fragility to physical impacts.

Appendix B

SfM-Based Method to Assess Gorgonian Forests (Paramuricea clavata (Cnidaria, Octocorallia)

Table B.1: Camera specifications and settings used for the Gopro Hero4 Black Edition (Woodman Labs, Inc., San Mateo, California, US)(GH) and the Sony NEX7 alpha digital (Sony Corporation, Minato, Tokyo, Japan) (SN)cameras used in this study

	Unit	GH	SN
Focal length	mm	2.98	12
Resolution	pixels	4000×3000	1920×1080
Sensor type	–	CMOS	CMOS
Sensor dimension	mm	6.17 x 4.55	23.50 x 15.60
Recording format	–	photo	video
Recording frame rate	frame s^{-1}	1	50
Housing port	–	flat	dome port

Table B.2: Number of images processed for each of the 1 m × 1 m quadrats conforming the Abundance Ground Truth (AGT) data set collected with the Gopro Black Edition (Woodman Labs, Inc., San Mateo, California, US) and the Sony alpha digital (Sony Corporation, Minato, Tokyo, Japan) cameras used in this study.

Colony	1	2	3	4	5	6	7	8	9
Gopro	51	58	71	59	60	66	69	58	60
Sony	49	57	71	63	57	63	73	65	62

Figure B.1: The point clouds of the nine dried colonies generated from SfM analysis. A dimensional reference of 10 cm × 1 cm × 1 cm was used to scale the point clouds.

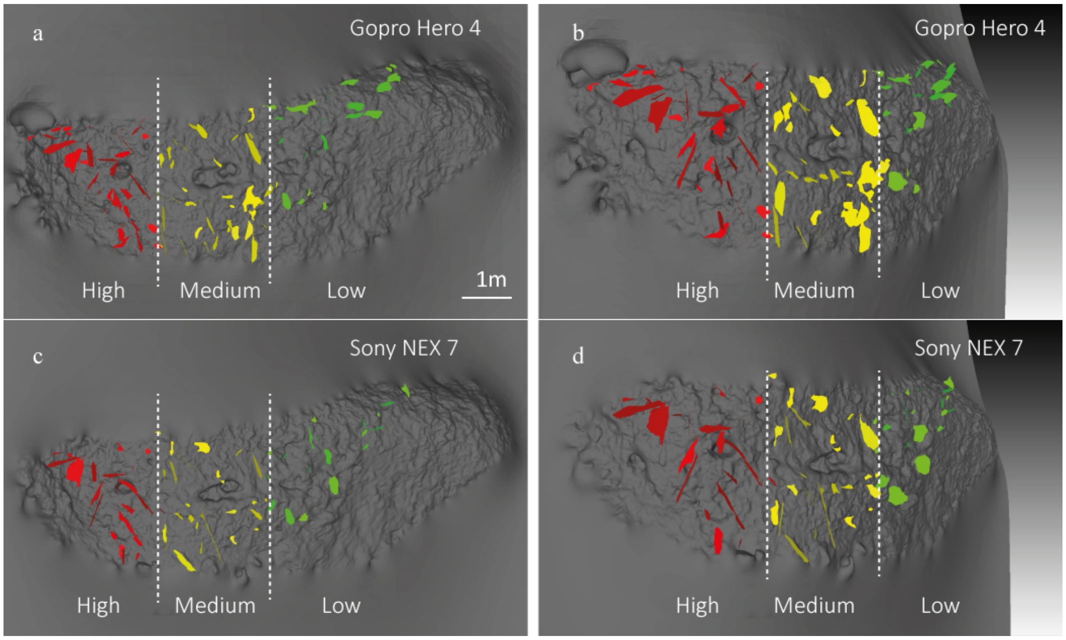

Figure B.2: Views over the 3D scene representing the study area with the gorgonians fan surfaces generated within the three strata by using the imagery recorded with the Gopro Hero4 Black Edition (Woodman Labs, Inc., San Mateo, California, US)(GP) (a, b) and the Sony NEX7 alpha digital (Sony Corporation, Minato, Tokyo, Japan) (SN) (c, d) cameras.

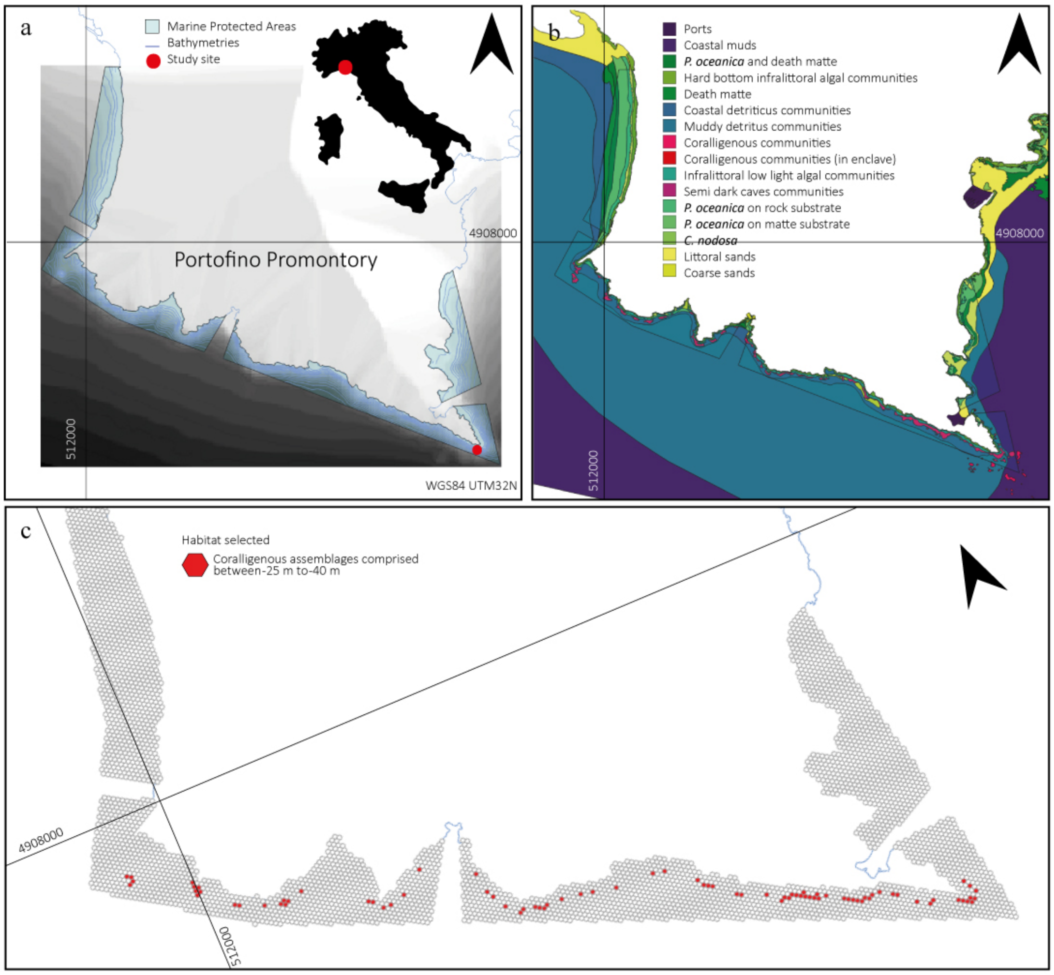

Figure B.3: The maps showing border of the Portofino Marine Protected Area (Italy) (a), the bathymetries at 20 m spatial resolution (a), the benthic biocenosis Diviacco (2009) (b), and the selected 8.63 Ha over a total of 22.22 Ha of coralligenous habitats comprised within the depth -25 m to -40 m, considered for the calculation of carbon and Energy contents of the gorgonians' forests living tissues